Francisca Borges Dias Monteiro da Silva

# Engineering immunotherapies for thyroid cancer

Universidade do Algarve

Faculdade de Medicina e Ciências Biomédicas

2023

Francisca Borges Dias Monteiro da Silva

# Engineering immunotherapies for thyroid cancer

Master in Oncobiology – Molecular Mechanisms of Cancer

This work was done under the supervision of:

Ir. Jeroen Deckers, (Supervisor)
Affiliation – Internal Medicine Department, Radboud UMC

Álvaro Tavares, (Co-Supervisor)

Affiliation – Departamento de Ciências Biomédicas e Medicina, Universidade do Algarve

Universidade do Algarve

Faculdade de Medicina e Ciências Biomédicas

2023

# Engineering immunotherapies for thyroid cancer

**Declaração de autoria de trabalho**

Declaro ser o autor deste trabalho, que é original e inédito. Autores e trabalhos consultados estão devidamente citados no texto e constam na listagem de referências incluída.

"*I declare that I am the author of this work that is original and unpublished. Authors and works consulted are properly cited in the text and included in the list of references.*"

X

Francisca Borges Dias Monteiro da Silva

*“Have no fear of perfection. You’ll never reach it.”*

-Salvador Dali

*“Todas as vitórias ocultam uma abdicação”*

-Simone de Beauvoir

## Acknowledgments

I would like to express my sincere gratitude to all those who have contributed to the successful completion of my master's dissertation. This research endeavor would not have been possible without the support, guidance, and encouragement of various people who have generously shared their knowledge and expertise with me.

First and foremost, I am immensely grateful to my supervisor, Jeroen Deckers, whose continuous support and guidance have been fundamental throughout this journey. His insightful feedback, constructive criticism, and constant belief in my abilities have significantly shaped the direction and quality of this research. I am indebted for the patience, dedication, and invaluable mentorship.

I would like to extend my heartfelt appreciation to the MulderLab members, particularly Prof. Willem Mulder, Yohana Toner, Thijs Beldman, Tom Anbergen, Yuri van Elsas, and Rianne Maas, for their expertise, guidance, and valuable inputs. Their commitment to academic excellence, willingness to share their knowledge, and commitment to my personal growth have been remarkable.

My sincere gratitude goes to my co-supervisor Prof. Álvaro Tavares, for his time, expertise, and valuable feedback.

I would like to acknowledge the Internal Medicine Department of the Radboud UMC for providing me with a conducive research environment and access to invaluable resources. To all the individuals who have crossed my path during my academic pursuit, including fellow students, research collaborators, and academic peers. Their intellectual stimulation, camaraderie, and shared experiences have made this journey truly enriching.

I would like to express my gratitude to all the new friends that this opportunity brought me, particularly Yohana, Brenda, Patricia, and Iris for their friendship and support during this time. Thank you to my friends back home, especially Mariana Meireles, Sofia Basílio, Mafalda Paredes, Mafalda Fazenda, and Diogo Dias for the love and friendship, for the long conversations over the phone, for the support and for keeping me going even when I couldn't.

To my boyfriend, João Gonçalves, for taking care of me even from a distance, for all the love and support, for never letting me give up, and for pushing me to always do my best.

Finally, I want to express my deepest gratitude to my family for their wavering support, understanding, and encouragement throughout this challenging journey. Their love, patience, and belief in my abilities even when I doubted myself.

To my mother Lilia Borges, and my father Luís Monteiro for all the effort, love, and support, and for always making me believe that my dreams are never too big or too hard to achieve.

To Gil Botelho for being the one person that I can always count on, for all the love, motivation, and support, and for never giving up on me.

To my siblings Mercês, Martim, Kiamy, Erik, and Benjamim for the happiness that they bring to my days, for all the love and understanding.

A special thank you to my grandmothers Rosa and Alcina, and my grandfathers, Zeca and Carlos for all the love and hope that they placed in me.

In conclusion, I extend my deepest appreciation to all those who have played a part in the completion of my master's dissertation. Their collective efforts and support have made this

accomplishment possible. I am forever grateful for their contributions, and I hope to carry forward the knowledge and experiences gained from this experience in my future endeavors.

## Abstract

Thyroid cancer affects millions of people worldwide, particularly women. While most thyroid cancer patients have a good long-term prognosis, advanced anaplastic thyroid cancer is one of the most aggressive human malignancies. For most patients suffering from anaplastic thyroid cancer, treatment options are severely limited as tumors are resistant to conventional treatments.

Anaplastic thyroid cancers typically have a highly immunosuppressive, pro-tumorigenic phenotype, characterized by high levels of immune checkpoint expression and the accumulation of tumor-associated macrophages that can account for more than 50% of the tumor volume. These immune-mediated mechanisms that facilitate rapid tumor growth represent attractive new treatment opportunities, particularly combinations of immunotherapies targeting T-cells and macrophages.

The concept of innate immune memory, also known as trained immunity, has recently gained significant attention in the study of the innate immune system. It has also been shown that the induction of trained immunity can help overcome immunosuppression and can be beneficial in the context of cancer. Given this fact, we proposed trained immunity as a therapy target to overcome the characteristic immunosuppressive environment of anaplastic thyroid cancer. The research was conducted to determine the best conditions for inducing trained immunity in bone marrow-derived macrophages. We focused on commonly used primary stimuli such as β-glucan, bacillus Calmette-Guérin (BCG) vaccine, and MDP and secondary bacterial stimuli. Furthermore, tumor culture medium was used as a secondary stimulus.

Through measurements of cytokine production, we detected the induction of trained immunity in bone marrow-derived macrophages trained with BCG and we observed that factors released by tumor cells can have a comparable effect as bacterial stimuli.

We also examined the effect of a tumor on the immune system, looking at the cytokine production of splenocytes and bone marrow-derived macrophages of tumor-bearing mice. At the same time, we analyzed immune cell populations of tumor-bearing mice using flow cytometry, focusing on myeloid, lymphoid, and progenitor cell populations.

In summary, this study provides fundamental new knowledge on how to target the bone marrow and induce trained immunity as a new treatment paradigm for anaplastic thyroid cancer.

**Keywords:** anaplastic thyroid cancer, bone marrow-derived macrophages, immune system, BCG, and trained immunity.

## Resumo

O cancro da tiroide afeta milhões de pessoas em todo o mundo, especialmente mulheres. Embora a maioria dos doentes com cancro da tiroide tenha um prognóstico favorável a longo prazo, o cancro anaplásico avançado da tiroide é um dos cancros mais agressivo, tendo um prognóstico negativo. O tratamento convencionalmente utilizado é a cirurgia seguida do uso de iodo radioativo para eliminação do restante tumor. No entanto, para a maioria dos doentes com cancro anaplásico da tiroide, as opções de tratamento são severamente limitadas, uma vez que os tumores são resistentes ao iodo radioativo. Este tipo de cancro da tiroide desenvolve tumores rapidamente e de tamanhos exacerbados, levando, em muitos casos, a morte por asfixia.

Os cancros anaplásicos da tiroide têm tipicamente um fenótipo altamente imunossupressor e pró-tumorigénico. Este é caracterizado por mutações - BRAF, TP53, RAS, TERT- responsáveis pela agressividade do tumor, e níveis elevados de recrutamento de macrófagos associados a tumores (TAMs), que podem representar mais de 50 % do volume tumoral. Estes mecanismos mediados imunologicamente que facilitam o crescimento rápido do tumor representam oportunidades atrativas para novos tratamentos, particularmente combinações de imunoterapias direcionadas a células T e macrófagos.

O conceito de memória imunitária inata, também conhecida como imunidade treinada, tem ganho recentemente uma atenção significativa para o estudo do sistema imunitário inato. Este conceito é caracterizado pela capacidade do sistema imunitário inato de responder de forma mais eficaz a um patógeno ou estímulo após um encontro anterior com diferentes patógenos ou estímulos. Esta resposta imune é caracterizada por alterações epigenéticas persistentes nas células imunes, acompanhadas de uma maior produção de citocinas pró-inflamatórias.

Ao contrário da imunidade adaptativa, que é mediada por linfócitos B e T e requer exposição prévia ao antígeno específico, a imunidade treinada é uma resposta imune inata, que envolve principalmente células como macrófagos e células natural killer (NK). Esta resposta imune pode ser regulada pelo uso de nanomateriais fabricados para inibir ou induzir imunidade treinada, dependendo do contexto da doença.

Tem sido demonstrado que a indução da imunidade treinada pode ajudar a superar a imunossupressão característica do microambiente tumoral e pode ser benéfica no contexto do cancro. Com base nesse facto, propusemos a imunidade treinada como alvo terapêutico para superar o ambiente imunossupressor característico do cancro anaplásico da tiroide.

O presente projeto teve como principais objetivos i) a otimização de condições indutoras de imunidade treinada em macrófagos derivados da medula óssea (BMDMs) de murganhos; ii) avaliar como estes BMDMs treinados reagiriam num contexto tumoral; iii) estabelecer o efeito de um tumor nas células imunes inatas e nos seus progenitores. Depois de concretizados estes primeiros objetivos, o projeto obtém linhas bases de conhecimento para avançar para o fabrico de nanomateriais direcionados à medula óssea. Estes terão como finalidade induzir imunidade treinada em macrófagos e será possível o seu teste em modelos animais de murganhos com cancro anaplásico da tiroide.

Metodologicamente, foram feitos variados ensaios de imunidade treinada focados em estímulos primários comumente utilizados, como o β-glucano, a vacina bacilo Calmette-Guérin (BCG) e o dipeptídio muramil (MDP), e estímulos secundários bacterianos como o lipopolissacarídeo (LPS). Para avaliar a resposta das células treinadas a fatores tumorais, ensaios de imunidade treinada foram realizados usando como estímulo secundário meio de cultura tumoral. Este meio de cultura contém fatores libertados por células de melanoma B16F10 (linha celular de melanoma de murganhos C57BL/6J).

Para verificar a indução de imunidade treinada nestes BMDMs depois dos diferentes estímulos, sobrenadantes foram recolhidos e realizamos medições da produção de citocinas pró-inflamatórias (TNF e IL-6), através de ELISA. Detetamos a indução da imunidade treinada em BMDMs treinados com BCG depois de reestimulados com LPS. Observamos também que fatores libertados pelas células tumorais podem ter um efeito comparável aos estímulos bacterianos. Portanto, BMDMs treinadas com BCG conseguem reagir num ambiente tumoral de uma forma pró-inflamatória, superando a imunossupressão do microambiente tumoral.

Em experiências complementares foram avaliados outros estímulos usados comumente em monócitos, como Heat Killed *Candida Albicans* e Pam-3-cys. Foi-nos possível avaliar a incapacidade de usar Pam-3-cys devido à sua agressividade e capacidade de induzir alta inflamação neste tipo de macrófagos. Para além disso, testes usando imagem por ressonância magnética (MRI) foram realizados de maneira a avaliar a capacidade de visualizar e medir a tiroide e possíveis tumores nestes murganhos. Estes testes são fundamentais para verificar a viabilidade dos próximos passos do projeto.

Com o intuito de perceber o efeito de um tumor no sistema imunitário inato, um modelo de melanoma em murganhos foi usado. Devido a limitações de tempo características do projeto

não foi possível estabelecer um modelo de cancro anaplásico da tiroide, portanto um modelo de melanoma já estabelecido foi usado.

Metodologicamente, células de melanoma foram inoculadas em murganhos por uma ou duas semanas antes do momento de eutanásia. Analisamos o estado de treino em esplenócitos e macrófagos derivados da medula óssea de murganhos portadores de tumor. Para isso estas células foram estimuladas com LPS e medimos a produção de citocinas pró-inflamatórias através de ELISA. Ao mesmo tempo, analisamos as populações de células imunitárias utilizando citometria de fluxo e focando-nos em populações de células mieloides, linfoides e progenitores.

Em resumo, este estudo fornece novos conhecimentos fundamentais sobre como atingir a medula óssea e induzir a imunidade treinada como um novo paradigma de tratamento para o cancro anaplásico da tiroide. Estes resultados contribuem para um crescente corpo de conhecimento destinado a superar os desafios apresentados pelo microambiente imunossupressor desta forma agressiva de cancro. Para além disso, estabelecemos uma linha base de conhecimento acerca do efeito de um tumor no sistema imunitário inato, que será utilizado para avaliar a eficácia de possíveis nanomateriais usados para terapia deste cancro anaplásico da tiroide.

Ao aproveitar o potencial da imunidade treinada e explorar abordagens inovadoras de imunoterapia, pretendemos melhorar os resultados do tratamento e, em última análise, aprimorar a qualidade de vida das pessoas que lutam contra o cancro anaplásico da tiroide.

**Palavras-chave:** Cancro anaplásico da tiroide, macrófagos derivados da medula óssea, sistema imunitário, BCG, e imunidade treinada.

## TABLE OF CONTENTS

## INDEX OF FIGURES

## INDEX OF TABLES

## INDEX OF ANNEXES

# ABBREVIATIONS

**Ab** Antibodies

**ABCA1** ATP-binding cassette transporter A1

**ABCG1** ATP-binding cassette transporter G1

**AKT1** Protein kinase B alfa

**APC** Antigen-presenting cells

**APO-A1** Apolipoprotein A-1

**ATC** Anaplastic Thyroid Carcinoma

**ATP** Adenosine triphosphate

**BCG** Bacille Calmette-Guerin vaccine

**BM** Bone marrow

**BMDMs** Bone-marrow derived macrophages

**CCL1** C-C motif chemokine ligand 1

**CMPs** Common myeloid progenitors

**CTLA-4** Cytotoxic T-lymphocyte antigen 4

**CXCL13** C-X-C motif chemokine ligand 13

**DAMPs** Damage-associated molecular patterns

**DC** Dendritic cell

**DNA** Desoxyribonucleic acid

**DNMTi** DNA methyltransferase inhibitor

**EMT** Epithelial-to-mesenchymal transition

**EPR** Enhanced permeability and retention

**FDA** Food and Drug Administration

**GEMMs** Genetically engineered mouse models

**GITR** Glucocorticoid-induced tumor necrosis factor family receptor

**GM-CSF** Granulocyte-macrophage colony-stimulating factor

**GMPs** Granulocyte-macrophage progenitors

**HATi** Histone acetyltransferase inhibitor

**HDACi** Histone deacetylase inhibitor

**HDL** High-density lipoprotein

**HDMi** Histone demethylase inhibitor

**HMTi** Histone methyltransferase inhibitor

**HSCs** Hematopoietic stem cells

**HSPCs** hematopoietic stem and progenitor cells

**ICIs** Immune Checkpoint Inhibitors

**IDO** Indoleamine 2,3-dioxygenase

**IFN** Interferon

**IFNR** Interferon receptor

**IL** Interleukin

**IL-1β** Interleukin-1β

**IL-6** Interleukin-6

**IL-10** Interleukin-10

**IL-12** Interleukin-12

**LT-HSC** Long-term hematopoietic stem cells

**lncRNA** Long coding RNA

**LPS** Lipopolysaccharides

**MAPK** Mitogen-activated protein kinase

**MDSCs** Myeloid-derived suppressor cells

**MDP** Muramyl dipeptide

**MHC** Major histocompatibility complex

**MMP** Matrix metalloprotease

**MPP** Multipotent progenitors

**MPP2** Megakaryocyte/erythroid-biased MPPs

**MPP3** Myeloid lineage-biased MPPs

**MPP4** Lymphoid lineage biased MPPs

**miRNAs** MicroRNAs

**mRNA** Messenger RNA

**mTOR** Mammalian target of rapamycin

**MyPs** Myeloid progenitors

**NF-kB** Nuclear factor kappa-light-chain-enhancer of activated B cells

**NK** Natural killer cells

**NOD2** Domain-containing protein 2

**PAMP** Pathogen-associated molecular pattern

**PD-L1** Programmed death-ligand 1

**PD-1** Programmed cell death-1

**PIK3CA** Phosphatidylinositol-4,5-bisphosphate 3-kinase catalytic subunit alpha

**PRRs** Pattern recognition receptors

**PTEN** Phosphatase and tensin homolog

**RAI** Radioactive iodine

**RAIR** Radioiodine-Refractory

**ROS** Reactive oxygen species

**siRNA** Small interfering RNA

**SR-BI** scavenger receptor class B type I

**ST-HSC** Short-term hematopoietic stem cells

**STING** Stimulator of interferon genes

**TAMCs** Tumor-associated mast cells

**TAMs** Tumor-associated macrophages

**TC** Thyroid cancer

**TCR** T-cell receptor

**TERT** Telomerase reverse transcriptase

**TGF** Tumor growth factor

**TGF-β** tumor growth factor-β

**TLR** Tool-like receptors

**TME** Tumor microenvironment

**TNF** Tumor necrosis factor

**VEGF** Vascular endothelial growth factor

**WHO** World Health Organization

**β-glucan** beta-1,3-glucan

# CHAPTER 1

# Introduction

# 1.1- Cancer

## 1.1.1-Epidemiology

According to estimates from the World Health Organization (WHO) in 2019 [1], cancer is still the leading cause of death in 112 countries around the world.[2] Globally, the incidence and mortality of cancer are increasing quickly. Aging and the growth of the population are seen as the main contributors to these increases.[3]

In 2020, 19.3 million new cases of cancer were diagnosed and almost 10 million cancer deaths occurred.[2] Breast cancer has the highest occurrence with 2.3 million new cases (11.7%), followed by lung (11.4%), colorectal (10.0%), prostate (7.3%), and stomach (5.6%). However, lung cancer remained the leading cause of death (18%), followed by colorectal (9.4%), liver (8.3%), stomach (7.7%), and female breast cancer (6.9%).[2]

The top 10 cancer types are represented in **Figure 1.1**, and for both sexes combined they account for >60% of the newly diagnosed cancer cases and >70% of cancer deaths.[2]

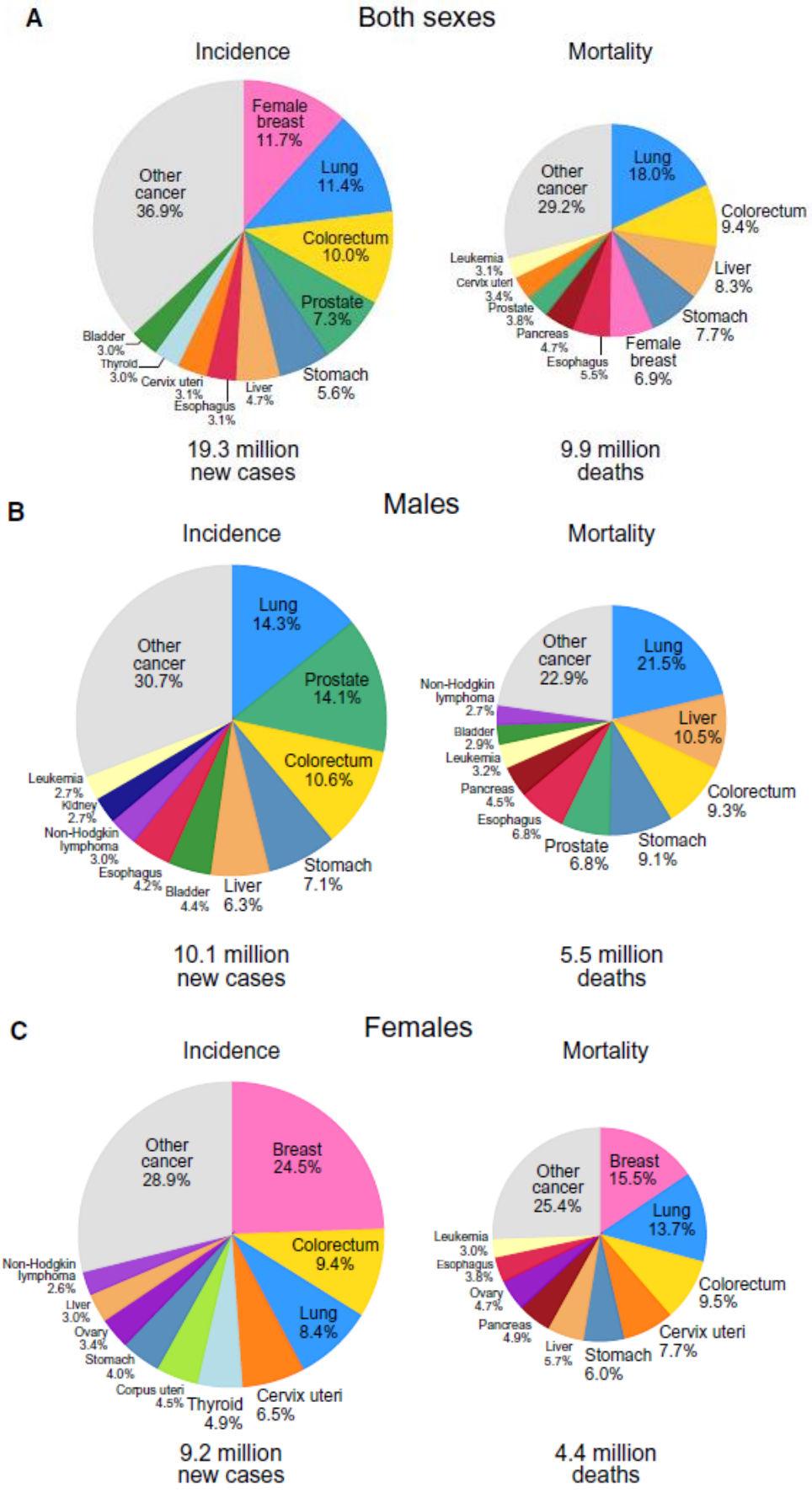
A
Both sexes
Incidence
Mortality
Female breast 11.7%
Lung 11.4%
Colorectum 10.0%
Prostate 7.3%
Stomach 5.6%
Liver 4.7%
Esophagus 3.1%
Cervix uteri 3.1%
Thyroid 3.0%
Bladder 3.0%
Other cancer 36.9%
19.3 million new cases
Lung 18.0%
Colorectum 9.4%
Liver 8.3%
Stomach 7.7%
Female breast 6.9%
Esophagus 5.5%
Pancreas 4.7%
Prostate 3.8%
Cervix uteri 3.4%
Leukemia 3.1%
Other cancer 29.2%
9.9 million deaths
B
Males
Incidence
Mortality
Lung 14.3%
Prostate 14.1%
Colorectum 10.6%
Stomach 7.1%
Liver 6.3%
Bladder 4.4%
Esophagus 4.2%
Non-Hodgkin lymphoma 3.0%
Kidney 2.7%
Leukemia 2.7%
Other cancer 30.7%
10.1 million new cases
Lung 21.5%
Liver 10.5%
Colorectum 9.3%
Stomach 9.1%
Prostate 6.8%
Esophagus 6.8%
Pancreas 4.5%
Leukemia 3.2%
Bladder 2.9%
Non-Hodgkin lymphoma 2.7%
Other cancer 22.9%
5.5 million deaths
C
Females
Incidence
Mortality
Breast 24.5%
Colorectum 9.4%
Lung 8.4%
Cervix uteri 6.5%
Thyroid 4.9%
Corpus uteri 4.5%
Stomach 4.0%
Ovary 3.4%
Liver 3.0%
Non-Hodgkin lymphoma 2.6%
Other cancer 28.9%
9.2 million new cases
Breast 15.5%
Lung 13.7%
Colorectum 9.5%
Cervix uteri 7.7%
Stomach 6.0%
Liver 5.7%
Pancreas 4.9%
Ovary 4.7%
Esophagus 3.8%
Leukemia 3.0%
Other cancer 25.4%
4.4 million deaths

**Figure 1.1**. **Distribution of Cases and Deaths for the Top 10 Most Common Cancers in 2020** for (A) Both Sexes, (B) Men, and (C) Women. For each sex, the area of the pie chart reflects the proportion of the total number of cases or deaths. From GLOBOCAN 2020.

## 1.1.2-Cancer as a multistep process

Cancer is a complex and multifaceted disease characterized by the uncontrolled growth and spread of abnormal cells in the body. It arises when healthy cells undergo genetic mutations that disrupt their ability to regulate cell division and growth.[4] These mutated cells, known as cancer cells, can form a mass of tissue called a tumor and have the potential to invade nearby tissues and even spread to distant parts of the body through a process called metastasis.[4]

Mutations, which are alterations in the DNA sequence of genes, play a crucial role in the development of cancer.[5] Mutations can occur spontaneously or be caused by various external factors, such as exposure to certain chemicals, radiation, or viruses. Additionally, some individuals inherit genetic mutations from their parents that increase their susceptibility to developing certain types of cancer.[5]

The DNA within our cells contains genes that act as instructions for the cell's normal growth, division, and death. When a mutation occurs in a gene involved in regulating these factors, it can disrupt this delicate balance. Mutations can affect different types of genes in various ways.[4,5]

Genes that - when affected by mutations - play a key role in tumorigenesis are generally distinguished into three classes: oncogenes, tumor suppressor genes, and DNA repair genes.[6]

Normally, oncogenes help regulate cell division and growth. However, when these genes acquire specific mutations, they become overactive, leading to uncontrolled cell growth and tumor formation. Tumor suppressor genes normally prevent the development of cancer by inhibiting cell division or promoting cell death. Mutations in these genes can disable their normal functions, allowing abnormal cells to grow and divide unchecked. DNA repair genes are responsible for fixing errors that occur during DNA replication. When mutated, they lose their ability to correct DNA damage, leading to an accumulation of further mutations in other genes and an increased risk of cancer.[6]

The process of tumorigenesis involves a series of steps. Initially, mutations in specific genes disrupt the normal controls over cell growth, enabling the affected cells to multiply rapidly. As the tumor grows, additional mutations occur, conferring advantages such as the ability to

promote blood vessel formation (angiogenesis) to sustain the growing mass or evade the immune system's surveillance.[7]

While the process of tumorigenesis is complex and variable, Douglas Hanahan and Robert Weinberg have tried to define the progression into cancerous cells by proposing the cellular Hallmarks of Cancer: self-sufficiency in growth signals; insensitivity to anti-growth signals; tissue invasion and metastasis; limitless replicative potential; sustained angiogenesis and evading apoptosis (**Figure 1.2**).[8]

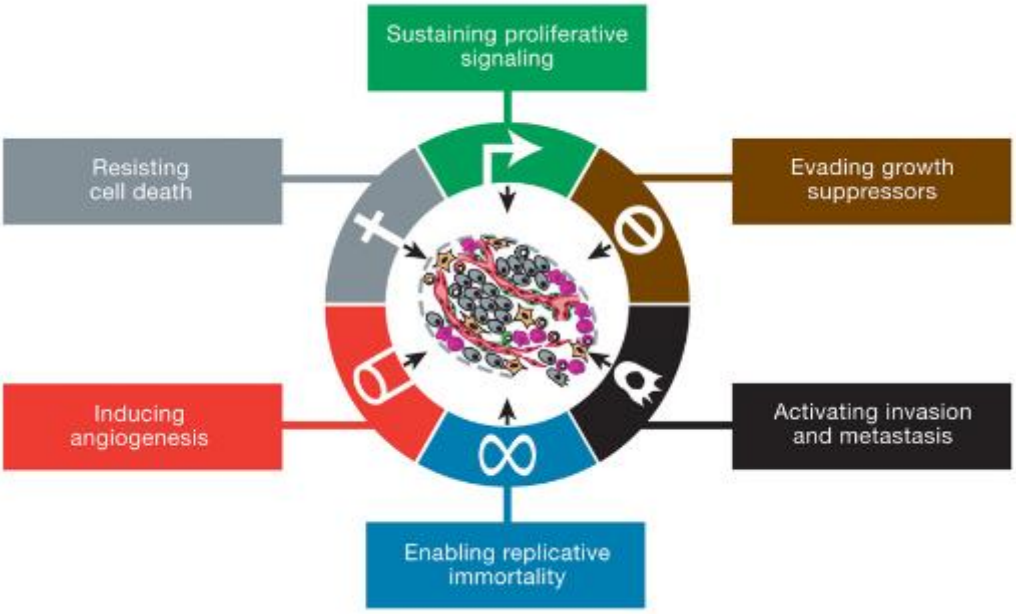


**Figure 1.2**. **The Hallmarks of Cancer.** From Hanahan et al, 2011.

However, five of these hallmarks are also present in benign tumors.[9] Therefore, a decade later, they revisited them to describe malignant tumors more accurately, suggesting two additional traits: genome instability and mutation and tumor-promoting inflammation. In addition, the dysregulation of cellular energetics and the avoidance of immunological destruction were proposed as two new hallmarks (**Figure 1.3**).[10,11]

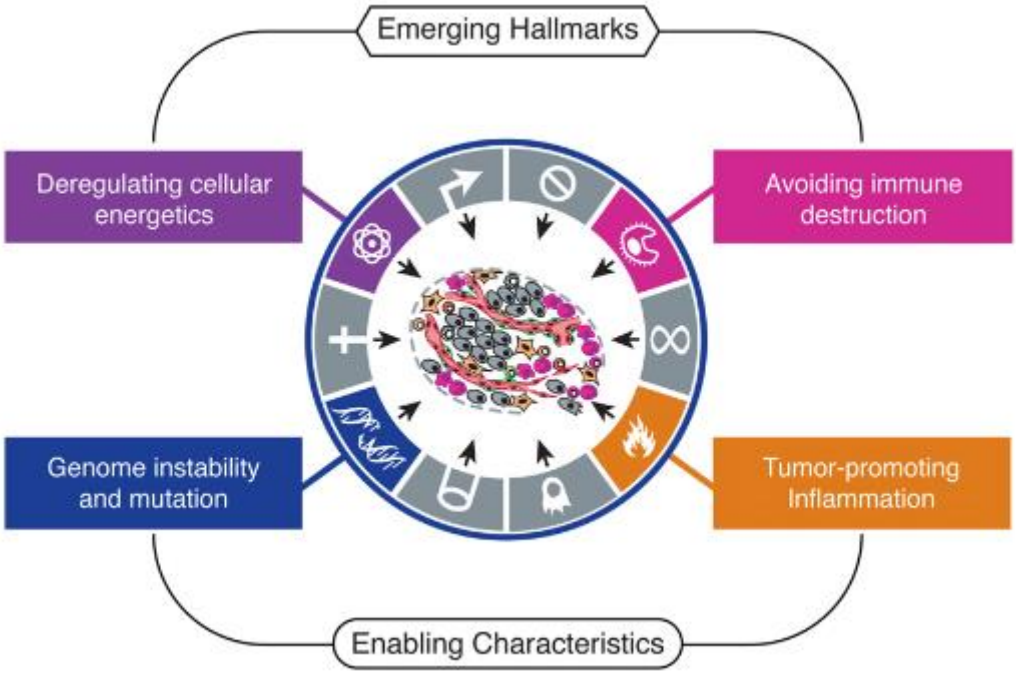


**Figure 1.3**. **Emerging Hallmarks and Enabling Characteristics.** From Hanahan et al, 2011.

### 1.1.3- Immune System and Tumorigenesis

The immune system is a highly complex and sophisticated defense mechanism that protects the body from harmful pathogens, such as bacteria, viruses, fungi, and parasites. It is composed of a network of cells, tissues, and organs working together to identify, target, and eliminate these foreign invaders, while also maintaining tolerance to the body's healthy cells and tissues.[12]

The immune system is constituted of two distinct components that work together to provide a comprehensive defense against pathogens: innate and adaptive immunity.

Innate Immunity is the first line of defense in the immune system that provides immediate, nonspecific protection. It does not require prior exposure to the specific pathogen or antigen, and its main role is to detect and eliminate pathogens quickly to prevent their spread. Innate immune cells detect and recognize pathogens through pattern recognition receptors (PRRs). PRRs recognize conserved structures called pathogen-associated molecular patterns (PAMPs) present in pathogens or damage-associated molecular patterns (DAMPs) released during cellular damage.[12]

On the other hand, adaptive immunity is a highly specialized and complex component of the immune system that provides targeted and specific defense against pathogens. It is characterized by its ability to recognize and respond to specific antigens, which are unique

molecules found on the surface of pathogens. This recognition happens through two primary cell types: B cells and T cells. These cells possess' antigens-specific receptors that recognize the antigens starting an immune response.[12]

After encountering a pathogen, cells and inflammatory substances move from infection sites to nearby lymph nodes. In these lymph nodes, antigens that don't belong to the host on the surface of antigen-presenting cells (APCs) are identified by receptors on host B and T lymphocytes. Adaptive immunity is comprised of both humoral and cellular elements.[13,14]

Humoral immunity describes B-cell response while cellular immunity describes T-cell response.

When a non-host antigen attaches to the antigen receptor on a B cell, it triggers a series of molecular signals that initiate B-cell activation. Once activated, B cells undergo differentiation, leading them to develop into either plasma or memory B cells.[12,13] Plasma cells are responsible for producing and releasing antibodies that specifically bind to the pathogen. On the other hand, memory B cells remain in a dormant state until they encounter the same antigen during a subsequent exposure and respond to it.[13]

On the other side, T cells when activated will differentiate into cells with cytotoxic, helper, or regulatory behavior. These cells undergo maturation before activation, this process occurs in the thymus and there they develop their T-cell receptor (TCR). T cell activation requires three signals: TCR binding to the antigen-major histocompatibility complex (MHC); co-stimulatory signals provided by the interaction between molecules on the APC and T cell surfaces; cytokines secreted by the APC that further influence T cell differentiation and function.[14,15]

Each one of the different behaviors that T cells may acquire has separate actions on immune defense. Helper T (Th) cells display the CD4 molecule on their surface. These cells assist other immune cells by releasing cytokines and providing help for B cell activation and enhancing function. Cytotoxic T cells (Tc) bear the CD8 molecule on their surface. Functioning as effector cells, they eliminate tissues that harbor intracellular pathogens. Regulatory T cells (Treg) help regulate the immune response by suppressing the other two subsets of T cells.[13,14]

This way of action also applies when it comes to cancer. When cancer develops, it often displays tumor antigens that can be recognized as foreign or abnormal by immune cells, such as T cells and natural killer (NK) cells, which are specialized components of the immune system. The

immune system's ability to recognize and eliminate cancer cells is known as immune surveillance.[16]

However, tumor cells have evolved various strategies to evade and suppress immune responses, allowing them to grow and spread. The mechanisms employed by cancer cells to escape immune surveillance include the downregulation of tumor antigens, inhibition of immune cell function, and the creation of an immunosuppressive environment by secreting immune inhibitory factors and recruiting immunosuppressive immune cells.[16]

One of the primary processes through which this recruitment occurs is known as chemotaxis. Here the cells are attracted to the tumor site by specific chemical signals released by the tumor cells themselves or the surrounding tissues. These signals, called chemokines, act as beacons, guiding the cells toward the tumor. Additionally, tumor cells can secrete growth factors and cytokines that stimulate the proliferation and migration of specific cell types (**Figure 1.4**).[17]

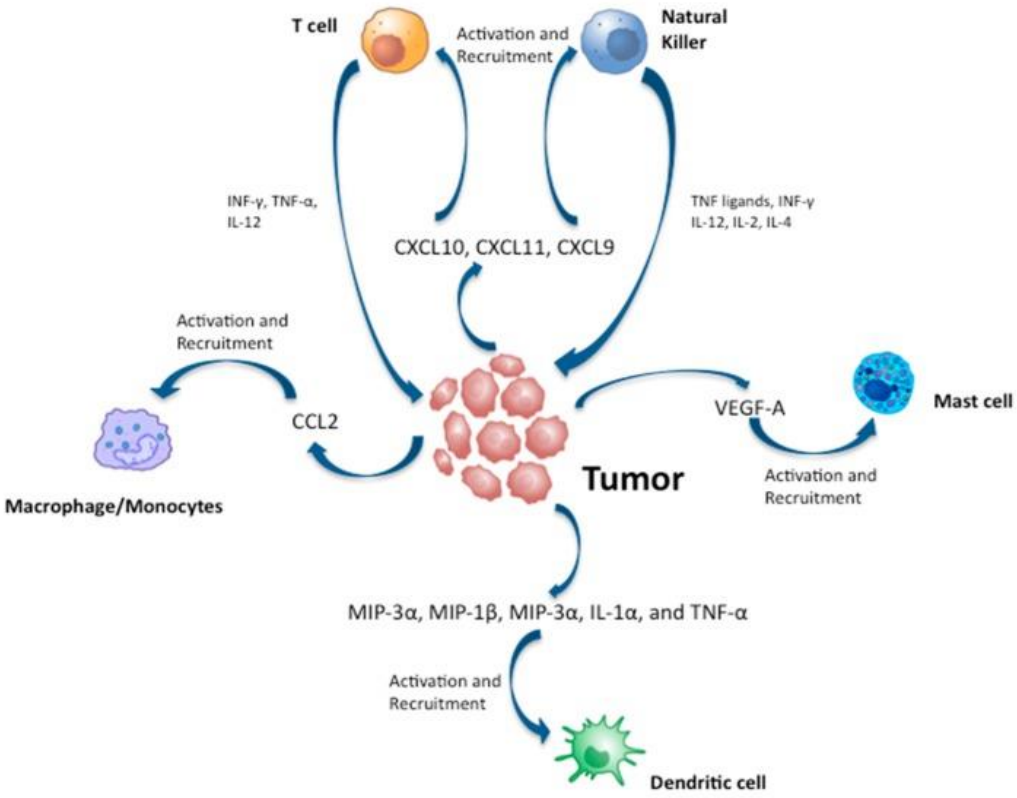


**Figure 1.4**. **Cytokines and chemokines released in thyroid cancer microenvironment and their role in recruiting inflammatory cells**. From Ferrari et al, 2019.

Myeloid-derived suppressor cells (MDSCs) are immune cells that originate from the bone marrow and can suppress immune responses, thereby promoting tumor growth and progression.

These cells exert their suppressive effects by inhibiting the activation and function of immune cells, such as T cells and NK cells.[18]

Tumor-associated macrophages (TAMs) are another type of immunosuppressive cells that infiltrate tumors and can exhibit diverse functions depending on the specific conditions within the tumor. These cells - when presenting an M2-like phenotype - can promote tumor growth and metastasis by providing growth factors and supporting the formation of new blood vessels (angiogenesis).[19]

Tumor-associated mast cells (TAMCs) are a very specific type of granulocytes found within the tumor microenvironment. Mast cells can release various factors that influence tumor progression, including angiogenesis, and tissue remodeling. However, their precise impact on cancer development is still an area of active research.[17,20]

Collectively, these cells work in favor of tumor growth and progression after recruitment, aiding in cancer's evasion of immune surveillance **(Figure 1.5)**.[17] Understanding their roles and functions is crucial for devising effective therapeutic strategies against cancer.

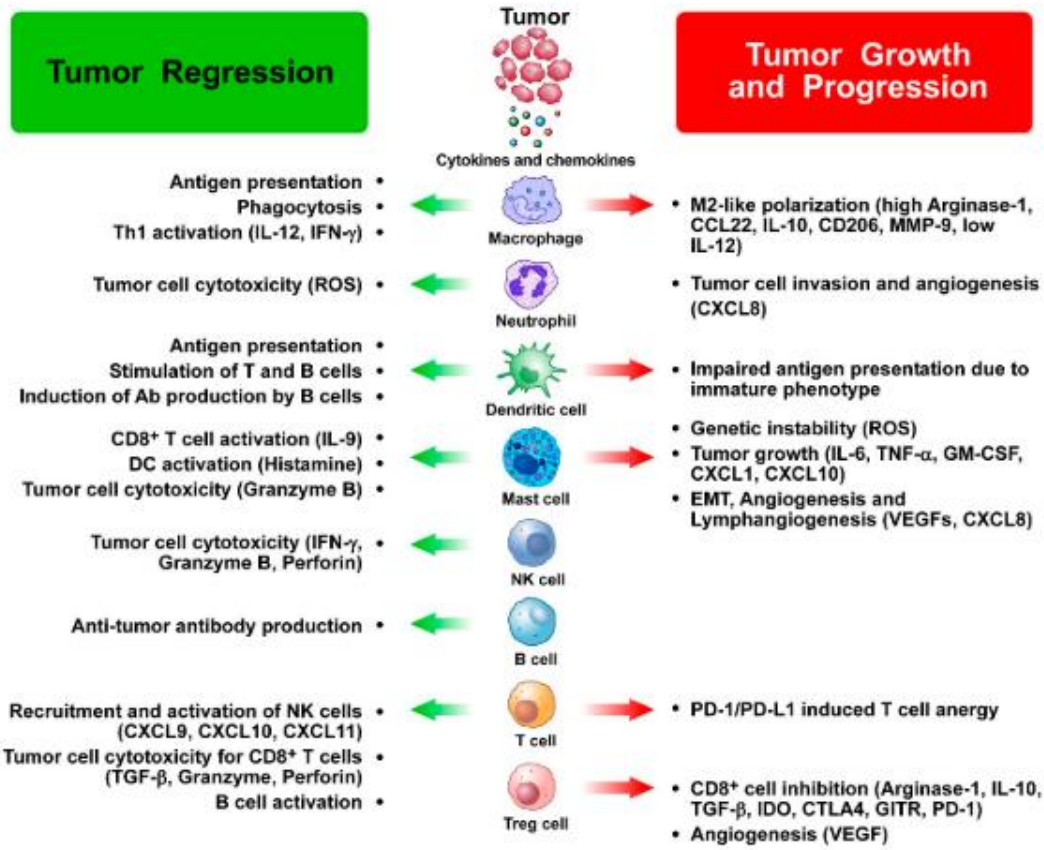


**Figure 1.5**. **Dual role of immune cells in thyroid cancer growth and progression.** Tumor-infiltrating immune cells can exert both antitumor and protumor functions in thyroid cancer and

interact with each other as well as with cancer cells. Several soluble factors (cytokines, chemokines, angiogenic, and lymphangiogenic factors) released by immune cells mediate the protumor as well as the antitumor effects of immune cells in thyroid cancer. List of abbreviations: Ab: antibodies; CTLA-4: Cytotoxic T-lymphocyte antigen 4; DC: dendritic cell; EMT: epithelial-to-mesenchymal transition; GITR: glucocorticoid-induced tumor necrosis factor family receptor; IDO: indoleamine 2,3-dioxygenase; IFN: interferon; IL: interleukin; MMP: matrix metalloprotease; NK: natural killer; PD-1: programmed cell death-1; PDL-1: programmed death-ligand 1; ROS: reactive oxygen species; TGF: tumor growth factor; TNF: tumor necrosis factor; VEGF: vascular endothelial growth factor. From Ferrari et al, 2019.

## 1.2- Thyroid Cancer

As mentioned before, cancer has the ability to withstand attacks from the immune system, which is an important characteristic of its development.[9] Thyroid cancer (TC) is an illustrative case of where this escape occurs.

TC is the 5$^{th}$ most diagnosed cancer in females (**Figure 1.6**) and is the most common endocrine cancer. Although an increase in cases in the last three decades has been observed, mortality rates have remained stable.[21]

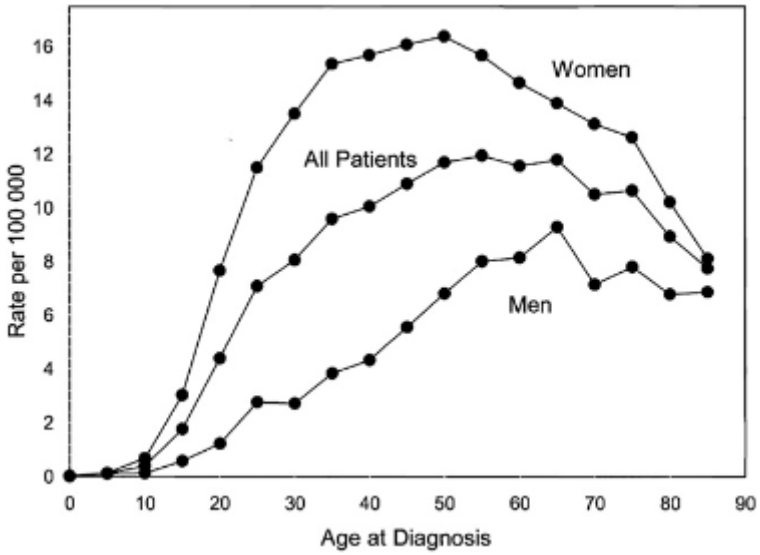


**Figure 1.6**. **Age at the time of diagnosis of thyroid cancer in men and women from 1975 to 2006.** The incidence rate per 100 000 is about 3-fold higher in women compared with men, and peak incidence occurs nearly 20 years earlier in women than men. From Sipo et al, 2010.

TC is generally divided into two categories, namely follicular-derived thyroid cancer (differentiated thyroid cancer and anaplastic thyroid cancer) and neuroendocrine C-cell-derived thyroid cancer (medullary thyroid cancer).[22]

Only 1-2% of thyroid malignancies are medullary thyroid cancer, which originates from the thyroid's parafollicular neuroendocrine cells and typically metastasizes to cervical lymph nodes.[22]

In follicular-derived TC, we can identify two different types: differentiated TC and anaplastic thyroid cancer.[23]

More than 95% of TC cases are differentiated thyroid carcinoma, which develops from thyroid follicular epithelial cells. Papillary thyroid cancer, follicular thyroid cancer, and Hurthle cell thyroid cancer all fall under the heading of well-differentiated thyroid cancers which are less aggressive than poorly differentiated thyroid carcinoma.[23]

Anaplastic thyroid cancer (ATC) is the rarest (<1%) but also the most aggressive form. The tumor is characterized by a heavy accelerated development pattern that results in a large neck mass.[23] Therefore, the death of ATC patients is often caused by tracheal and esophageal obstruction, leading to asphyxiation.[24] The median survival is 3-6 months, accounting for 50% of TC-related mortalities.[25]

It frequently develops from differentiated thyroid cancer, but it can also occur de novo. It typically contains distant metastases in the lungs, bones, and brain. ATC presents a high mutation burden, which includes mutations in TP53, telomerase reverse transcriptase (TERT) promoter, PI3K/AKT/mTOR pathways effectors, RAS, and BRAF.[26]

TP53 is a tumor suppressor gene that regulates cell cycle arrest, DNA repair, and apoptosis. Mutations in TP53 are commonly found in ATC and are associated with the loss of its tumor suppressor function. TP53 mutations lead to the uncontrolled growth and division of cells, attributing to the aggressive behavior of ATC.[26]

The TERT gene encodes an enzyme involved in maintaining the length of telomeres, the protective caps at the end of chromosomes. Mutations in the promoter region of TERT have been found in various cancers, including ATC. These mutations enhance the activity of the TERT gene, leading to increased telomerase activity and allowing cells to replicate indefinitely.[26]

The PI3K/AKT/mTOR pathway is a signaling pathway involved in cell growth, proliferation, and survival. Mutations or amplifications in PIK3CA (phosphatidylinositol-4,5-bisphosphate 3-kinase catalytic subunit alpha) or PTEN (phosphatase and tensin homolog) can activate the pathway, leading to uncontrolled cell growth and survival. Additionally, mutations in AKT1

(protein kinase B alpha) and alterations in mTOR (mammalian target of rapamycin) signaling have also been observed in ATC, further driving tumor progression and resistance to therapy.[26]

The RAS pathway plays a critical role in regulating cell proliferation, survival, and differentiation. In ATC, activating mutations in RAS genes, including HRAS and KRAS, are frequently found. These mutations lead to constitutive activation of the RAS pathway, promoting uncontrolled cell growth and proliferation. RAS mutations are associated with a more aggressive phenotype in ATC.[26]

BRAF is a gene that encodes a protein involved in the RAS-RAF-MEK-ERK signaling pathway. In ATC, a specific mutation known as $BRAF^{V600E}$ is often present.[27] This mutation leads to constitutive activation of the signaling pathway, resulting in increased cell proliferation and survival. BRAF mutations are associated with a more aggressive disease course in ATC.[26]

ATC is distinctively characterized by a high infiltration of the TME by TAMs with an M2-like phenotype.[28,29] This oncogenic polarization of macrophages is associated with the tumor microenvironment. TAMs secrete a variety of chemokines and cytokines such as CCL2 and IL-10 that suppress the immune system and promote angiogenesis, invasion, and metastasis.[30,31]

The standard course of care for TC is surgery, frequently followed by radioactive iodine ($I^{131}$) therapy for remnant ablation. Unfortunately, ATC patients are commonly refractory to radioiodine therapy.[32]

Radioactive iodine refractoriness most frequently develops in the context of loss of thyroid differentiation features. The ability of follicular cells to concentrate iodine is crucial in this therapy. Radioactive iodine enters the cell and emits particles that destroy the follicular cell. However, in a subset of ATCs, the ability to trap the iodine is lost, resulting in therapy resistance.[33]

There are few choices available in these situations, and the prognosis is still poor. Therefore, it is critical to develop novel therapies for these TC patients.

### 1.2.1- Research Approach in Anaplastic Thyroid Cancer

Research in ATC involves a multi-faceted approach. Investigation of gene mutations and signaling pathways, exploration of potential therapeutic targets, and the development of preclinical and clinical models for testing new treatments.

Mouse models are widely used in preclinical research due to their genetic and physiological similarity to humans, making them an excellent tool to study complex biological processes and diseases. One of the major advantages of using mouse models is that they provide a controlled experimental environment, allowing researchers to manipulate variables and observe outcomes with limited variations and high reproducibility. Additionally, mice have a relatively short lifespan, which enables the study of various interventions in a relatively short period of time.[34,35]

There are several thyroid cancer mouse models with genetically engineered mouse models (GEMMs), and xenograft models being the most commonly used. GEMMs involve the introduction of oncogenic mutations in the thyroid follicular cells to develop ATC, while xenografts models involve the implantation of human ATC cell lines into immunocompromised mice.[34,35] However, generating GEMMs can be a time-consuming process, requiring multiple generations of breeding to establish a stable line that expresses the desired genetic alterations. Similarly, establishing xenograft models can be time-consuming as it requires optimizing the implantation technique and monitoring tumor growth over time. Additionally, the development of robust and clinically relevant models often involves iterative experimentation and optimization, which can further extend the timeline for model development.[34,35] Another disadvantage to be considered in xenograft models is the lack of a functional immune system. This can be limited when it comes to the study of a disease where the immune system plays such an important role - as in ATC.

Despite these limitations, mouse models offer an excellent platform to investigate and explore novel therapeutic targets for ATC. Such studies play a crucial role in advancing our understanding of ATC and may lead to the development of innovative strategies for this challenging disease. [34,35]

# 1.3- Mechanisms of the immune system as a cancer therapy target

## 1.3.1- Trained immunity

The immune system is divided into two parts, adaptive immunity, and innate immunity. The innate immune system, in contrast to adaptive immune responses, has historically been thought of as rudimentary and generic, unable to distinguish between different pathogen species or the frequency of contacts. However, a convincing collection of clinical and experimental evidence currently supports a change in how we see innate immune responses. It has recently been shown that the cellular elements of innate immunity, such as monocytes, macrophages, natural killer

(NK) cells, and innate lymphoid cells, can recall a past foreign encounter and, thus, possess immunological memory.[36]

This newfound phenomenon was termed "trained immunity" to highlight the immune system's capacity to adapt and "remember" previous encounters. This trained immunity was initially observed in the early 2000s when some vaccines, such as the Bacillus Calmette-Guérin (BCG) vaccine, were noticed to have broader effects on the immune system beyond their targeted pathogens.[37] Through more intensive studies, in the last years, it was discovered that innate immune cells possess the ability to undergo reprogramming or functional changes upon encountering a pathogen or stimulus. This reprogramming led to an enhanced immune response upon subsequent encounters with different pathogens, even if they were unrelated to the initial exposure.[36]

The establishment of innate memory responses involves two main mechanisms: epigenetic remodeling and the rewiring of intracellular metabolic pathways. Through epigenetic modifications, certain genes involved in immune responses are activated or suppressed, leading to long-lasting changes in the immune system's behavior. Additionally, intracellular metabolic pathways are reprogrammed to sustain a proinflammatory state, resulting in enhanced production of cytokines when subjected to a secondary stimulus.[36]

As already mentioned, innate immune cells possess specialized receptors – PRRs- which recognize PAMPs present on pathogens or DAMPs released during cellular damage. Upon encountering a pathogen, PRRs on innate immune cells bind the PAMPs/DAMPs, triggering a cascade of signaling events that activate the immune response.

Through this mechanism, they can adapt and respond to a wide range of external or internal challenges. As innate immune cells migrate from the bone marrow into the bloodstream and tissues, they continue to adapt to enhance or regulate immune responses.[38] The specific way in which they respond is influenced by factors such as the intensity and duration of the challenges they encounter. This dynamic response of innate immune cells encompasses various processes, including cell differentiation, priming, tolerance, and trained immunity. Each one of these responses has been characterized.[39]

The functional status of innate immune cells before secondary challenges is the main factor that distinguishes between the different responses (**Figure 1.7**). The processes of innate immune cell 'differentiation' involves the transformation of immature cells into their mature counterpart, accompanied by long-term changes in cell function and morphological

characteristics influenced by alterations in the tissue environment or chronic exposure to stimuli. In 'priming', the initial stimulus alters the functional state of the cells, and their immune status does not return to baseline levels before subsequent stimulation or infection. As a result, the effect of a second stimulus on primed cells is often additive or synergistic with the effects of the first challenge.[40]

In contrast, 'trained immunity' differs from priming in that the functional immune status induced by the first stimulus returns to baseline levels after the stimulus is removed, while the epigenetic alterations persist. However, when exposed to similar or different challenges, both gene transcription and cell function are significantly enhanced compared to levels observed during priming. On the other hand, in innate immune 'tolerance', the cell becomes unable to activate gene transcription and perform its functions upon restimulation.[40]

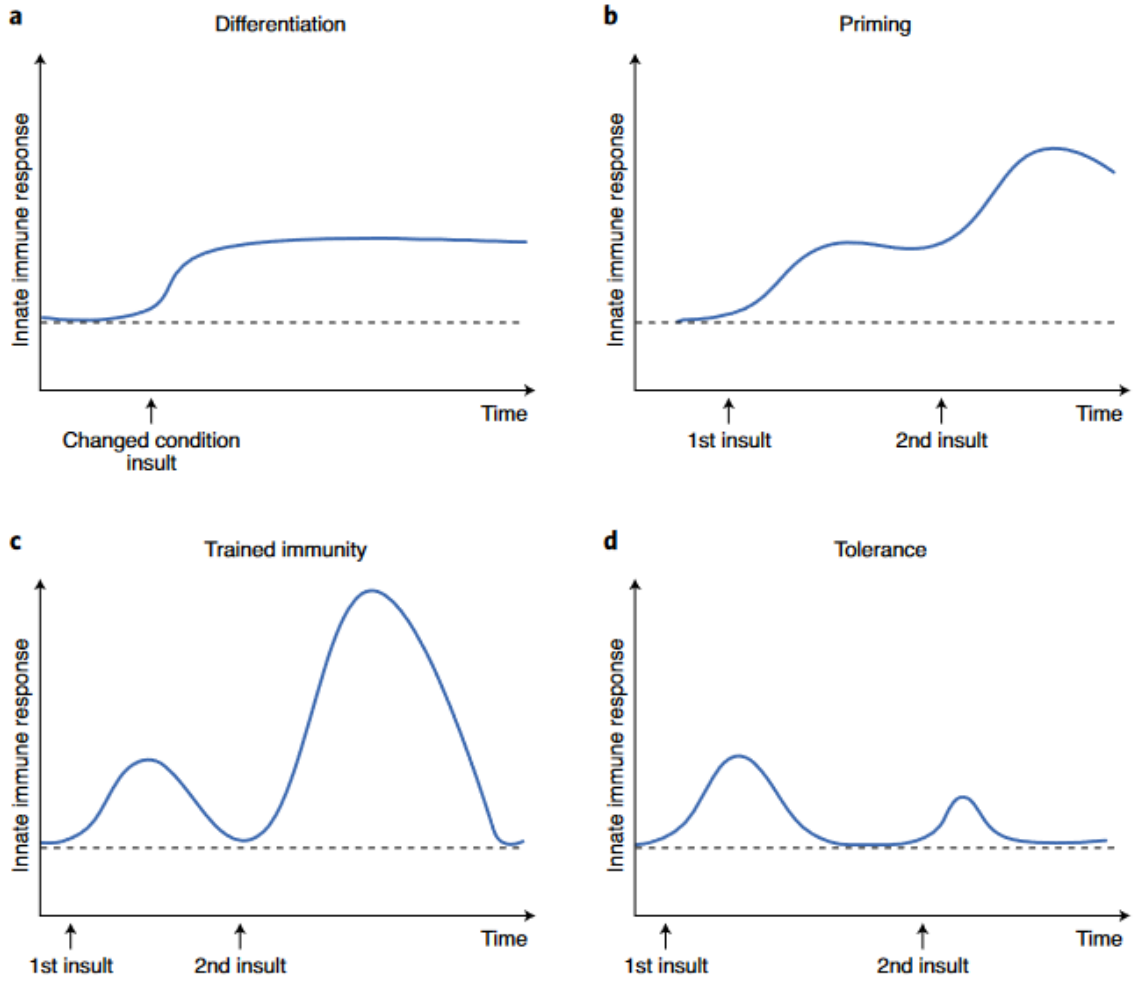


**Figure 1.7. Schematic presentation of the behavior of innate immune responses during the different adaptive programs induced in innate immune cells.** a- Differentiation. b- Priming. c- Trained immunity (innate immune memory). d- Tolerance. From Divangahi et al, 2021

Trained immunity involves complex mechanisms that contribute to the enhanced immune state observed and play a crucial role in host defense against infections.[40] Trained immunity can be induced by exposure to PAMPs derived from bacteria, fungi, or viruses. These PAMPs include components such as lipopolysaccharides (LPS), β-glucans, or viral nucleic acids.[39] Additionally, DAMPs released by stressed or damaged cells can also activate trained immunity pathways. DAMPs include molecules like ATP, uric acid, or high-mobility group box 1 (HMGB1).[40]

Toll-like receptors (TLRs) are a major group of PRRs involved in trained immunity. TLRs such as TLR2, TLR4, and TLR7/8, recognize specific PAMPs and DAMPs, initiating downstream signaling cascades. Upon PAMP or DAMP recognition, downstream signaling pathway cascades, such as NF-kB (nuclear factor kappa-light-chain-enhancer of activated B cells), MAPK (mitogen-activated protein kinase), and PI3K (phosphoinositide 3-kinase) are activated.[39,40]

Activation of these pathways triggers a cascade of events, including the production and release of pro-inflammatory cytokines such as interleukin-6 (IL-6), tumor necrosis factor (TNF), and interferons (IFNs).[39,40]

These cytokines mediate inflammation, recruit other immune cells, and enhance the immune response against pathogens. One of the critical features of trained immunity is the induction of epigenetic alterations in innate immune cells. These alterations involve modifications in histones and DNA methylation, leading to long-term changes in gene expression. Specific genes involved in immune responses, such as cytokines and PRRs, are upregulated, contributing to the heightened immune state.[39,40]

The immunological phenotype of trained immunity has been proven to last at least 3 months and, in some cases, even up to several years. Recent work has shown that trained immunity can occur in hematopoietic stem and progenitor cells (HSPCs) in the bone marrow (central trained immunity), as well as in blood monocytes and tissue macrophages (peripheral trained immunity) (**Figure 1.8**).[39]

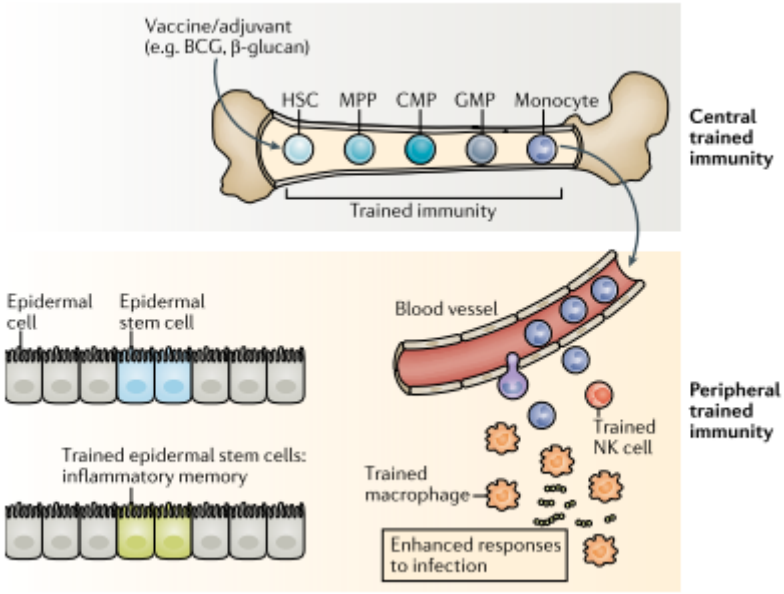


**Figure 1.8. Central and peripheral trained immunity.** From Netea et al, 2020.

Therefore, central, and peripheral factors, or a combination of both, can impact the duration and maintenance of trained immunity.

Monocytes - cells of the mononuclear phagocyte lineage where trained immunity was initially established -have a short lifespan and are unlikely to pass on their memory phenotype to their offspring and give long-lasting protection.[39]

Hematopoietic stem cells (HSCs), in contrast, are long-lived, self-renewing cells found in the bone marrow. HSCs give rise to the whole range of myeloid and lymphoid cell types continuously undergoing asymmetric division in the bone marrow, which is one of the sites of hematopoiesis, myelopoiesis, and lymphopoiesis. HSCs with a trained phenotype can pass on this phenotype to their daughter cells which then move to peripheral organs to exert their immune functions with an increased effector capability against various pathogen types.[39]

The primary defense mechanism against re-infection is immune memory, which plays a critical role in improving survival rates. However, it is important to note that the inadvertent activation of trained immunity can have contrasting effects, leading to either immunodepression or hyperinflammation, depending on whether the induction is heightened or diminished. The specific disease context determines the appropriate utilization of the immune system as a therapy target (**Figure 1.9**). For instance, inducing trained immunity can be beneficial in the treatment of cancer and immune paralysis associated with sepsis.[41] On the other hand, it is

preferable to inhibit an excessively trained innate immune state when managing chronic inflammatory diseases or preventing organ rejection in transplantation cases.[42]

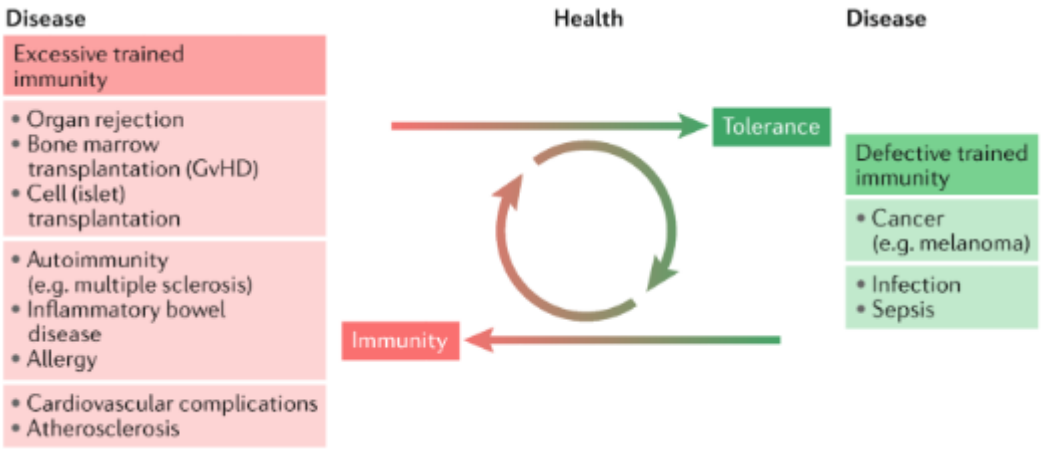


**Figure 1.9. Excessive and defective trained immunity in disease**. Conditions that are characterized by excessive trained immunity, including organ rejection, cardiovascular diseases, and autoimmune diseases, and conditions in which defective trained immunity facilitates disease progression, such as cancer, represent two sides of the 'same immunological coin'. Therefore, regulating trained immunity can be developed into a therapeutic avenue to treat such diseases. Therapeutically engaging trained immunity is compelling as it allows for durable responses, yet these are reversible. GvHD, graft versus host disease. From Mulder et al, 2019.

## 1.3.2- Immunotherapy

The understanding of the immune system enabled us to create several promising immunotherapeutic approaches for cancer. Nowadays, the most used therapies rely principally on cytokines and the cellular stage of adaptive immunity.[37]

The discovery of T cell immune checkpoints and immune checkpoint inhibitors (ICIs) changed clinical cancer care.[43] These checkpoints are proteins on the surface of the immune and cancer cells that act as "breaks" to prevent the immune response from becoming too strong and causing harm.[44] Cancer cells can take advantage of these checkpoints to evade immune surveillance, expressing high levels of these proteins. ICIs target these inhibitory receptors and reinvigorate anti-tumor immune responses.

The most frequently employed specific antibodies are against the proteins cytotoxic T lymphocyte-associated antigen 4 (CTLA4), programmed cell death 1 (PD-1), and its ligand PD-L1, more commonly known as checkpoint inhibition therapy.[45]

Another strategy that has gained popularity is CAR T-cell therapy (Chimeric Antigen Receptor T-cell therapy). It involves genetically modifying the patient's T cells (autologous therapy) or using T cells from a healthy donor (allogeneic therapy) to express a chimeric antigen receptor (CAR) on their surface. This receptor is designed to recognize specific proteins in cancer cells. Once the CAR T cells are infused into the patient, they can specifically target and destroy cancer cells expressing the targeted protein.[46]

Dendritic cell therapy is another emerging immunotherapy that entails exposing tumor-specific antigens to dendritic cells to trigger a tumor-specific T-cell response.[37,43]

However, these types of therapies still encounter several challenges and limitations. The immunosuppressive tumor microenvironment, the lack of targetable antigens, and the tumor heterogeneity are some of the reasons why they are less responsive in some cancer types, such as ATC.[45–47]

Whereas cancer immunotherapies focus on the adaptive immune system, there is mounting evidence that the innate immune system plays a crucial role as well, making it a somewhat unexplored target for cancer immunotherapy.

However, - with today's knowledge – the first immunotherapy was already applied in the 1800s. William B. Coley identified cases of spontaneous cancer regression following infection in the late 19$^{th}$ century, sparking the creation of the first non-infectious disease immunotherapeutic strategy.[37] Coley administered a cocktail of bacteria - that became known as "Coley's toxin" - to a variety of cancer patients many of which he was able to heal.[37,43] However, other options including chemotherapy, radiation, and surgery started to be used in its place because of its unpredictable and dangerous treatment outcomes.[37,43] The mechanisms of Coley's toxin's activity wouldn't become apparent for more than fifty years until we had a better understanding of the major sepsis mediators, such as interleukins, interferons, and chemokines.[48]

Nowadays, there have been remarkable advancements in our understanding of the innate immune system, paving the way for innovative approaches to target its mechanisms. One such breakthrough is the development of nano-immunotherapy, which utilizes nanotechnology to precisely target and manipulate innate immune responses. This exciting development in immunotherapy holds the potential for improving treatment outcomes and personalized medicine.

### 1.3.3- Nano-immunotherapy

Nanomedicine is an emerging field that aims to use the properties and physical characteristics of nanomaterials to diagnose and treat diseases at a molecular level.[49]

Nanomaterials can be engineered to have multiple functions being particularly useful for medical applications. Nanoparticles are used in medicine to enhance drug delivery to the site of disease and/or improve its pharmacokinetic and pharmacodynamic properties.[49,50]

Oral, local, topical, and intravenous administration of some nanoparticles has already received Food and Drug Administration (FDA) approval.[51] The targeting and desired outcome of the treatment determines the administration strategy.

Many nanoparticle-based approaches for cancer treatment make use of intratumoral injections. This strategy aims to minimize potential side effects in other organs while concentrating the therapeutic effects at the tumor location. However, this route of administration still presents a series of disadvantages. First of all, it can only be applied to solid tumors that are accessible and the heterogeneity of tumors makes the nanoparticle delivery uneven throughout the tumor while neglecting potential metastatic lesions. At the same time, leakage of the drugs out of the tumor can still lead to – severe – adverse effects.[49]

For intravenous use of nanoparticles, there are two delivery strategies, namely passive and active targeting.[52]

Passive targeting makes use of the enhanced permeability and retention (EPR) effect that occurs in solid tumor vasculature.[52,53] Tumor vessels show high permeability to macromolecular compounds that get trapped inside the tumor tissue for a long period. The fact that tumors have a poor lymphatic system helps with this accumulation. This buildup further enhances the retention of drugs or drug carriers within the tumor. Once trapped, the drug can be released, leading to localized and targeted therapy while minimizing systemic side effects.[50,53] However, usually these particles suffer from a lack of cell specificity and off-target effects, accumulating in healthy tissues like the liver.

On the other hand, active targeting exploits the heterogeneity between target and non-target cells and organs, such as the expression levels of certain cellular receptors. Through the incorporation of an antibody directed against a receptor that is exclusively or highly expressed on the target cell, the nanoparticle can be routed toward target cells and organs.[43,44,45]

A relatively new way of using nanoparticles to target the immune system is the use of high-density lipoprotein (HDL)-like nanoparticles, coined nanobiologics.[54] HDL is a type of lipoprotein and consists of a combination of proteins and lipids. HDL transports cholesterol and other lipids through the bloodstream and plays a crucial role in the reverse cholesterol transport process. It picks up excess cholesterol from the peripheral tissues, including artery walls, and transports it back to the liver for excretion or recycling. This process helps to prevent the buildup of cholesterol in the arteries and reduces the risk of heart disease.[54]

Apolipoprotein A1 (Apo-A1), is the primary protein component of HDL particles. It plays a crucial role in the structure and function of HDL by binding lipids for their transportation through the body.

This new nanoparticle platform leverages the inherent properties of Apo-A1 to deliver therapeutic agents to specific cells and tissues. Effectively modulating the innate immune response.[55]

Apo-A1 interacts with various cell surface receptors, such as ATP-binding cassette transporter A1 (ABCA1), scavenger receptor class B type I (SR-BI), and ATP-binding cassette transporter G1 (ABCG1).[54] These receptors are highly expressed by myeloid cells - including monocytes and macrophages - and HSPCs residing in the bone marrow.[54] By using this innate avidity, therapeutic agents can be selectively delivered to the desired immune cells, enhancing treatment efficacy, and minimizing off-target effects.[56]

The use of only natural components is another major advantage of this platform, minimizing potential toxicity and unwanted side effects. The biocompatibility allows prolonged circulation time, facilitating sustained and controlled release of therapeutic agents.[55]

Although most of the nanoparticles that have been developed engage the adaptive immune system, engaging the innate immune system – and specifically trained immunity – through ApoA1-based nanoparticles can be a compelling therapeutic strategy (**Figure 1.10**).[54]

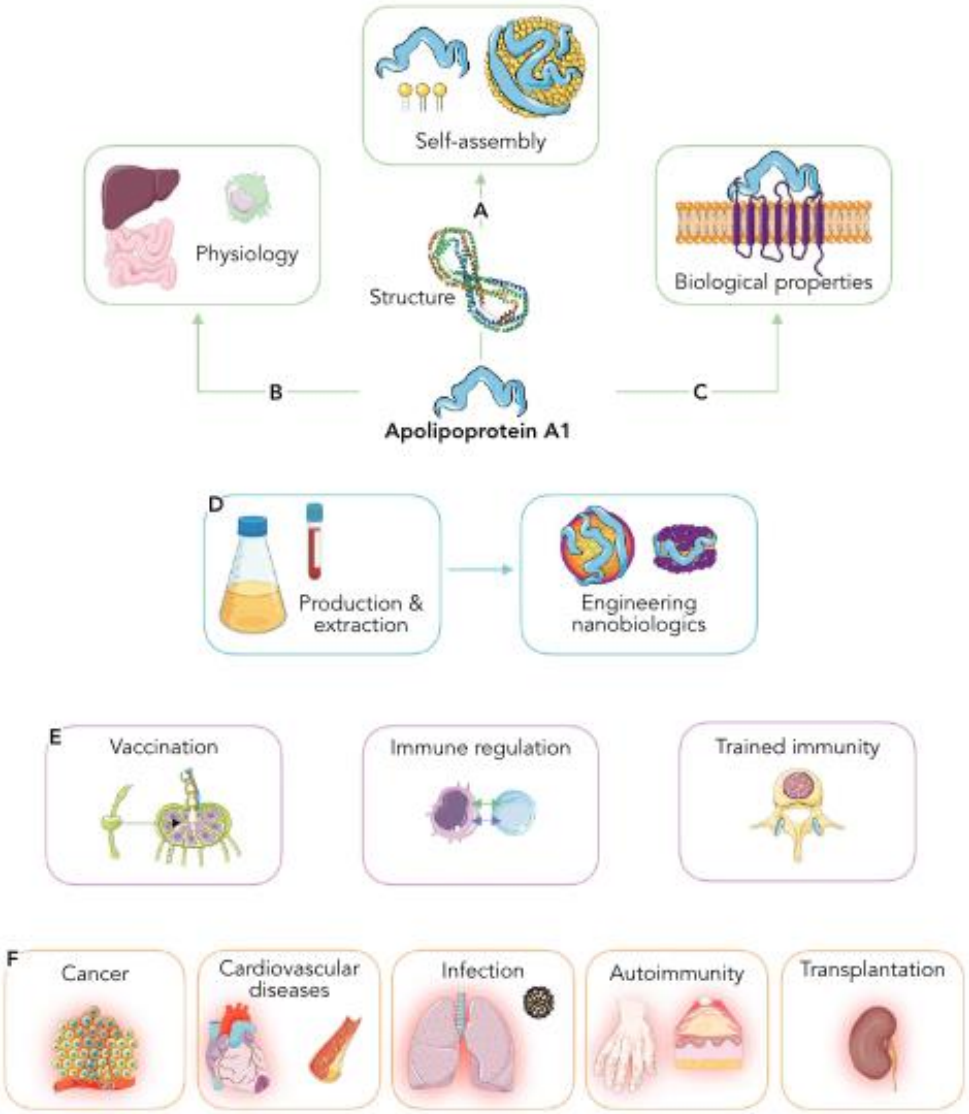


**Figure 1.10. Overview of the chemical, physiological, and biological properties of apolipoprotein A1 (apoA1), and its function as an engineerable therapeutic platform to treat diseases.** A–C) Properties and function of apoA1. D) Production and engineering of A1-nanomaterials. E) A1-nanotherapeutics as a platform for immunotherapy. F) Treating diseases using A1-nanotherapeutics**.** From Schrijver et al, 2021

The design of nanomedicines for trained immunity targeting must consider the different levels at which it might be targeted. Myeloid-cell-rich hematopoietic organs, like the spleen and bone marrow, are interesting targets, due to their relatively high proportion of HSPCs.[56]

As mentioned before, the fact that HSPCs give rise to a range of innate immune cells makes them an intriguing target for nanomaterials that aim to regulate trained immunity.

Nano-delivery platforms can be applied to target these cells in the main hematopoietic organs, such as the bone marrow and spleen. In the last few years, a variety of nanomedicine platforms have been developed for immunomodulatory drug delivery, as shown in **Figure 1.11.**[57]

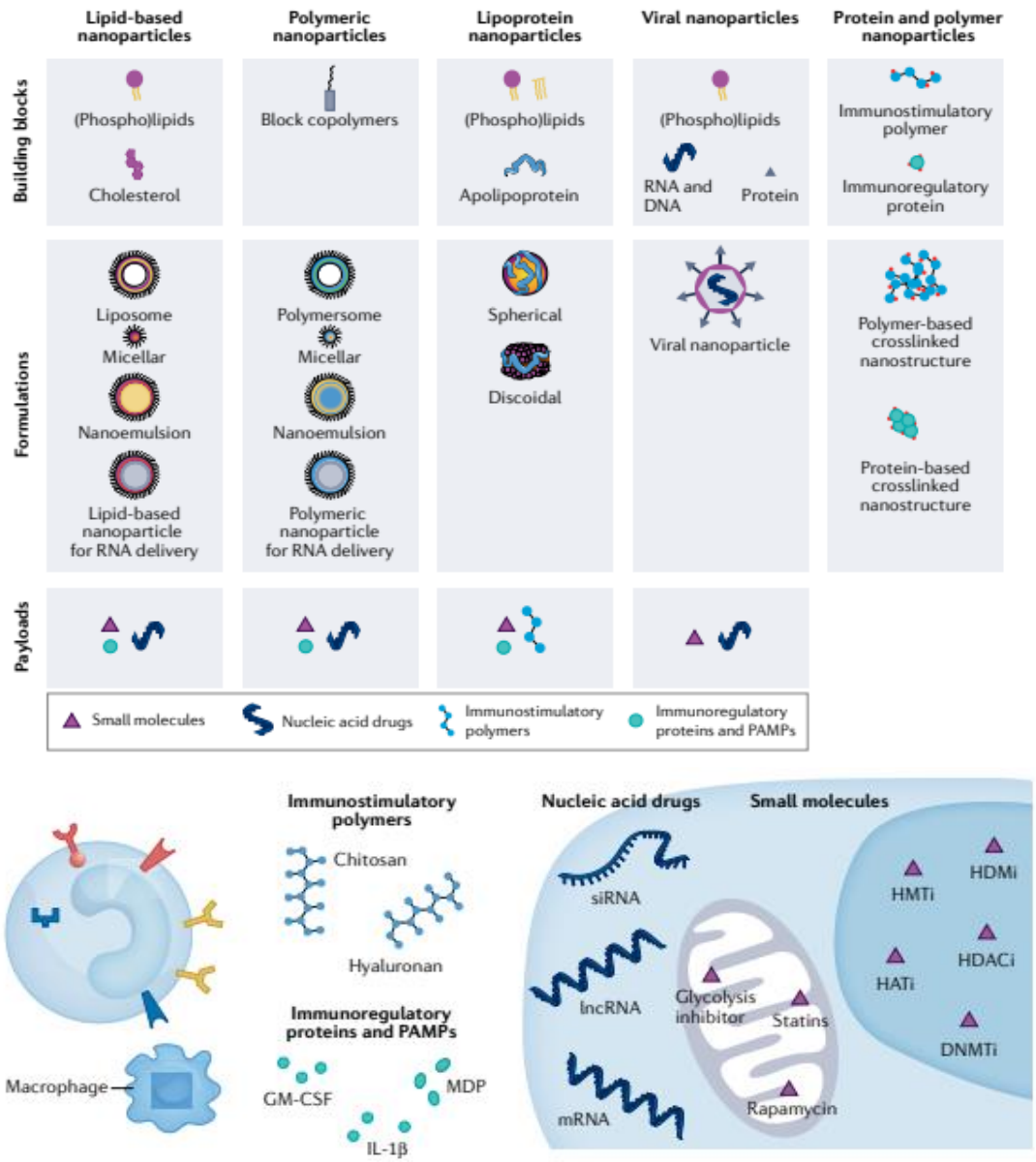


**Figure 1.11. Nanoparticle platforms**. An overview of nanoparticle platforms that can deliver immunomodulatory payloads, including small molecules, RNA therapeutics, immunoregulatory proteins, and immunostimulatory polymers. DNMTi, DNA methyltransferase inhibitor; GM-CSF, granulocyte-macrophage colony-stimulating factor; HATi, histone acetyltransferase inhibitor; HDACi, histone deacetylase inhibitor; HDMi, histone demethylase inhibitor; HMTi, histone methyltransferase inhibitor; IL-1β, interleukin-1β; lncRNA, long non-coding RNA; MDP, muramyl dipeptide; PAMP, pathogen-associated molecular pattern; siRNA, small interfering RNA. From van Leent et al, 2022.

This nano-immunotherapy, if administered intravenously, will have the ability to interact with HSPCs in the bone marrow. Although they can be designed to have a propensity to engage the bone marrow, they can often concentrate in other hematopoietic organs, like the liver and spleen. As mentioned before, the mechanism of action of these nanoparticles will rely on the disease context. Whether they have an inflammatory phenotype or molecular structures that inhibit trained immunity will depend on the desired therapy outcome. (**Figure 1.12**).[37]

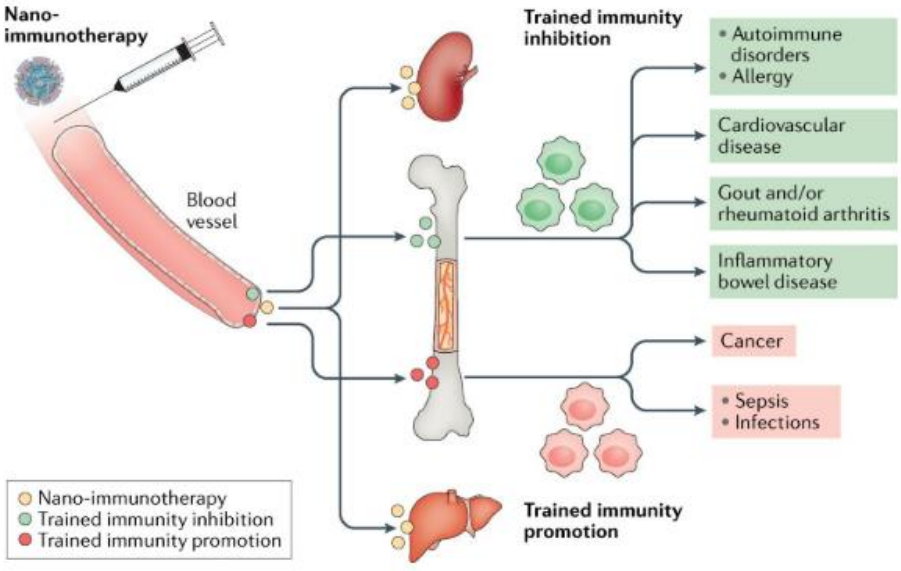


**Figure 1.12**. **Regulating trained immunity with nanotechnology**. Long-term therapeutic benefits can theoretically be achieved by the intravenous administration of nanomaterials that engage myeloid cells and their stem and progenitor cells in the bone marrow. Intravenously administrable nanomaterials (yellow circles) typically accumulate in the liver and spleen but can be designed to exhibit bone marrow proclivity. Induction of trained immunity can be prevented by functionalizing these nanomaterials with molecular structures that inhibit epigenetic and metabolic pathways that regulate trained immunity (green circles). The resulting 'green' cells have an alternatively activated phenotype. Conversely, by incorporating molecular structures derived from pathogen-associated molecular patterns (PAMPs) that activate dectin 1 or nucleotide-binding oligomerization domain-containing protein 2 (NOD2), nanomaterials (red circles) can be applied to promote trained immunity. These 'red' cells have an inflammatory phenotype. Systemically inhibiting trained immunity using this nanotechnology-based approach may be employed to treat a variety of conditions, ranging from cardiovascular disease and its clinical consequences myocardial infarction and stroke to autoimmune disorders. Therapeutically inducing trained immunity may find use in overcoming immunoparalysis in sepsis and infections and in treating cancers. From Mulder et al, 2019.

## 1.4- Macrophages as targets to ATC and prospects

Patients with ATC have extremely few therapeutic options and a very dismal prognosis. Therefore, it is crucial to develop new therapies. Recently, it has been identified that the innate

immune system - and trained immunity in particular - plays a crucial role in thyroid cancer disease progression.[58]

A recent study by Rabold et. al focused on understanding the behavior of myeloid cells and their progenitors in patients with non-medullary thyroid carcinoma. The data revealed that the immunosuppressive phenotype of myeloid cells in cancer is determined at a much earlier stage than currently thought. The results supported the hypothesis that significant changes occur in immune cell progenitors within the bone marrow. Notably, the analysis of bone marrow-derived progenitor cell types has demonstrated a reduction in the proportion of myeloid/ multipotent progenitor cells in TC samples (**Figure 1.13**).[58]

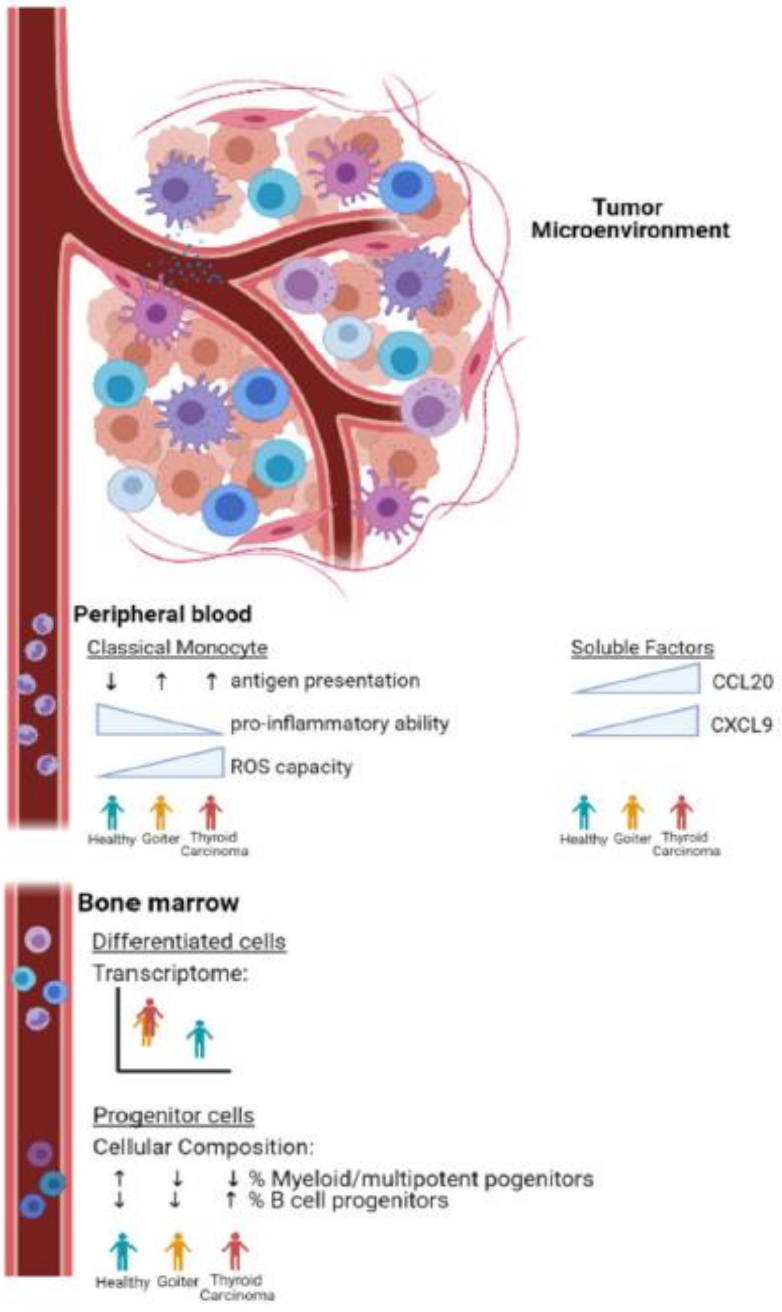

**Figure 1.13. Graphical summary of main findings.** From Rabold et. al

The findings underscore the critical involvement of the immune system in the development and spread of thyroid cancer, emphasizing the potential for immunotherapeutic interventions to target trained immunity and improve patient outcomes.[58]

The hypothesis is that the immunotolerance characteristic of the tumor microenvironment can be overcome by targeting the bone marrow cells to induce trained immunity and rewire the immune cells.[45]

As introduced earlier, Apo-A1-based nanomaterials have a relatively high accumulation in the bone marrow and can thus serve as an interesting technology for the targeting of trained immunity and thus also for the treatment of thyroid cancer (**Figure 1.14**).

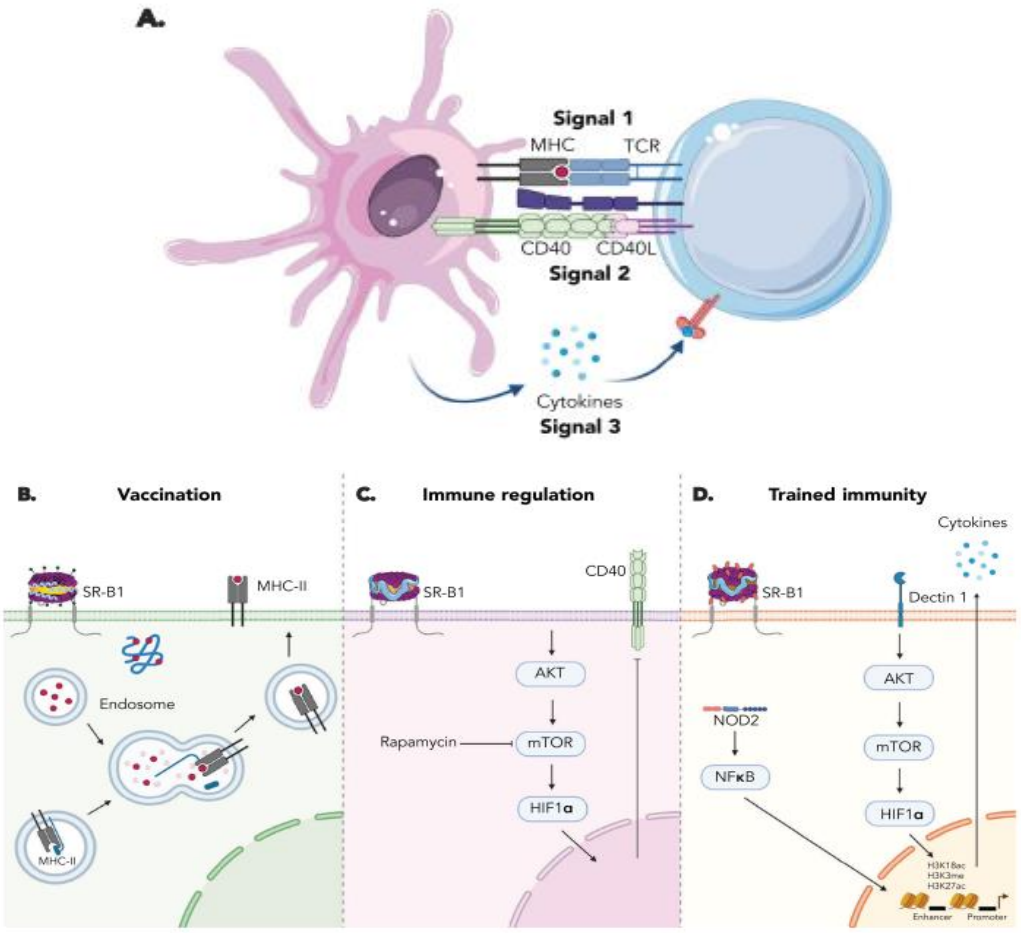

**Figure 1.14. Exploiting Apo-A1-nanotherapeutics as a platform for immunotherapy**. A) APCs can activate T-cells via MHC protein complexes-facilitated antigen presentations (signal 1), co-stimulation (signal 2), and cytokines (signal 3). B) ApoA1 mimetic discs harboring antigens and adjuvants can serve as a vaccination strategy to provide signal 1. C) Regulating immune responses via signal 2 by incorporating small molecules such as rapamycin. D) Inducing trained immunity using NOD2 agonist containing A1-nanotherapeutics, which primarily modifies the cytokine profile (signal 3). From Schrijver et al, 2021.

In a cancer setting, signals "play" with the plasticity of macrophages leading to a variety of TAMs phenotypes.[29] The functional plasticity of TAMs in a pro-tumor mode is strongly influenced by cytokines (such as IL-10) and chemokines (such as CCL2 and CCL18) produced from tumor cells. As was previously indicated, M2-like polarization of TAMs refers to functional programs linked with tumor growth and suppression of effective adaptive immunity.[59]

Reshaping TAMs is fundamental to the activation of innate and adaptive immune responses in the context of cancer. Given that TAMs can make up to 50% of the tumor volume in ATC, they make for a convincing immunotherapeutic target in ATC **(Figure 1.15)**.[50]

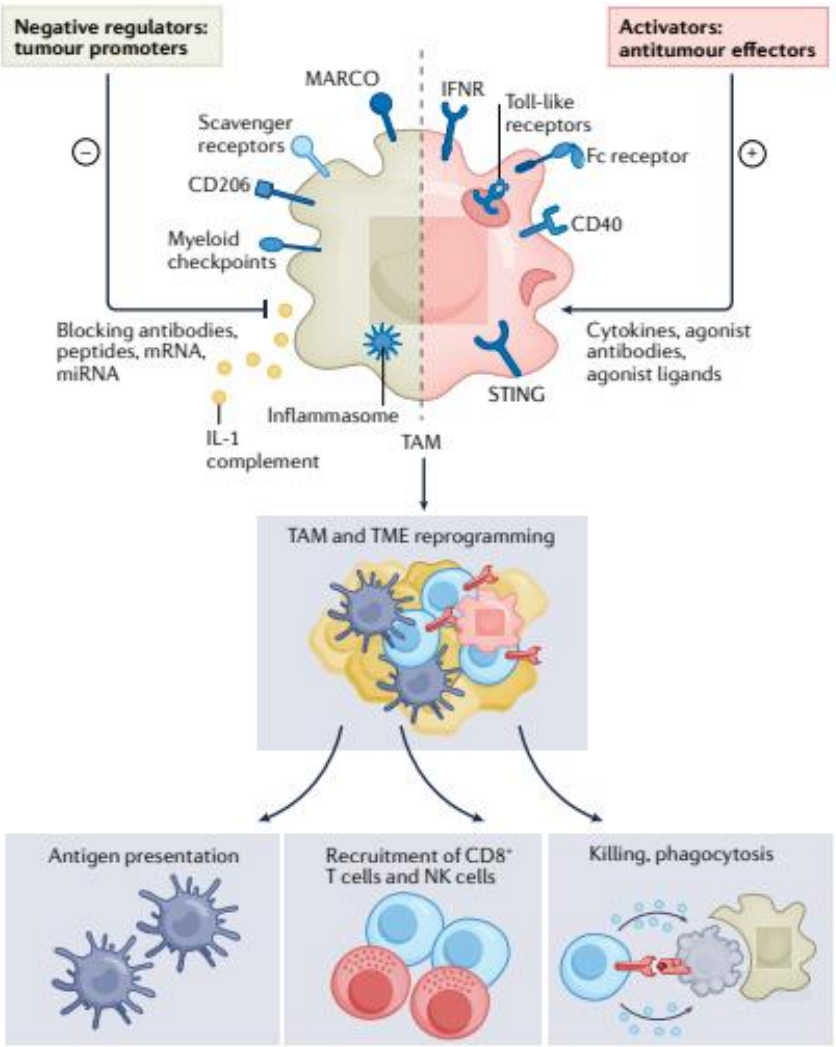


**Figure 1.15. Macrophage reprogramming and activation of innate and adaptive immune responses.** Cytokines (such as interferons), Toll-like receptors, stimulators of interferon genes (STING) agonists, and monoclonal antibodies activate macrophage-mediated tumor cell killing (red shading). A number of signals, including complement, inflammasome activators, ligands for scavenger receptors MARCO and CD206, and myeloid checkpoints can set macrophages in a pro-tumor mode (brown shading). MicroRNAs (miRNAs) and mRNA represent strategies to reprogram macrophage functions. Macrophage reprogramming induces macrophage-mediated killing of cancer cells, recruitment, and activation of innate and adaptive lymphoid cells, and reshaping of the tumor microenvironment. IFNR, interferon receptor; NK, natural killer; TAM, tumor-associated macrophages. From Mantovani A. et al, 2022.

# CHAPTER 2

# Aims

The immunotherapy field has been growing throughout the last decade, with multiple ways of action such as through monoclonal antibodies, and immune checkpoint inhibitors (ICIs). This field of therapy has been used for the treatment of many diseases such as auto-immune diseases, heart complications, and cancer.[43]

Whereas all cancers are defined by the ability to evade immune surveillance, one specific type - i.e., anaplastic - of thyroid cancer is characterized by the concurrent recruitment and accumulation of pro-tumorigenic myeloid cells.[26] Although rare (less than 1 % of all thyroid cancers)[60], this form of thyroid cancer is extremely lethal, and to date, no effective treatments have been identified. Thus, engineering immunotherapies that could potentially be used for the treatment of anaplastic thyroid cancer was the major goal of this study.

It has already been shown in previous studies that macrophages can be targeted to treat different types of cancer.[30] A recent study on thyroid cancer specifically also shows that cancer itself actively rewires the immune cells and their progenitors in the bone marrow, inducing an immunosuppressive state on a tumor as well as systemic level.[58,61,62] So based on these facts, we hypothesized that targeting immunotherapies to the bone marrow to revert this systemic immunosuppression could be a new therapeutic solution.

More specifically, by inhibiting migration and tumor infiltration of proinflammatory myeloid cells and polarizing the tumor microenvironment towards an anti-tumor phenotype. This would be achieved by inducing trained immunity [63] in bone marrow-derived macrophages to overcome the characteristic tolerance of the tumor microenvironment (TME). Knowing that >50% of the TME of anaplastic thyroid cancer is composed of TAMs [26] it is possible that changing the macrophage phenotype towards a more M1-like phenotype helps stop the tumor progression. (**Figure 2.1**).

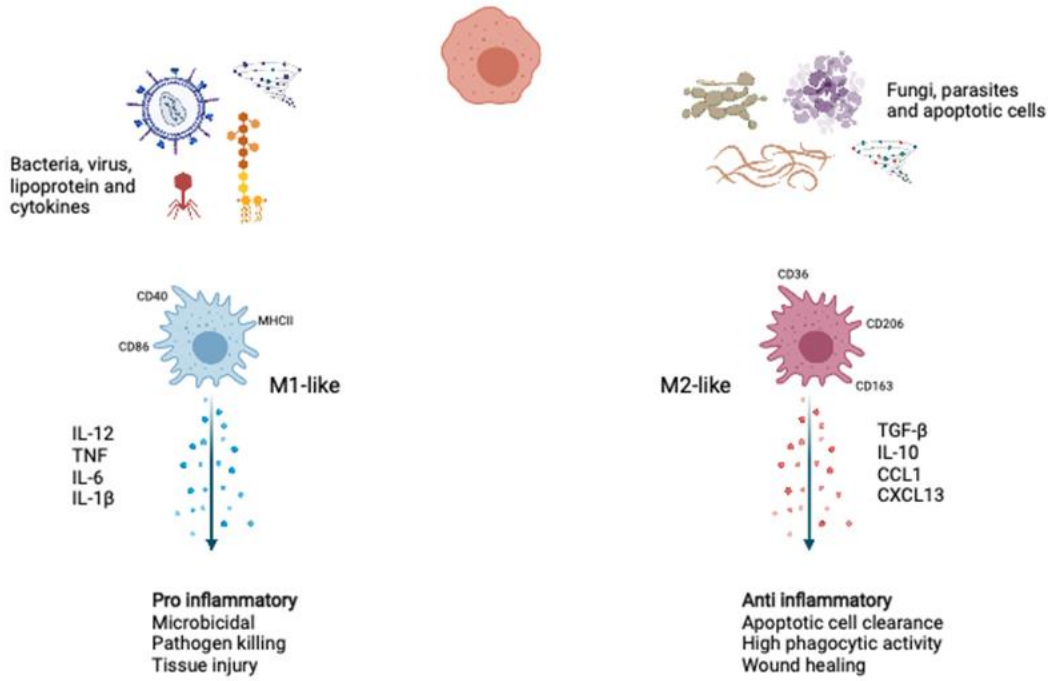


**Figure 2.1. Macrophage polarization.** During activation upon stimuli, such as type 1 cytokine, intracellular pathogens, and lipoproteins, the macrophages polarized to the M1-like phenotype show inflammatory and microbicidal. Upon stimuli, such as apoptotic cells and type 2 cytokines, the macrophages polarized to the M2-like phenotype function as anti-inflammatory, wound healing, and apoptotic cell clearance. IL-12, Interleukin-12; TNF, tumor necrosis factor; IL-6, Interleukin-6; IL-1β, Interleukin-1β; TGF-β, tumor growth factor-β; IL-10, Interleukin-10; CCL1, C-C motif chemokine ligand 1; CXCL13, C-X-C motif chemokine ligand 13. From Zubair et al. 2021.

Compared to untrained macrophages, trained ones can react more forcefully both quantitatively and qualitatively.[30]

Prior studies have shown that environmental stimuli such as LPS, β-glucan, MDP, and Bacillus Calmette–Guérin (BCG), as well as certain metabolites, can induce trained immunity.[63] These assays were mainly established in human monocytes.

However, there are few studies focused on inducing trained immunity in vitro in murine-derived cells. As mentioned before, the use of mice as research subjects presents a series of advantages, such as easy access, low variability of outcomes, and the eventual similarity to a therapeutic model.

Having this in mind, one of the goals of this research project was to ascertain the feasibility of inducing trained immunity in murine bone marrow-derived macrophages (BMDMs) and

optimize a so-called trained immunity assay for these cells,[63] to assist subsequent phases of the research.

The next step was the establishment of a mouse model to further investigate possible immunotherapies for ATC. Due to the limited timeline of the project, setting up an ATC mouse model was not feasible; therefore, an established melanoma mouse model was utilized for this study. Using this model, the aim was to establish the effect of the tumor on the immune cells and its progenitors in the bone marrow.

# CHAPTER 3

# Materials and Methods

## 3.1- Mice

C57BL/6J female wild-type mice were purchased from Charles River Germany and were between 8 and 12 weeks of age. All mice were housed in a pathogen-free facility at the Radboudumc's Animal Research facility at 25±2 ºC and 50±5 % humidity with a 12-h dark/light cycle and fed with *ad libitum* rodent diet. Mice were allowed to acclimate to the housing facility for at least 1 week. All experiments were performed following relevant laws and guidelines approved by the Central Authority for Scientific Procedures on Animals (CCD) in the Netherlands.

## 3.2- Reagents

β-1,3-(D)-Glucan from *Candida Albicans* was kindly provided by Professor David Williams (College of Medicine, Johnson City, USA), BCG (vaccine Statens Serum Institut) was obtained from The Netherlands Vaccine Institute, MDP (N-acetylmuramyl-ananyl-D-isoglutamine) was obtained from Sigma-Aldrich (catalog number A-9519), *Candida albicans* (UC820) was heat-inactivated for 30 minutes at 95 ºC. *Escherichia coli* lipopolysaccharide (LPS, serotype O55:B5; Sigma-Aldrich) was purified as described previously (Hirschfeld, M et al. 2000), and Pam-3-Cys was obtained from EMC Microcollections (catalog number L2000).

## 3.3- Cell culture

### 3.3.1- Bone Marrow derived macrophages (BMDMs) isolation and culturing

C57BL/6J female wild-type mice were euthanized using a CO2 chamber and whole femurs were taken and placed on ice-cold PBS 1X (Phosphate Buffered Saline, Thermo Fisher, Gibco™). The bones were cleaned and placed in 70 % Ethanol for 30 seconds and then placed in ice-cold PBS. The ends of the bone were cut with sterile material. Using a 10 mL syringe filled with ice-cold with a blue needle (BD needle- 0,60 x 30 mm) the bone marrow was flushed through a 70 µm strainer (Corning, Falcon) to a 50 mL falcon tube.

The cells were then spun down for 5 minutes at 4 ºC and 400 x g (Rotina 380R Hettich Centrifuge) and resuspended in 20 mL medium; 17 mL RPMI-1640 medium with Glutamax (Roswell Park Memorial Institute, Thermo Fisher, Gibco™), supplemented with 10 % heat-inactivated FBS (fetal bovine serum, Thermo Fisher, Gibco™) and 1 % Penicillin-Streptomycin (Thermo Fisher, Gibco™) and 3 mL LCM (L929-conditioned medium containing M-CSF). The cells were then plated and allowed to grow on a TC-treated culture dish (Tissue culture treated, 145 x 20 mm, sterile, CELLSTAR).

To guarantee macrophage differentiation and avoid cell stress, the cells were allowed to grow for 7 days before use with the addition of medium (10 mL) on day 3 and a change of medium (20 mL) on day 6, always maintaining a ratio of 85:15 RPMI: LCM.

### 3.3.2- Cell lines

B16F10 murine melanoma cell line (ATCC) was cultured in DMEM (Dulbecco's Modified Eagle Medium, Thermo Fisher, Gibco™) supplemented with 10 % heat-inactivated FBS (fetal bovine serum, Thermo Fisher, Gibco™) and 1 % Penicillin-Streptomycin (Thermo Fisher, Gibco™). The cell line was maintained at 37 ºC in a humidified incubator with 5 % $CO_2$ (Heracell 150i).

All cell lines were subjected to a Mycoplasma test (MycoStrip™ Mycoplasma detection kit) before use to ensure that there were no mycoplasma contaminations.

#### 3.3.2.1- Subculture and cellular conditions

Cell lines were first cultured in 25 $cm^3$ culture flasks (Thermo Fisher) with complete growth culture medium composed of DMEM (Dulbecco's Modified Eagle Medium, Thermo Fisher, Gibco™) or RPMI-1640 medium with Glutamax (Roswell Park Memorial Institute, Thermo Fisher, Gibco™), supplemented with 10 % heat-inactivated FBS (fetal bovine serum, Thermo Fisher, Gibco™) and 1 % Penicillin-Streptomycin (Thermo Fisher, Gibco™), and maintained at 37 ºC in a humidified incubator with 5 % $CO_2$ (Heracell 150i).

To avoid metabolic stress due to space and nutrient restrictions, and to allow exponential growth, the cells were passed to 75 or 175 $cm^3$ culture flasks (Thermo Fisher) when cells were at a ~80 % confluency. For this procedure, the medium was aspirated and TrypLE (cell culture dissociation reagent, Thermo Fisher, Gibco™) was added followed by a 3-minute incubation at 37 ºC to promote cell detachment. After this time, the TrypLE was neutralized by the addition of fresh medium. The resulting cell suspension was transferred to a 50 mL falcon tube from which 20 µL was taken and added to a CASY cup filled with 10 mL of CASY ton to determine cell density using a CASY cell counter (OMNI Life Science). Based on the cell density the cells were then passed to a new flask using a set of dilutions, ranging from 1:2 to 1:20 according to the specific doubling time for each cell line.

All experiments were carried out in an aseptic environment in a level II biosafety cabinet (Clean Air) and the culture solutions were preheated in a 37 ºC water bath (Julabo) to be at the ideal temperature for use.

It was important to control changes in the genotype and phenotype of the cell lines. This was achieved by maintaining a low number of passages, through regular freezes in high concentration, in exponential growth, and with the lowest number of passages possible.

The cell suspension was spun down at 4 ºC and 400 x g for 5 minutes (Rotina 380R Hettich Centrifuge), from where the sediment containing the cells was resuspended in preheated complete medium to a $1x10^6$ cells/mL concentration. The cells were then collected in cryotubes (Thermo Fisher); 1 mL of freezing medium - containing 80 % FBS (fetal bovine serum, Thermo Fisher, Gibco™) and 20 % DMSO (dioxide dimethyl, Sigma-Aldrich) – was added in a slow drop-wise manner to 1 mL of the cell suspension in the cryotubes. Finally, the cryotubes were placed in a freezing container (Corning CoolCell LX Cryo 1 ºC) at -80 ºC. This method provides alcohol-free freezing at the rate of -1 °C per minute which prevents abrupt and aggressive freezing of the cells. After the gradual freezing, the cryovials were placed in a -150 ºC freezer.

Thawing of the cells was carried out by heating the cryovial in a 37 ºC water bath and then added to a fresh medium to neutralize the DMSO. The cell suspension was then centrifuged at 400 x g for 5 minutes (Rotina 380R Hettich Centrifuge) to completely remove the DMSO from the cells. The supernatant was aspirated and discarded, and the pellet was resuspended in 5 mL of fresh medium and finally placed in a 25 $cm^3$ culture flask (Thermo Fisher) and kept at 37 ºC and 5 % $CO_2$ (Heracell 150i).

## 3.4- Trained Immunity assays in BMDMs

To determine the optimal method of inducing trained immunity in Bone Marrow-Derived Macrophages (BMDMs), a series of trained immunity assays were conducted. These assays involved the utilization of various stimuli, concentrations, and rest time combinations, as schematic in **Figure 3.1**.

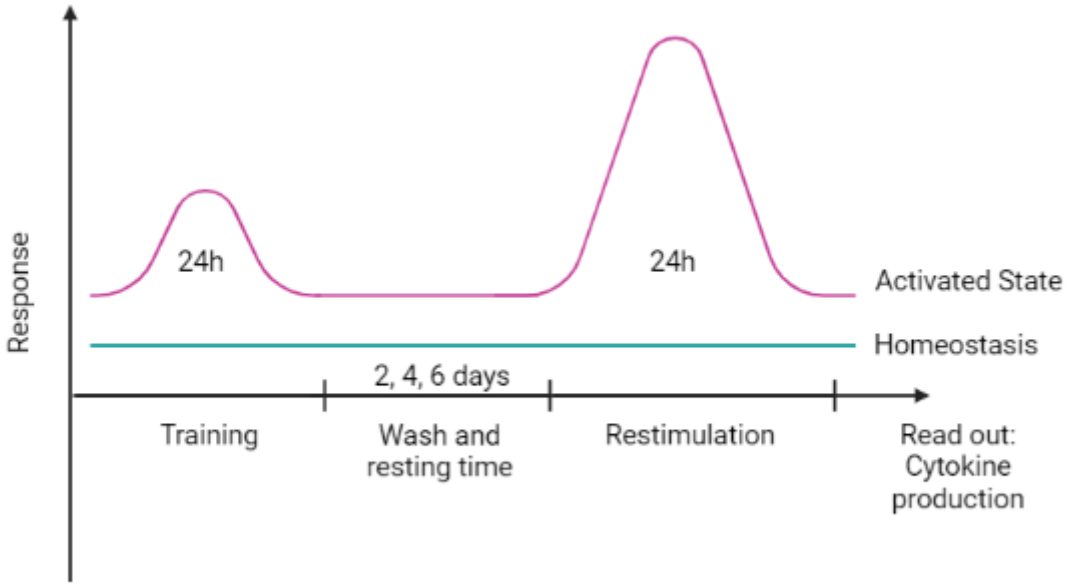


**Figure 3.1. Schematic overview of trained immunity methodology. Created with BioRender.com**

Before every trained immunity assay, fresh BMDMs were harvested from a previously plated culture dish. For this procedure, the medium was aspirated and 10 mL of TrypLE (cell culture dissociation reagent, Thermo Fisher, Gibco™) was added followed by a 5-minute incubation at 37 ºC to promote cell detachment. After this time, the TrypLE was neutralized by the addition of fresh RPMI-1640 medium with Glutamax (Roswell Park Memorial Institute, Thermo Fisher, Gibco™), supplemented with 10 % heat-inactivated FBS (fetal bovine serum, Thermo Fisher, Gibco™) and 1 % Penicillin-Streptomycin (Thermo Fisher, Gibco™). The cells were then harvested, and the resulting cell suspension was transferred to a 50 mL falcon tube from which 20 µL was taken and added to a CASY cup filled with 10 mL of CASY ton to determine cell density using a CASY cell counter (OMNI Life Science). The cells were then spun down for 5 minutes at 400 x g (Rotina 380R Hettich Centrifuge) and resuspended to the desired concentration in fresh medium: 15 % LCM (L929-conditioned medium containing M-CSF) and 85 % RPMI-1640 medium with Glutamax (Roswell Park Memorial Institute, Thermo Fisher, Gibco™), supplemented with 10 % heat-inactivated FBS (fetal bovine serum, Thermo Fisher, Gibco™) and 1 % Penicillin-Streptomycin (Thermo Fisher, Gibco™).

### 3.4.1- Trained immunity assay to establish first stimuli

BMDMs (100,000 cells/well) were added in triplicate to a flat-bottom 96-well plate (TPP$^{R}$ tissue culture plates). After incubation for at least 2 hours at 37 ºC to allow adherence, BMDMs

were incubated with culture medium as a negative control or 1,3,9 µg/mL β-glucan, 5,15,45 µg/mL BCG, or 5,15,45 µg/mL MDP for 24 hours (in 200 µL/well with 15 % LCM). After the incubation time, supernatants were collected, the cells were washed once with 200 µL of warm PBS 1X and incubated for 2 or 4 days in culture medium: 15 % LCM (L929-conditioned medium containing M-CSF) and 85 % RPMI-1640 medium with Glutamax (Roswell Park Memorial Institute, Thermo Fisher, Gibco™), supplemented with 10 % heat-inactivated FBS (fetal bovine serum, Thermo Fisher, Gibco™) and 1 % Penicillin-Streptomycin (Thermo Fisher, Gibco™). The medium was changed once on day 2 for cells resting for 4 days. Cells were restimulated with 200 µL RPMI, or 10 ng/mL LPS. After 24h, supernatants were collected. All supernatants were stored at -20 ºC until used for further analysis.

### 3.4.2- Trained immunity assay with HK *Candida Albicans* and Pam-3-cys

For this assay, BMDMs (100,000 cells/well) were added in triplicate to a flat-bottom 96-well plate (TPP$^{R}$ tissue culture plates). After incubation for at least 2 hours at 37 ºC to allow adherence, macrophages were incubated with culture medium as a negative control or 45 µg/mL BCG, or 1x10$^{5}$ cells/mL HK *Candida Albicans* for 24 hours (in 200 µL/well with 15 % LCM). After the incubation time, supernatants were collected, the cells were washed once with 200 µL of warm PBS 1X and incubated for 2 days, 4 days, or 6 days in culture medium: 15 % LCM (L929-conditioned medium containing M-CSF) and 85 % RPMI-1640 medium with Glutamax (Roswell Park Memorial Institute, Thermo Fisher, Gibco™), supplemented with 10 % heat-inactivated FBS (fetal bovine serum, Thermo Fisher, Gibco™) and 1 % Penicillin-Streptomycin (Thermo Fisher, Gibco™). The medium was changed once on day 3 for cells resting for 4 and 6 days. Cells were restimulated with 200 µL RPMI, 10 ng/mL LPS, or 1 µg/mL P3C. After 24h, supernatants were collected. All supernatants were stored at -20 ºC until further analysis.

### 3.4.3- Trained immunity assay to access Pam-3-Cys inflammatory response

BMDMs (100,000 cells/well) were added in triplicate to a flat-bottom 96-well plate (TPP$^{R}$ tissue culture plates). After incubation for at least 2 hours at 37 ºC to allow adherence, macrophages were incubated with culture medium as a negative control or 45 µg/mL BCG, or 1x10$^{5}$ cells/mL HK Candida for 24 hours (in 200 µL/well with 15 % LCM). After the incubation time, supernatants were collected, the cells were washed once with 200 µl of warm PBS 1X and incubated for 4 days, in culture medium: 15 % LCM (L929-conditioned medium containing M-CSF) and 85 % RPMI-1640 medium with Glutamax (Roswell Park Memorial Institute, Thermo Fisher, Gibco™), supplemented with 10 % heat-inactivated FBS (fetal bovine serum, Thermo Fisher, Gibco™) and 1 % Penicillin-Streptomycin (Thermo Fisher, Gibco™). The

medium was changed once on day 2. Cells were restimulated with 200 µL RPMI, 0.125, 0.25, 0.5, 1, 5, and 10 µg/mL P3C. After 24h, supernatants were collected. All supernatants were stored at -20 ºC until further analysis.

### 3.4.4- Trained immunity assay with Tumor Culture Medium (TCM)

BMDMs (100,000 cells/well) were added in triplicate to a flat-bottom 96-well plate (TPP$^{R}$ tissue culture plates). After incubation for at least 2 hours at 37 ºC to allow adherence, macrophages were incubated with culture medium as a negative control or 45 µg/mL BCG for 24 hours (in 200 µL/well with 15 % LCM). After the incubation time, supernatants were collected, the cells were washed once with 200 µL of warm PBS 1X and incubated for 4 days in culture medium: 15 % LCM (L929-conditioned medium containing M-CSF) and 85 % RPMI-1640 medium with Glutamax (Roswell Park Memorial Institute, Thermo Fisher, Gibco™), supplemented with 10 % heat-inactivated FBS (fetal bovine serum, Thermo Fisher, Gibco™) and 1 % Penicillin-Streptomycin (Thermo Fisher, Gibco™). The medium was changed once on day 2. Cells were restimulated with different stimuli including 200 µL RPMI, B16F10 TCM (40 % or 70 %), and 10 ng/mL LPS. After 24h, supernatants were collected. All supernatants were stored at -20 ºC until cytokine measurement. For tumor culture medium collection, B16F10 cells were cultured until ~80% confluency. The tumor culture medium supernatant was stored at -80 ºC in aliquots until use.

## 3.5- Nitrite Assay

After a 24-hour stimulation period, 150 µL of the culture medium was extracted from each well for analysis. To determine the nitrite content the culture medium was incubated with Griess reagent (Griess Reagent Kit for Nitrite Determination (G-7921), Molecular Probes) at room temperature for 30 minutes. Subsequently, the absorbance was measured at 548 nm using a microplate reader. The nitrite content was calculated based on a standard curve constructed using $NaNO_2$.

## 3.6- Cell Proliferation Assay

To assess the viability of BMDMs following the trained immunity assays and exposure to stimuli, a cell proliferation assay was conducted (CyQUANT® Cell Proliferation Assay Kit, Invitrogen) following the manufacturer protocol. The DNA content was calculated based on a standard curve constructed using a standard DNA solution.

## 3.7- Thyroid Magnetic Resonance Imaging (MRI)

High-resolution MR imaging of the mouse thyroid was done on a Bruker 7T Biospec 70/30 scanner equipped with a 200 mT/m gradient coil (Bruker Biospin MRI). Mice were anesthetized with 1 % isoflurane gas during scanning and monitored using a small animal physiological monitoring system for respiration (SA Instruments).

Mouse thyroid images were acquired using T2-weighted fast spin-echo rapid acquisition with relaxation enhancement (RARE) sequence with a 0.4-mm-thick transversal slice, and a spatial resolution of 150 × 150 µm. For acquisition, an echo time of 61 ms and RARE factor 8 was used.

## 3.8- Scale down BMDMs culture

Bone marrow cells were isolated as previously described. Then the cells were spun down for 5 minutes at 4 ºC and 400 x g (Rotina 380R Hettich Centrifuge).

Cells were then resuspended in 20 (one femur), 8 (1/2 of a femur), 2.94 (1/6 of a femur), or 1.2 (1/15 of a femur) mL medium; 17, 6.8, 2.5 or 1.02 mL RPMI-1640 medium with Glutamax (Roswell Park Memorial Institute, Thermo Fisher, Gibco™), supplemented with 10 % heat-inactivated FBS (fetal bovine serum, Thermo Fisher, Gibco™) and 1 % Penicillin-Streptomycin (Thermo Fisher, Gibco™) and 3, 1.2, 0.44 or 0.18 mL LCM (L929-conditioned medium containing M-CSF). The cells were then plated and allowed to grow on a TC-treated culture dish (Tissue culture treated, 145 x 20 mm/ 100 x 15 mm/ 60 x 15 mm/ 30 x 10 mm, sterile, CELLSTAR).

To guarantee macrophage differentiation and avoid cell stress, the cells were allowed to grow for 7 days before use with the addition of medium (10, 4, 1.47, 0.6 mL) on day 3 and a change of medium (20, 8, 2.94, 1.2 mL) on day 6, always maintaining a ratio of 85:15 RPMI: LCM.

BMDMs were harvested, a small fraction was taken for flow cytometry analysis, and the remnant was seeded in a flat-bottom 96-well plate (TPP$^{R}$ tissue culture plates) at 100,000 cells per well, two times in triplicate. After incubation for at least 2 hours at 37 ºC to allow adherence, BMDMs were incubated with culture medium as a negative control or 10 ng/mL LPS. After 24h, supernatants were collected. All supernatants were stored at -20 ºC until further analysis.

## 3.9- Phenotyping B16F10 to establish a mouse model

### 3.8.1- Cell preparation

B16F10 murine melanoma cells were cultured as previously described until reaching a ~80 % confluence. The cells were then harvested, counted using a CASY Counter (OMNI Life Science), and diluted to $1x10^6$ cells/mL in warm sterile 1X PBS supplemented with 0.5 % fetal bovine serum (FBS Thermo Fisher, Gibco™)

### 3.8.2- Mouse injections

For tumor experiments, $1x10^5$ B16F10 murine melanoma cells were injected subcutaneously into the right anterior flank of each mouse. The tumor was allowed to grow for 1 or 2 weeks before euthanizing the mice and collecting the organs for consequent analysis.

### 3.8.3- Preparation of Single cells Suspensions

C57BL/6 mice were euthanized 1 or 2 weeks after tumor inoculation. Blood was collected by cardiac puncture, placed in 250-500 µL $K_2$EDTA microtainers (BD), and kept on ice. Mice were subsequently perfused with 20 mL cold PBS and spleen and 2 femurs were collected from each mouse. All organs were kept in PBS and on ice until further processing.

150 µL of blood was incubated with 1 mL of RBC Lysis buffer (BioLegend) for 7 min on ice. PBS was added after 7 minutes to quench the lysis. The cells were then centrifuged at 4 ºC and 400 x g for 5 minutes (Rotina 380R Hettich Centrifuge). This lysis process was repeated twice, and cells were resuspended in flow buffer (PBS 1X, 0.5% BSA; 2 mM EDTA). Bone marrow was flushed out of one femur (per mouse) with a syringe filled with 10 mL of flow buffer using a blue needle (BD needle- 0,60 x 30 mm), filtered through a 70 µm cell strainer (Corning, Falcon) into a 50 mL falcon tube, incubated with 1 mL RBC Lysis buffer (BioLegend) for 1 min at room temperature, washed with 5 mL flow buffer and finally resuspended in flow buffer. Samples were then ready for flow cytometry analysis.

In sterile conditions, one femur (per mouse) was cleaned and placed in 70 % Ethanol for 30 seconds and then placed in ice-cold PBS 1X (Phosphate Buffered Saline, Thermo Fisher, Gibco™). The ends of the bone were cut with sterile material. Using a 10 ml syringe filled with ice-cold PBS 1X (Phosphate Buffered Saline, Thermo Fisher, Gibco™) with a blue needle (BD needle- 0,60 x 30 mm) the bone marrow was flushed through a 70 µm strainer (Corning, Falcon) to a 50 mL falcon tube. The cells were then incubated with 1 mL RBC Lysis buffer (BioLegend) for 1 min at room temperature and washed with 5 mL of RPMI-1640 medium with Glutamax

(Roswell Park Memorial Institute, Thermo Fisher, Gibco™), supplemented with 10 % heat-inactivated FBS (fetal bovine serum, Thermo Fisher, Gibco™) and 1 % Penicillin-Streptomycin (Thermo Fisher, Gibco™). The cells were counted with a CASY counter (OMNI Life Science), spun down for 5 minutes at 4 ºC and 400 x g (Rotina 380R Hettich Centrifuge), and resuspended in fresh medium to a concentration of $0.5x10^6$ million cells/mL.

In sterile conditions, spleens were cut into small pieces and pushed through a 70 µm strainer (Corning, Falcon) to a 50 mL falcon tube with 5 mL of ice-cold 1X PBS. The cells were then incubated with 2 mL RBC Lysis buffer (BioLegend) for 4 min at room temperature and washed with 8 mL of RPMI-1640 medium with Glutamax (Roswell Park Memorial Institute, Thermo Fisher, Gibco™), supplemented with 10 % heat-inactivated FBS (fetal bovine serum, Thermo Fisher, Gibco™) and 1 % Penicillin-Streptomycin (Thermo Fisher, Gibco™). The cells were counted with a CASY counter (OMNI Life Science), spun down for 5 minutes at 4 ºC and 400 x g (Rotina 380R Hettich Centrifuge), and resuspended in fresh medium to a concentration of $5x10^6$ million cells/mL. A small fraction of the final volume was taken for flow cytometry analysis.

### 3.8.4- In vitro bone marrow and splenocytes re-stimulation

Bone marrow cells were seeded in a flat-bottom 96-well plate ($TPP^R$ tissue culture plates) at 100,000 cells per well, two times in triplicate. After incubation for at least 2 hours at 37 ºC to allow adherence, bone marrow cells were incubated with culture medium as a negative control or 10 ng/mL LPS. After 24h, supernatants were collected. All supernatants were stored at -20 ºC until further analysis.

Splenocytes were seeded in a flat-bottom 96-well plate ($TPP^R$ tissue culture plates) at 500,000 cells per well, two times in triplicate. After incubation for at least 2 hours at 37 ºC to allow adherence, splenocytes were incubated with culture medium as a negative control or 100 ng/mL LPS. After 24h, supernatants were collected. All supernatants were stored at -20 ºC until further analysis.

### 3.8.5- In vitro BMDMs re-stimulation

Approximately 3 million bone marrow cells (per sample) were taken into culture on a TC-treated culture dish (Tissue culture treated, 60 x 15mm, sterile, CELLSTAR).

For this, cells were resuspended in 2.94 mL culture medium: RPMI-1640 medium with Glutamax (Roswell Park Memorial Institute, Thermo Fisher, Gibco™), supplemented with 10 % heat-inactivated FBS (fetal bovine serum, Thermo Fisher, Gibco™) and 1 % Penicillin-

Streptomycin (Thermo Fisher, Gibco™) with 15 % LCM (L929-conditioned medium containing M-CSF), and finally plated and allowed to grow.

To guarantee macrophage differentiation and avoid cell stress the cells were allowed to grow for 7 days before use with a medium addition (1.47 mL) on day 3 and medium change (2.94 mL) on day 6.

On day 7 bone marrow-derived macrophages were harvested and seeded in a flat-bottom 96-well plate (TPP$^{R}$ tissue culture plates) at 100,000 cells per well, two times in triplicate. After incubation for at least 2 hours at 37 ºC to allow adherence, BMDMs were incubated with culture medium as a negative control or 10 ng/mL LPS. After 24h, supernatants were collected. All supernatants were stored at -20 ºC until further analysis.

## 3.9- Cytokine Measurements

In order to evaluate the proinflammatory cytokine production after training assays, cytokine concentration in supernatants was measured using commercial ELISA (ELISA MAX™ Deluxe Set, Biolegend) kits for mouse TNF and IL-6, following the manufacturer's instructions. Sample absorbance was measured at 450 nm in a microplate reader (BioTek 800 TS Absorbance Reader, Agilent). Analyses were performed according to the manufacturer's protocols.

## 3.10- Flow cytometry

### 3.10.1- Flow cytometry for analysis of scaled-down BMDMs

1x10$^{6}$ cells/ mL BMDMs were washed with PBS, incubated with Viakrome 808, blocked with Fc-Block, and stained for 30 min at 4 ºC in the dark with the following antibodies: anti-Ly6C, anti-CD115, anti-CD206, anti-CD11b, anti-CD68, and anti-F4/80. Cells were subsequently washed and resuspended in flow buffer. All data was acquired on a CytoFLEX LX Flow Cytometer (Beckman Coulter).

### 3.10.2- Myeloid and lymphoid flow cytometry from B16F10 Phenotyping

Bone marrow, spleen, and blood cells were washed with PBS, incubated with Viakrome 808, blocked with Fc-Block, and stained for 30 min at 4 ºC in the dark with myeloid or lymphoid antibody cocktails. For the myeloid panel, cells were incubated with anti-CD115, anti-F4/80, anti-Ly6C, anti-Ly6G, anti-CD11b, anti-Cd45, and anti-CD11c. For lymphoid panel anti-CD3, anti-CD4, anti-CD8a, anti-CD19, anti-CD11b, anti-CD45, and anti-NK1.1 was added. Cells were subsequently washed and resuspended in flow buffer. All data was acquired on a

CytoFLEX LX Flow Cytometer (Beckman Coulter). Cells were identified as shown in **Tables 3.1 and 3.2.**

| **Myeloid Panel** | |
|---|---|
| Leukocytes | CD45+ |
| Myeloid cells | CD45+ CD11b+ |
| DCs | CD45+ CD11b+ CD11c+ |
| Neutrophils | CD45+ CD11b+ Ly6G+ |
| Macrophages | CD45+ CD11b+ F4/80+ |
| Monocytes | CD45+ CD11b+ CD115+ F4/80- |
| Monocytes Ly6C high | CD45+ CD11b+ CD115+ F4/80- Ly6C(High) |
| Monocytes Ly6C Low | CD45+ CD11b+ CD115+ F4/80- Ly6C(Low) |

**Table 3.1. Flow cytometry gating strategy for myeloid cell populations**.

| **Lymphoid Panel** | |
|---|---|
| Leukocytes | CD45+ |
| Lymphoid cells | CD45+ CD11b- |
| NK cells | CD45+ CD11b- CD3- NK-1.1+ |
| B-cells | CD45+ CD11b- CD19+ |
| T cells | CD45+ CD11b- CD3+ |
| Cytotoxic T cells, CD8 | CD45+ CD11b- CD3+ CD8+ |
| T helper cells, CD4 | CD45+ CD11b- CD3+ CD4+ |

**Table 3.2. Flow cytometry gating strategy for lymphoid cell populations**.

## 3.10.3- Progenitors flow cytometry from B16F10 Phenotyping

For progenitor flow cytometry, bone marrow cells were washed with PBS, incubated with Viakrome 808, and stained with the following antibodies: anti-CD117, anti-Ly6A/E, anti-Cd34, anti-CD135, anti-CD16/32, anti-CD48, anti-CD41, anti-CD150, and a lineage cocktail containing anti-CD3, anti-CD11b, anti-CD45R/B220, anti-Ly76, anti-Ly6G, and Ly6C. Cells were subsequently washed and resuspended in flow buffer. All data was acquired on a

CytoFLEX LX Flow Cytometer (Beckman Coulter). Cells were identified as shown in **Table 3.3.**

| **Progenitors Panel** | |
|---|---|
| Lineage – (negative) | Lin- |
| Hematopoietic stem cells, HSCs [LSKs] | Lin- cKit+ Sca1+ |
| Short-term hematopoietic stem cells, ST-HSC | Lin- cKit+ Sca1+ CD48- CD150- |
| Long-term hematopoietic stem cells, LT-HSC | Lin- cKit+ Sca1+ CD48- CD150+ |
| Myeloid-biased LT-HSC | Lin- cKit+ Sca1+ CD48- CD150+ CD41+ |
| Multipotent progenitors, MPP | Lin- cKit+ Sca1+ CD48+ CD150- |
| MPP3, myeloid lineage-biased MPPs | Lin- cKit+ Sca1+ CD48+ CD150- CD135- |
| MPP4, lymphoid lineage-biased MPPs | Lin- cKit+ Sca1+ CD48+ CD150- CD135+ |
| MPP2, megakaryocyte/erythroid (ME)-biased MPPs | Lin- cKit+ Sca1+ CD48+ CD150+ CD135- |
| Myeloid progenitors, MyPs | Lin- cKit+ Sca1- |
| Granulocyte-macrophage progenitors, GMPs | Lin- cKit+ Sca1- CD16/32+ CD34+ |
| Common myeloid progenitors, CMPs | Lin- cKit+ Sca1- CD16/32- CD34+ |

**Table 3.3. Flow cytometry gating strategy for progenitor cell populations**.

## 3.11-Microscopy

Cell morphology was studied by conventional light microscopy during incubation each day.

## 3.12- Statistic Analysis

Data were tested using a two-tailed Student's t-test (when comparing two groups) or two-way ANOVA (to test multiple groups) in GraphPad Prism version 7.0 software, as indicated in the figure legends. p values $< 0.05$ were considered significant, with levels of significance as follows: *$p < 0.05$; **$p < 0.01$; ***$p < 0.001$; ****$p < 0.0001$; ns, not significant. Data are shown as means ± standard errors of the means.

# CHAPTER 4

# Results

## 4.1- In Vitro training of murine bone marrow-derived macrophages using different stimuli and resting periods.

As was shown previously, 24h incubation with β-glucan, BCG, or MDP induces - in human monocytes - a trained immunity phenotype. This is characterized by increased production of proinflammatory cytokines upon restimulation with heterologous stimuli.

However, this kind of reprogramming has not been optimized for murine-derived cells. For that reason, the aim was to develop and optimize a training assay in murine-derived BMDMs.

We investigated the training capacity of β-glucan, BCG, and MDP in BMDMs (**Fig. 4.1**) and evaluated their induction of trained immunity after consequent restimulation. Furthermore, different resting periods between stimuli were assessed to find how temporal changes in the timing of the second stimulus impact the development of the trained immunity phenotype. (**Fig. 4.2**).

The proinflammatory cytokines tumor necrosis factor (TNF) and interleukin-6 (IL-6) were used as surrogate trained immunity markers. BMDMs were stimulated with different concentrations of β-glucan, BCG, and MDP for 24 hours. After a resting period of 2 or 4 days, the cells were restimulated with LPS (24h). As a positive control, non-trained cells stimulated with LPS were used. ELISA readout on TNF and IL-6 was performed on supernatants collected after the first (**Fig 4.1**) and second stimulation (**Fig 4.2**).

BCG stimulation induced a higher production of TNF and IL-6 when compared with β-glucan and MDP stimulation (**Fig 4.1**), being more prominent at a concentration of 45µg/mL. It was also observed that training with BCG (45µg/mL) induced the strongest increase in cytokine production upon LPS restimulation (**Fig 4.2**). β-glucan and MDP did not induce trained immunity when compared to the positive control.

The influence of the resting time between stimuli was noticeable when training with a higher concentration of BCG. After a resting time of 2 days, the cells reacted more strongly to LPS restimulation, producing higher concentrations of TNF and IL-6 (**Fig 4.2**).

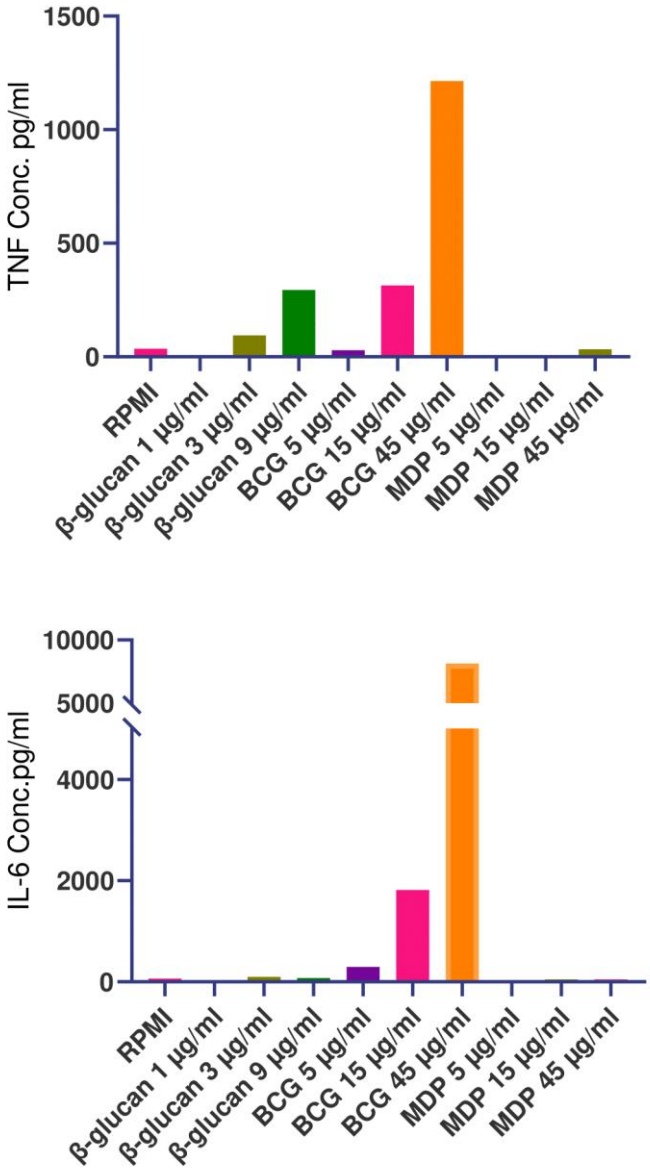


**Figure 4.1. Pro-inflammatory cytokine production after first stimulation.** TNF and IL-6 production after the first stimulus. Cells were stimulated for 24 hours with β-glucan, BCG, or MDP. RPMI-stimulated cells were used as a control. Data are shown as means ± standard errors of the means. p values < 0.05 were considered significant, with levels of significance as follows: *p < 0.05; **p < 0.01; ***p < 0.001; ****p < 0.0001; ns, not significant. P values were derived from a two-way analysis of variance (ANOVA) with a multiple-comparison test.

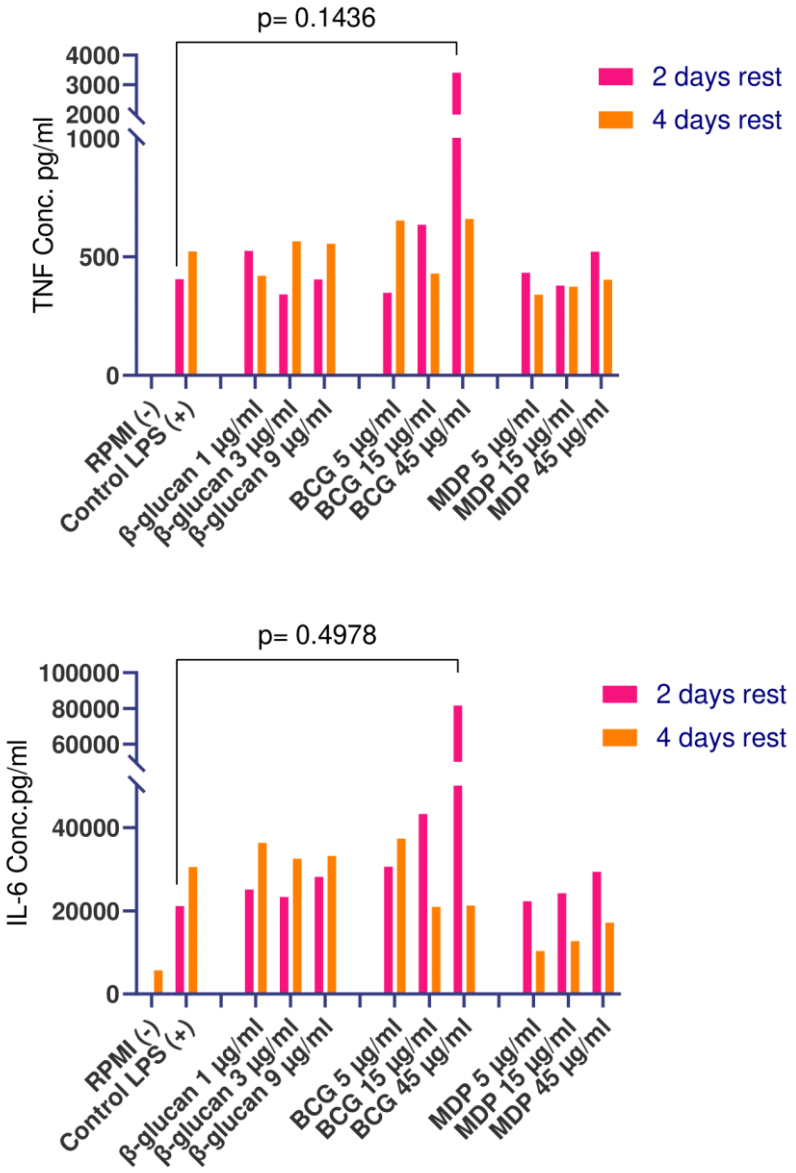


**Figure 4.2. Proinflammatory cytokine production is dependent on training and resting time.** TNF and IL-6 production after LPS restimulation (24h). After training the cells rested for 2 or 4 days. RPMI-stimulated cells were used as a negative control and LPS stimulated as a positive control. Data are shown as means ± standard errors of the means. p values < 0.05 were considered significant, with levels of significance as follows: *p < 0.05; **p < 0.01; ***p < 0.001; ****p < 0.0001; ns, not significant. P values were derived from a two-way analysis of variance (ANOVA) with a multiple-comparison test.

Together, these data suggest that trained immunity can be induced in BMDMs. It suggests that BCG as a first challenge is the best inducer. We can also observe that the time between stimuli can influence the reprogramming of the cells toward a trained immunity phenotype.

### 4.1.1- Stimulation Boosts the Production of Nitric Oxide

In addition to cytokines, nitric oxide (NO) production can also serve as a readout for the degree of activation of myeloid cells like macrophages. The principal metabolic pathway of NO involves its rapid oxidation into higher nitrogen oxides, namely nitrite, and nitrate. While nitrite ($NO_2$) can be detected using the colorimetric Griess reagent, the detection of nitrate requires its conversion to $NO_2$. In the case of bone marrow-derived macrophages, the spectroscopic estimation of NO production involves the measurement of formed $NO_2$. Following its synthesis, NO produced by BMDM dissolves in the culture medium and undergoes oxidation, resulting in the generation of both nitrate and nitrite.

To complement the previous results, and access the activation of the BMDMs, the production of NO was accessed.

As shown in **Figure 4.3**, after the first stimulation, individual stimuli show low NO concentrations, but once again BCG (45 µg/mL) induces a more prominent activation (**Fig. 4.3 a**).

However, after LPS restimulation, BMDMs show a greater production of NO, and on average, the concentration of NO remains the same after 2 and 4 days of rest (**Fig. 4.3 b**). Cells stimulated with BCG show a high production of NO after 2 days of resting period which is consistent with the cytokine production verified before. This indicates that BCG stimulation, at a high concentration, is the best option when it comes to inducing a trained immunity phenotype upon LPS restimulation.

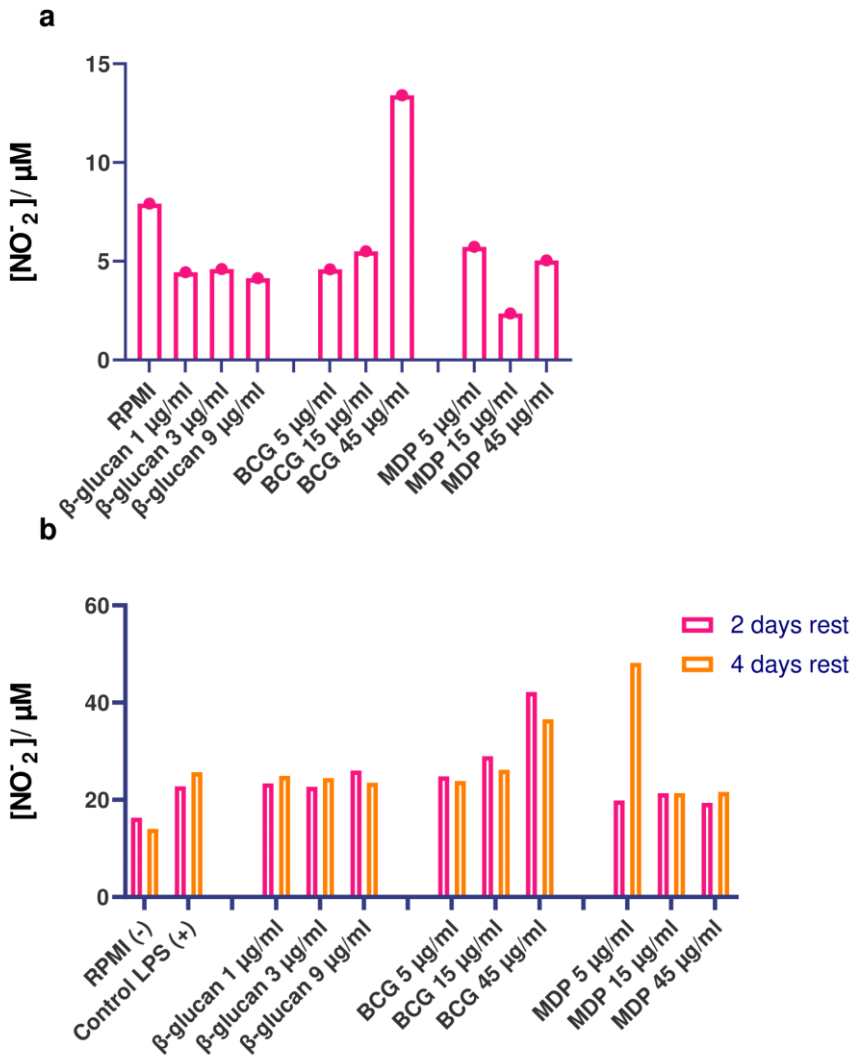


**Figure 4.3. Stimulation Boosts the Production of Nitric Oxide (NO). (a)-** NO concentration/ (µM) after the first 24 hours of stimulation. **(b)-** NO concentration/ (µM) after LPS restimulation after 2 or 4 days of resting time. RPMI-stimulated cells were used as a negative control and LPS stimulated as a positive control.

## 4.2- Training is induced by BCG and Heat Killed Candida upon restimulation with LPS but not upon Pam-3-cys restimulation

Enhanced trained immunity responses are induced by exposure to certain infectious agents. Previous research[64,65] conducted on human monocytes demonstrated that both Heat Killed *Candida Albicans* (HK Candida) and Pam-3-Cys (P3C) exhibit promising potential as inducers of trained immunity.

HK Candida refers to *Candida albicans* cells that have undergone a heat treatment which renders them non-viable, however, they can still be used as an antigen source. The use of HK

Candida presents a series of advantages when compared to live *Candida albicans* in training assays. Reasons like safety, standardization of experimental conditions, controlled immune stimulations, and consistent antigen presentation, makes HK Candida the preferred stimuli in these kinds of experiments.

On the other hand, Pam-3-cys is a synthetic molecule derived from the bacterial cell wall. It acts as a ligand for TLR2 and can initiate immune responses.

Consequently, they were selected and evaluated as the primary and secondary stimuli for BMDMs (**Fig. 4.4, 4.5, and 4.6**). Once again, in vitro training experiments were performed, and the pro-inflammatory cytokines tumor necrosis factor (TNF) and interleukin-6 (IL-6) were used as surrogate trained immunity markers. For that, BMDMs were incubated with BCG (45 µg/mL), or HK Candida for 24 hours. After 2, 4, or 6 days of resting time, the cells were restimulated with LPS or P3C. As a positive control, non-trained cells stimulated with LPS or P3C were used. ELISA readout was performed on supernatants collected after the first (**Fig. 4.4**) and second stimulation (**Fig. 4.5 and 4.6**).

As was evaluated in the first assays, temporal changes between the first and second stimulus can impact the degree of training. Thus, again, different resting periods were used.

BMDMs showed higher production of proinflammatory cytokines after BCG stimulation, while with HK Candida that wasn't observed (**Fig. 4.4**).

As was already expected, and reinforced by the previous results, BCG stimulation induced a higher proinflammatory cytokine production after LPS restimulation (**Fig. 4.5 and 4.6**). When it comes to HK Candida, even though it did not induce the production of proinflammatory cytokines by itself, a trained phenotype was observed when restimulated with LPS. However, this phenomenon was only observed after a 6-day resting period (**Fig. 4.5 and 4.6**).

However, Pam-3-cys showed, by itself, a high pro-inflammatory effect, and ended up decreasing the training effect on BCG-stimulated BMDMs after a 2-day rest time.

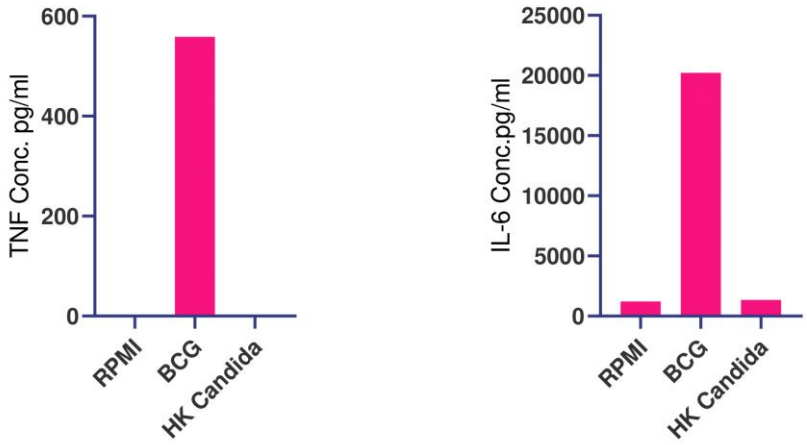


**Figure 4.4. Pro-inflammatory cytokine production after first stimulation with BCG or HK Candida.** TNF and IL-6 production after the first stimulus. Cells were stimulated for 24 hours with BCG or HK Candida. RPMI-stimulated cells were used as a control. Data are shown as means ± standard errors of the means. p values < 0.05 were considered significant, with levels of significance as follows: *p < 0.05; **p < 0.01; ***p < 0.001; ****p < 0.0001; ns, not significant. P values were derived from a two-way analysis of variance (ANOVA) with a multiple-comparison test.

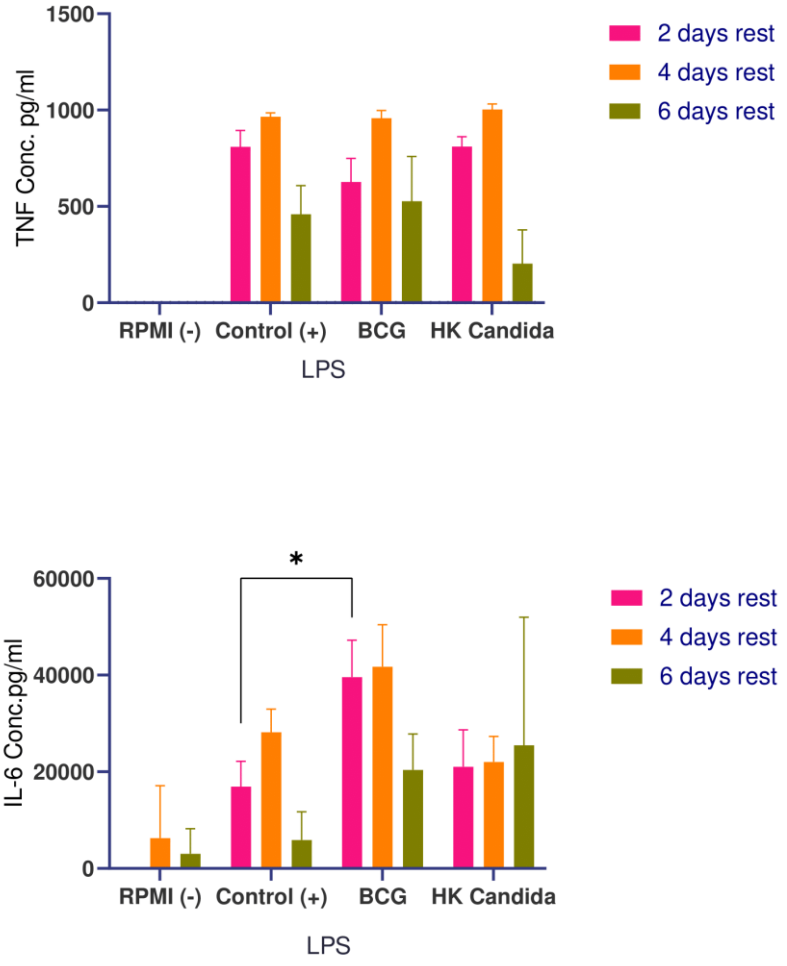

**Figure 4.5. Training is induced by BCG and Heat Killed Candida upon restimulation with LPS.** TNF and IL-6 production after LPS restimulation. After training the cells rested for 2,4 or 6 days. RPMI-stimulated cells were used as a negative control and LPS stimulated as a positive control. Data are shown as means ± standard errors of the means. p values < 0.05 were considered significant, with levels of significance as follows: *p < 0.05; **p < 0.01; ***p < 0.001; ****p < 0.0001; ns, not significant. P values were derived from a two-way analysis of variance (ANOVA) with a multiple-comparison test.

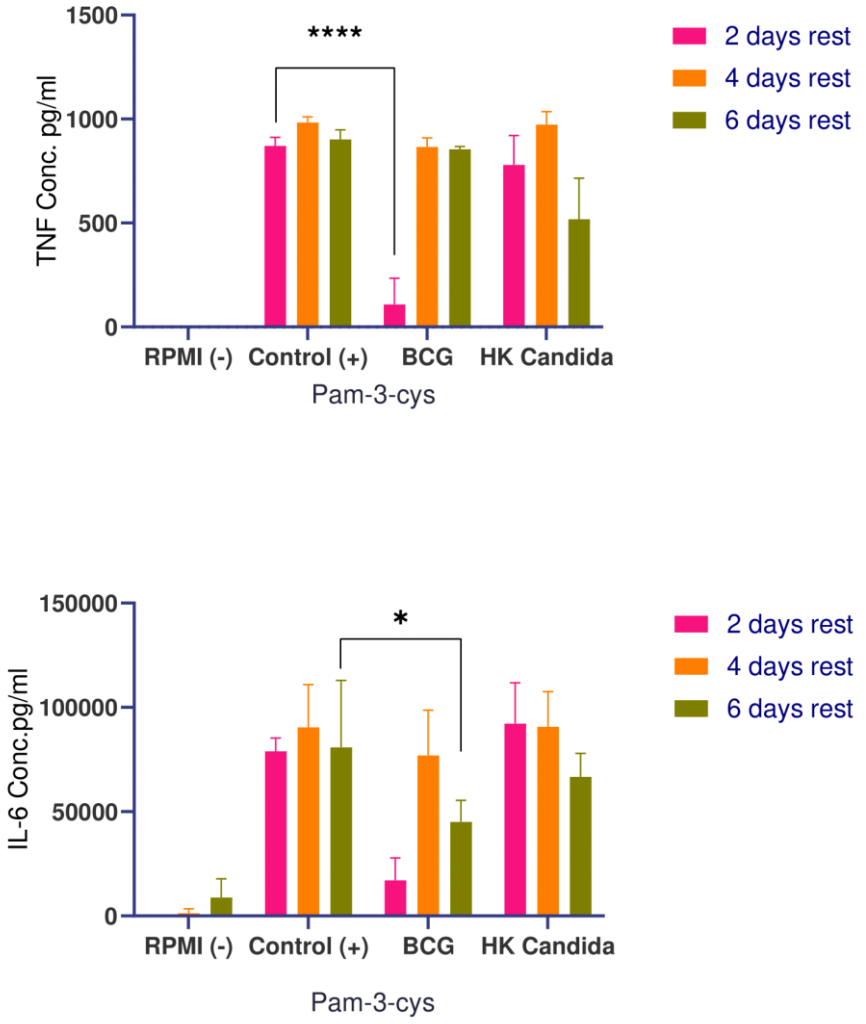


**Figure 4.6. Training is not induced by BCG and Heat Killed Candida upon restimulation with Pam-3-cys.** TNF and IL-6 production after P3C restimulation. After training the cells rested for 2,4 or 6 days. RPMI-stimulated cells were used as a negative control and P3C stimulated as a positive control. Data are shown as means ± standard errors of the means. p values < 0.05 were considered significant, with levels of significance as follows: *p < 0.05; **p < 0.01; ***p < 0.001; ****p < 0.0001; ns, not significant. P values were derived from a two-way analysis of variance (ANOVA) with a multiple-comparison test

These results suggest that both BCG and HK Candida can be used to induce trained immunity in BMDMs, nonetheless, BCG remains the best inducer of this trained phenotype. As a second stimulus, LPS obtains the best results, since P3C induced a high inflammatory state even on non-trained cells. With these observations, we can conclude that LPS acts as a better second insult than P3C, as the latter elicits an excessively inflammatory response on its own, unable to induce a stronger innate immune response when applied to BCG-trained cells.

### 4.2.1-Stimulations do not affect cell viability

Based on the previous results, a viability assay was performed to ensure that the BMDMs weren't affected by the high inflammatory responses (**Fig. 4.7**). This kind of assay also ensures that the viability of the cells is not the cause for differences in measured cytokine concentration, making the readouts viable and trustful.

The cells were analyzed after supernatant collection, following restimulation. The concentration of DNA, assessed for each well, was calculated based on fluorescence measurements made using a microplate reader with excitation at 480 nm and emission detection at 520 nm.

BMDMs showed no significant alterations in DNA concentration after the stimulations when compared with non-stimulated cells (**Fig. 4.7 a, b**). On cells stimulated with P3C, the DNA concentration was similar to the RPMI-stimulated ones (**Fig. 4.7 b**).

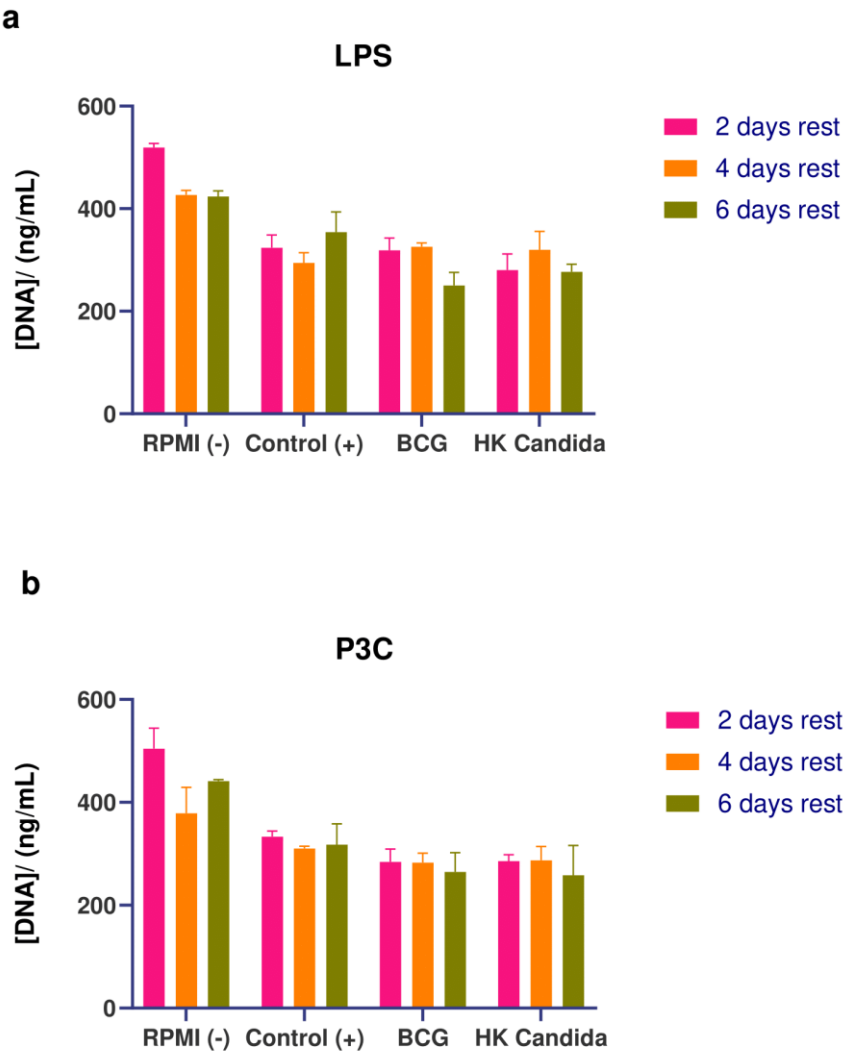


**Figure 4.7. Stimulations do not affect cell viability. (a)-** DNA concentration (ng/mL) after LPS restimulation. **(b)-** DNA concentration (ng/mL) after P3C restimulation. Data are shown as means ± standard errors of the means.

## 4.3- Pam-3-cys show increased inflammation

Pam-3-cys is a TLR1/TLR2 agonist used as a second stimulus to induce trained immunity in immune cells, like monocytes. However, based on our first trial using this second stimulus, we hypothesized that Pam-3-cys induces a high increase in inflammation rather than inducing trained immunity in BMDMs.

To address this issue, a trained immunity assay was performed using both BCG and HK candida to train the BMDMs (**Fig. 4.8**), and a range of different Pam-3-cys concentrations as a second stimulus (**Fig. 4.9**). For that, BMDMs were incubated with BCG (45 µg/mL), or HK Candida for 24 hours. The cells were then restimulated with P3C. As a positive control, non-trained cells

stimulated with P3C were used. ELISA readout was performed on supernatants collected after the first (**Fig. 4.8**) and second stimulation (**Fig. 4.9**).

When comparing trained and non-trained cells, in all the different Pam-3-cys concentrations, non-trained cells show already a high proinflammatory cytokine production (**Fig. 4.9**). Furthermore, trained cells have a lower cytokine production noticeably lower in HK Candida-trained cells compared to BCG training (**Fig. 4.9**).

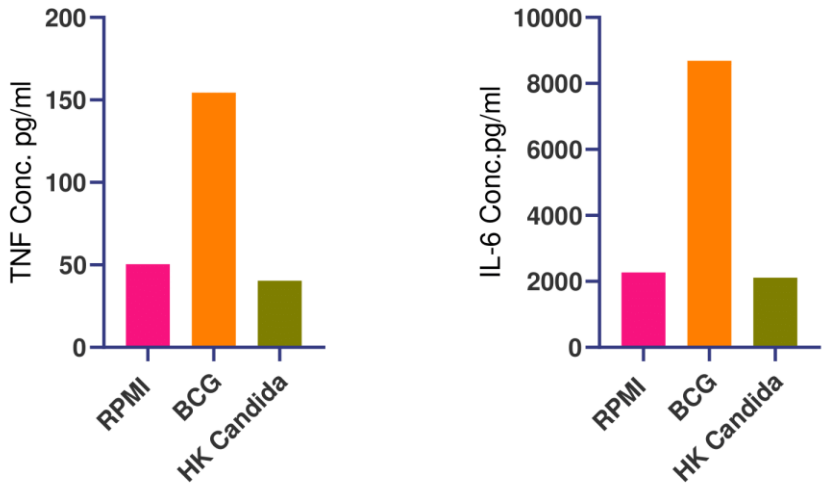


**Figure 4.8. Pro-inflammatory cytokine production after first stimulation with BCG or HK Candida.** TNF and IL-6 production after the first stimulus. Cells were stimulated for 24 hours with BCG or HK Candida. RPMI-stimulated cells were used as a control. Data are shown as means ± standard errors of the means. p values < 0.05 were considered significant, with levels of significance as follows: *p < 0.05; **p < 0.01; ***p < 0.001; ****p < 0.0001; ns, not significant. P values were derived from a two-way analysis of variance (ANOVA) with a multiple-comparison test.

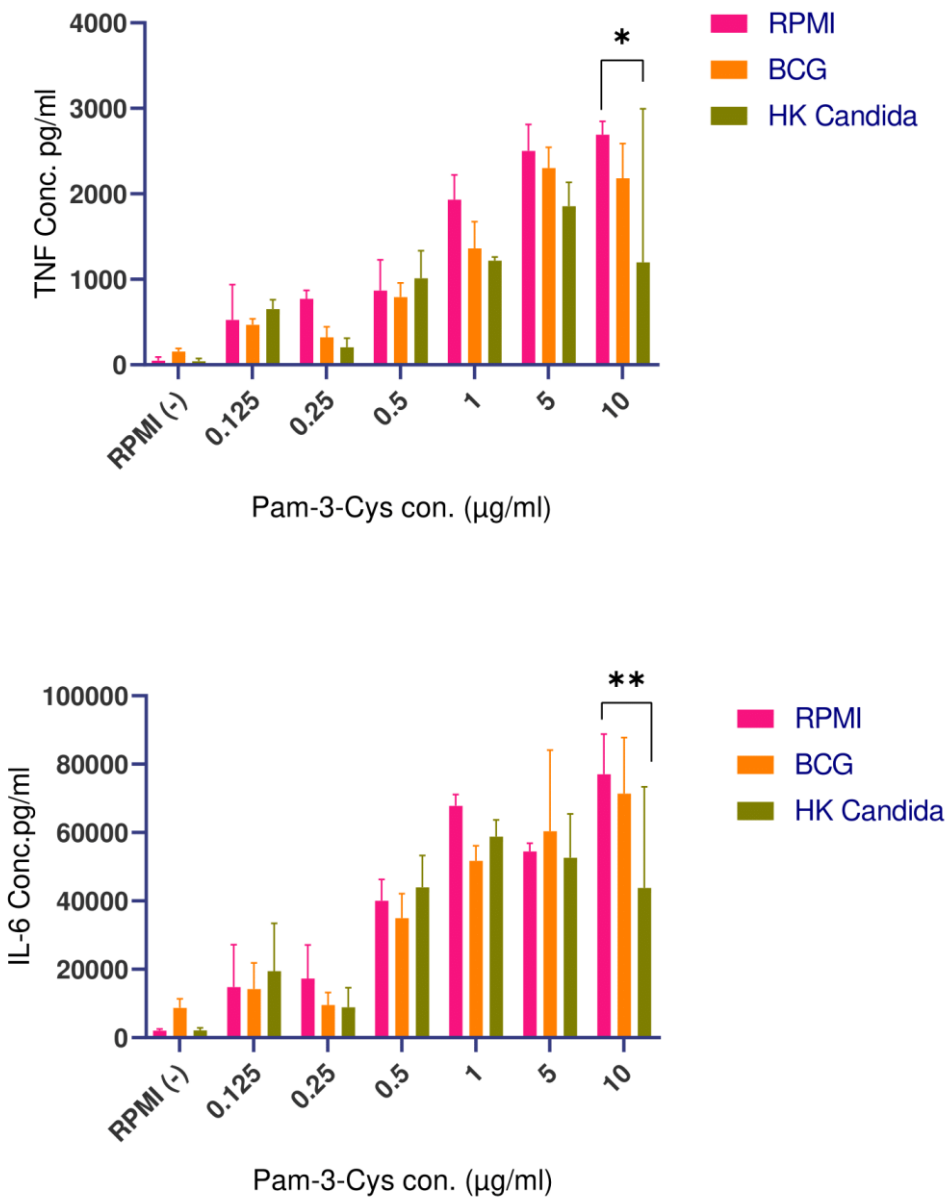


**Figure 4.9. Pam-3-cys induces high inflammation**. TNF and IL-6 production after P3C restimulation. P3c was used in 0.125; 0.25; 0.5; 1; 5; 10 µg/mL After training the cells rested for 4 days. RPMI-stimulated cells were used as a negative control and P3C stimulated as a positive control. Data are shown as means ± standard errors of the means. p values < 0.05 were considered significant, with levels of significance as follows: *p < 0.05; **p < 0.01; ***p < 0.001; ****p < 0.0001; ns, not significant. P values were derived from a two-way analysis of variance (ANOVA) with a multiple-comparison test.

These results suggest that besides Pam-3-Cys works as an excellent second stimulus in monocytes, it is too inflammatory by itself when it comes to macrophages, preventing a trained immunity phenotype from developing.

## 4.4-Trained immunity is induced in trained cells when re-stimulated with Tumor Culture Medium and LPS

LPS has been commonly used as a secondary stimulus to induce a trained response. Once it was understood that LPS could lead to a trained immunity response in BMDMs, we wanted to address whether these cells could respond to tumor-secreted factors. To access this B16F10 culture supernatants were used as a secondary stimulus (**Fig. 4.10 and 4.11**).

A trained immunity assay was performed using BCG to train the BMDMs, and tumor culture medium (TCM) at different concentrations (40 and 70 %) as a second stimulus. After training, the cells rested for 4 days and then were restimulated with TCM (**Fig. 4.10**). As a positive control, non-trained cells stimulated with TCM were used. ELISA readout was performed on supernatants collected after the first and second stimulation.

BCG-trained BMDMs produced a significantly higher TNF and IL-6 when restimulated with B16F10 culture supernatant at a 70 % concentration when compared to untrained controls (**Fig. 4.10**). Based on these first results, we hypothesized that restimulating these cells with LPS would have an accumulative effect on the TCM-induced trained immunity.

To this end, BMDMs were trained with BCG in the presence of TCM (40 and 70 %), and after 4 day resting period, LPS was added. TCM and LPS show a clear synergetic effect on inducing a trained immunity phenotype, by showing a much higher cytokine production (**Fig. 4.11**).

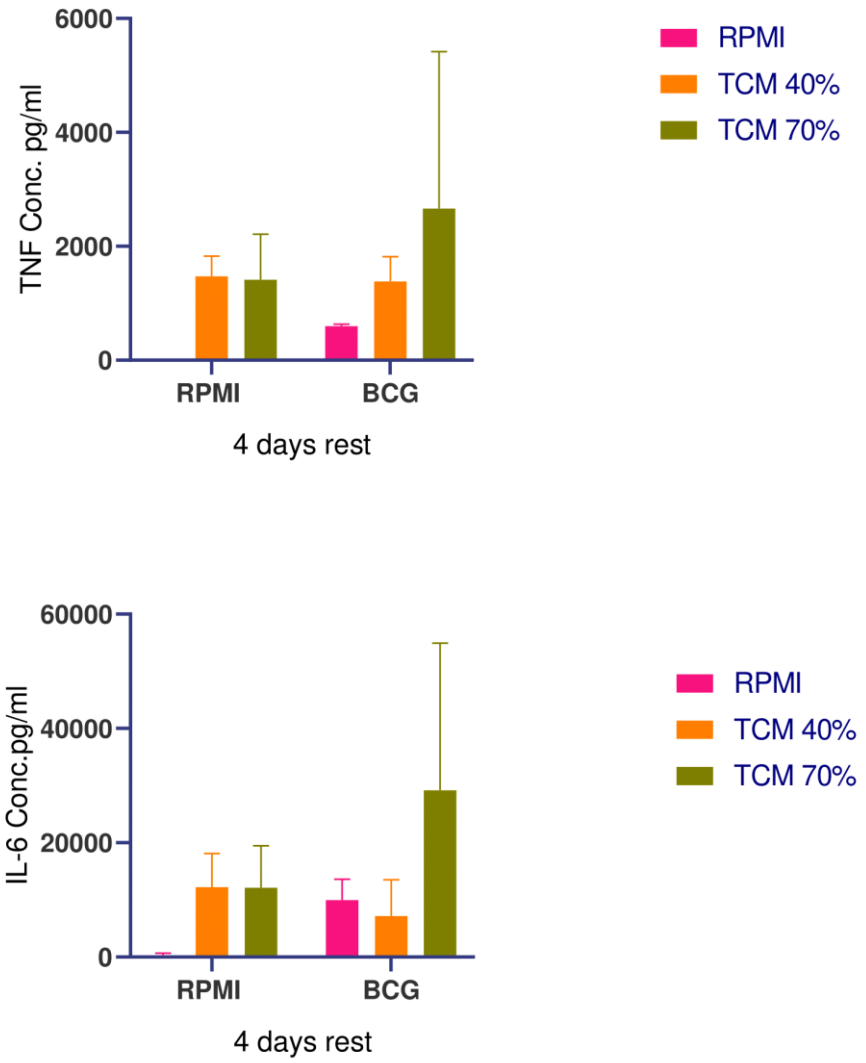


**Figure 4.10. TCM induces trained immunity phenotype**. TNF and IL-6 production after TCM restimulation. Cells were stimulated for 24 hours with BCG. After training cells rested for 4 days. BMDMs were restimulated with TCM. RPMI-stimulated cells were used as a control. Data are shown as means ± standard errors of the means. p values < 0.05 were considered significant, with levels of significance as follows: *p < 0.05; **p < 0.01; ***p < 0.001; ****p < 0.0001; ns, not significant. P values were derived from a two-way analysis of variance (ANOVA) with a multiple-comparison test.

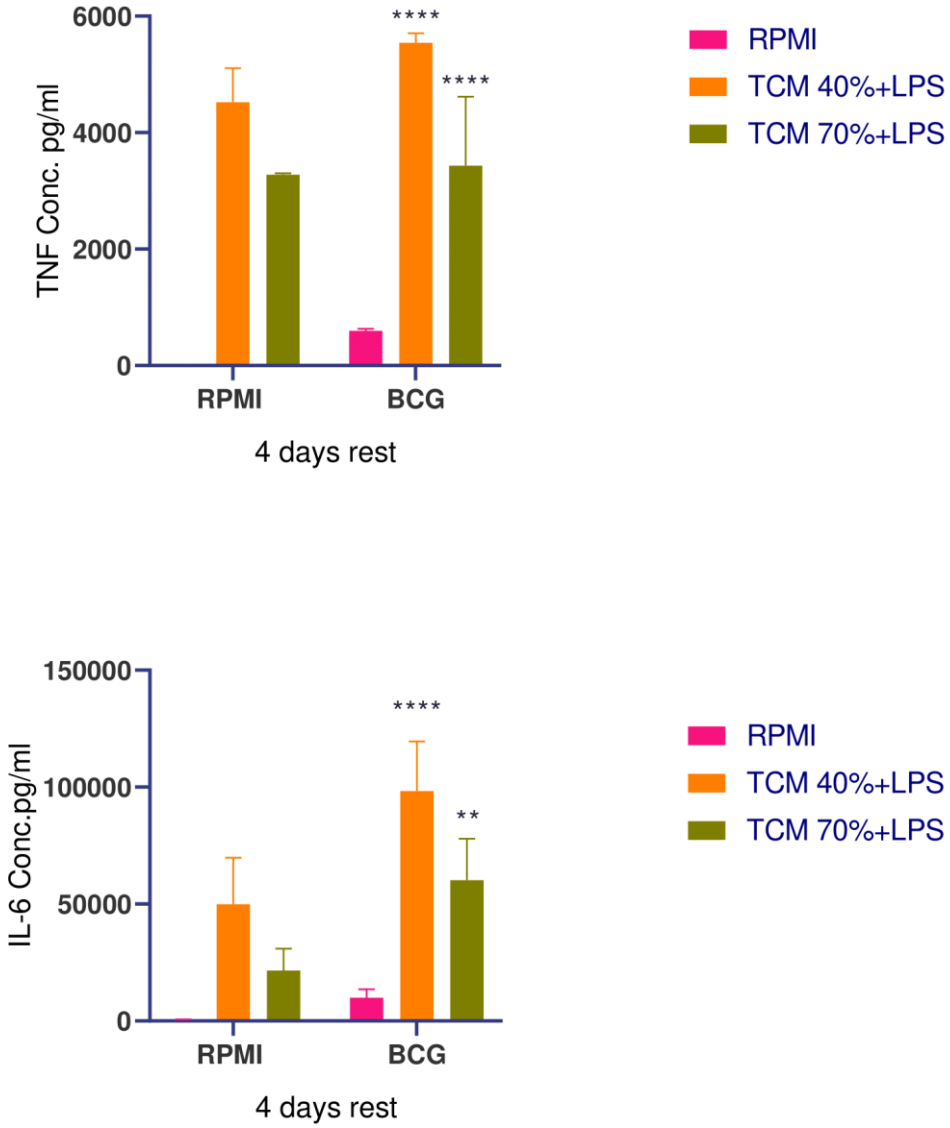


**Figure 4.11. TCM and LPS induce trained immunity phenotype**. TNF and IL-6 production after TCM and LPS restimulation. Cells were stimulated for 24 hours with BCG. After training cells rested for 4 days. BMDMs were restimulated with TCM and LPS. RPMI-stimulated cells were used as a control. Data are shown as means ± standard errors of the means. p values < 0.05 were considered significant, with levels of significance as follows: *p < 0.05; **p < 0.01; ***p < 0.001; ****p < 0.0001; ns, not significant. P values were derived from a two-way analysis of variance (ANOVA) with a multiple-comparison test.

These results suggest that BCG-trained macrophages elicit a trained response upon re-exposure not only to LPS but also to tumor-derived factors.

## 4.5-Magnetic Resonance Imaging (MRI) allowed thyroid visualization

With the goal of establishing a thyroid cancer mouse model in mind, a small imaging pilot was carried out.

The small size of the thyroid gland in a C57BL/6J mouse (usually measuring 20-30 mm in length and 10-15 mm in width) made it necessary the development of this pilot. To further understand the feasibility of accessing tumor growth in the thyroid gland in the upcoming mouse model.

Using magnetic resonance imaging (MRI), the possibility and feasibility of precisely visualizing the mouse thyroid gland were evaluated (**Figure 4.12**).

Thyroid tissues were classified according to the World Health Organization criteria for the evaluation of mouse thyroid tumors.[66] The mouse thyroid was situated in the sub hyoid region, just below the laryngeal prominence, near the cricoid cartilage, on the first three or four tracheal rings. The gland was more deeply located compared with humans. Neighboring structures, such as submandibular salivary glands, and trachea were all visible.

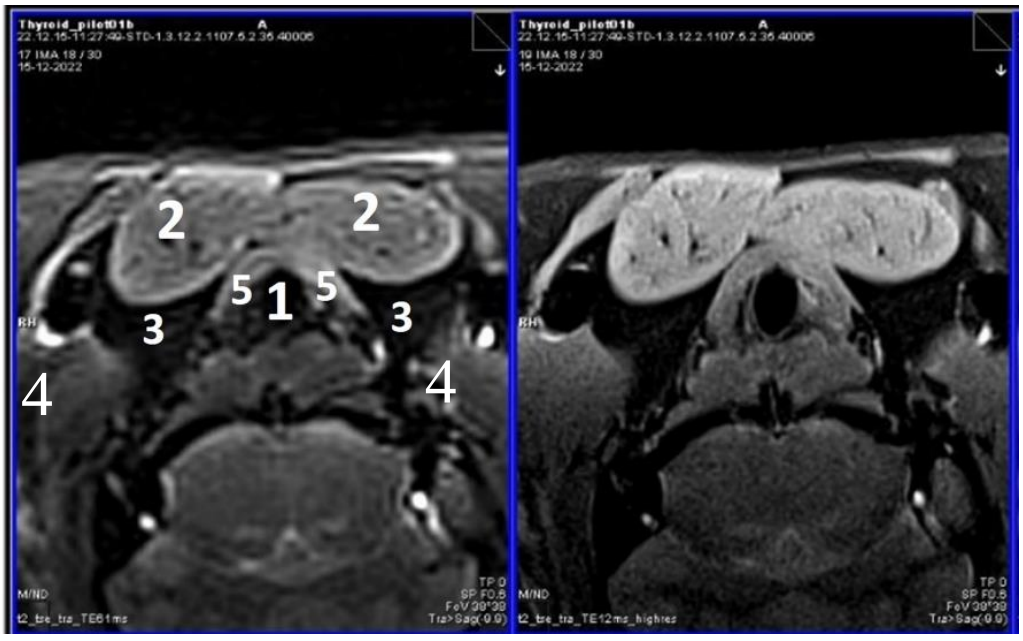


**Figure 4.12. Identification of thyroids component through MRI.** MRI transversal images of the sub hyoid and tracheal regions (thyroid region) in a normal mouse. Visible structures include (1) tracheal cartilage ring; (2) salivary gland; (3) sternohyoid and sternothyroid muscles; (4) sternomastoideus muscle; (5) thyroid lobes.

These results confirm that if a mouse ATC model was established, we could use MRI to evaluate the dimension and morphology of the mouse thyroid gland as well as tumor size and development.

## 4.6- BMDMs present the same phenotype in different-size dishes

A scale-down model is physically a smaller version of a large-scale process already established. This kind of model improves the process of the experiment, reduces costs, increases the speed, and helps with the overall feasibility of experiments.

For that reason and having in mind the next steps of the project, the process of culturing and differentiating BMDMs was scaled down and the differentiating state of the macrophages was tested (**Fig. 4.13)** as well as their training state (**Fig. 4.14**).

To assess this, different amounts of bone-marrow cells were cultured in different-sized TC-treated dishes and allowed to grow for 7 days in the presence of LCM. All dishes had the same treatment, and the number of cells per dish was calculated based on the growth area of each dish.

Finally, on day 7, BMDMs were harvested from each dish and tested via flow cytometry for the main macrophages' markers (**Fig. 4.13**), and ELISA for TNF and IL-6 production after direct LPS stimulation (**Fig 4.14**). The regularly used size dish (145x20 mm) with cells from 1 whole femur was used as a control.

Flow cytometry analyses revealed similar marker expression on all the different-size dishes. As expected, the main M1-macrophages markers F4/80 and CD11b showed a much higher expression on these cells (**Fig. 4.13**). Consequently, markers for M2-like macrophages, such as CD68 and CD206 showed almost no expression on these BMDMs.

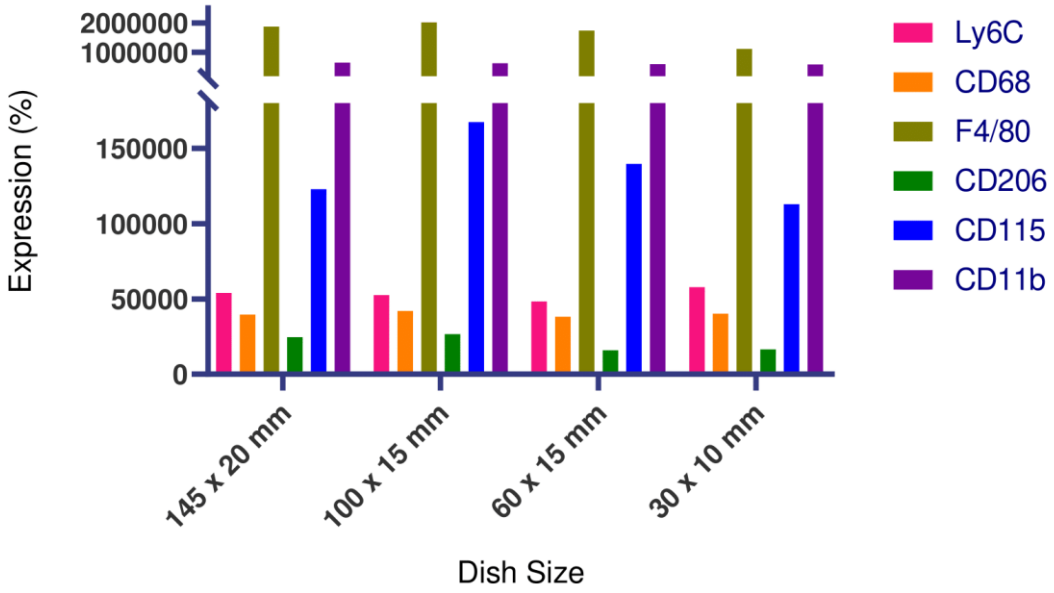


**Figure. 4.13. Dish size and number of cells cultured do not affect macrophage markers expression.** The graph shows the expression (%) of macrophage markers (Ly6C, CD68, F4/80, CD206, CD115, and CD11b) on BMDMs for each one of the different dishes.

However, the production of pro-inflammatory cytokines after LPS stimulation did not have the same results throughout all the dish sizes. The cells obtained from the smaller dish (30x10 mm) had noticeably less TNF (**Fig. 4.14 a**) and IL-6 (**Fig. 4.14 b**) production after LPS stimulation when compared with all the other dishes. These results indicate that these cells possess a different phenotype- less macrophage-like- and for that reason, this dish can't be used for BMDMs culture to ensure consistency in the experiments.

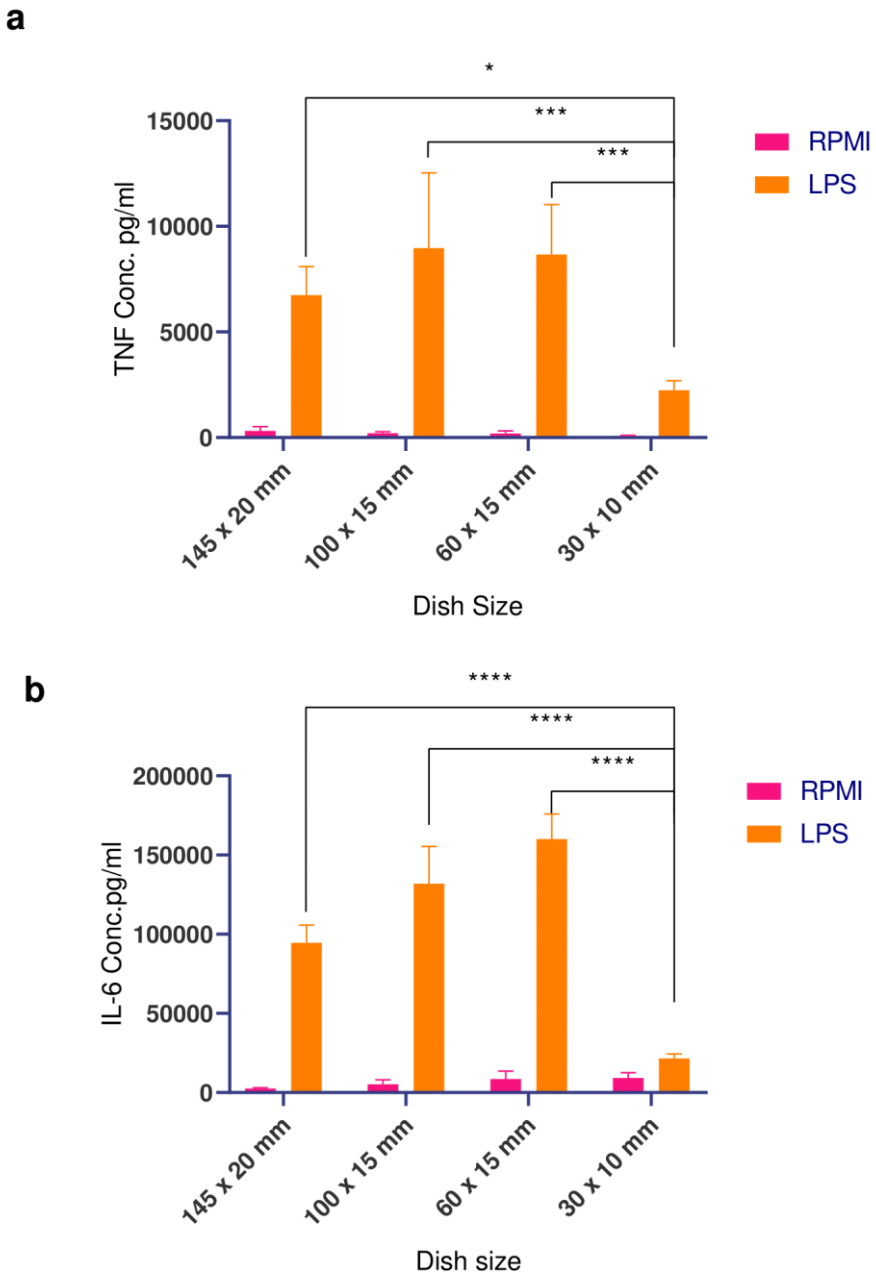


**Figure 4.14. Smaller dish affected proinflammatory cytokine production. (a)-** TNF and **(b)-** IL-6 production after LPS stimulation. RPMI-stimulated cells were used as a negative control. Data are shown as means ± standard errors of the means. p values < 0.05 were considered significant, with levels of significance as follows: *p < 0.05; **p < 0.01; ***p < 0.001; ****p < 0.0001; ns, not significant. P values were derived from a two-way analysis of variance (ANOVA) with a multiple-comparison test.

Together, these results show that culturing BMDMs in the next set of experiments could be done in smaller-sized dishes. The smallest size that can be used without compromising the

quality and viability of the BMDMs is 60x15mm. Using this dish size would facilitate the feasibility of the next experiments, allowing the culture of BMDMs from multiple samples.

## 4.7- Immune system is affected by B16F10 melanoma tumor

The interactions between a tumor and the immune system are made through complex mechanisms that can affect tumor growth, immune surveillance, and the potential of immunotherapies.

Taking this into account, we wanted to further understand the effect of a tumor on the immune cells and its progenitors. To ensure the continuality of the project with the eventual engineering of immunotherapies for ATC we used an already established melanoma mouse model.

To that aim, we performed an *in vivo* study in C57BL/6 mice that were subcutaneously injected with $1x10^5$ B16F10 melanoma cells. We established a control group without tumor inoculation (naive mice), a 1-week tumor inoculation group, and a 2-week tumor inoculation group (n=7 per group). In all tumor-bearing mice, palpable tumors were established.

At indicated periods after tumor inoculation, mice were euthanized, blood was collected, and the spleen and two femurs were harvested.

To analyze the effect of tumor inoculation and time after tumor inoculation in immune cells and their progenitors, cells from blood, spleen, and bone marrow were analyzed by flow cytometry (**Fig. 4.15, 4.16, and 4.17**).

Myeloid (**Fig 4.15**) and lymphoid cells (**Fig 4.16**) from all different samples, didn’t reveal significant differences between the control and tumor groups. In addition, the cells evaluated in the progenitors' panel (**Fig 4.17**) showed similar results between all three groups.

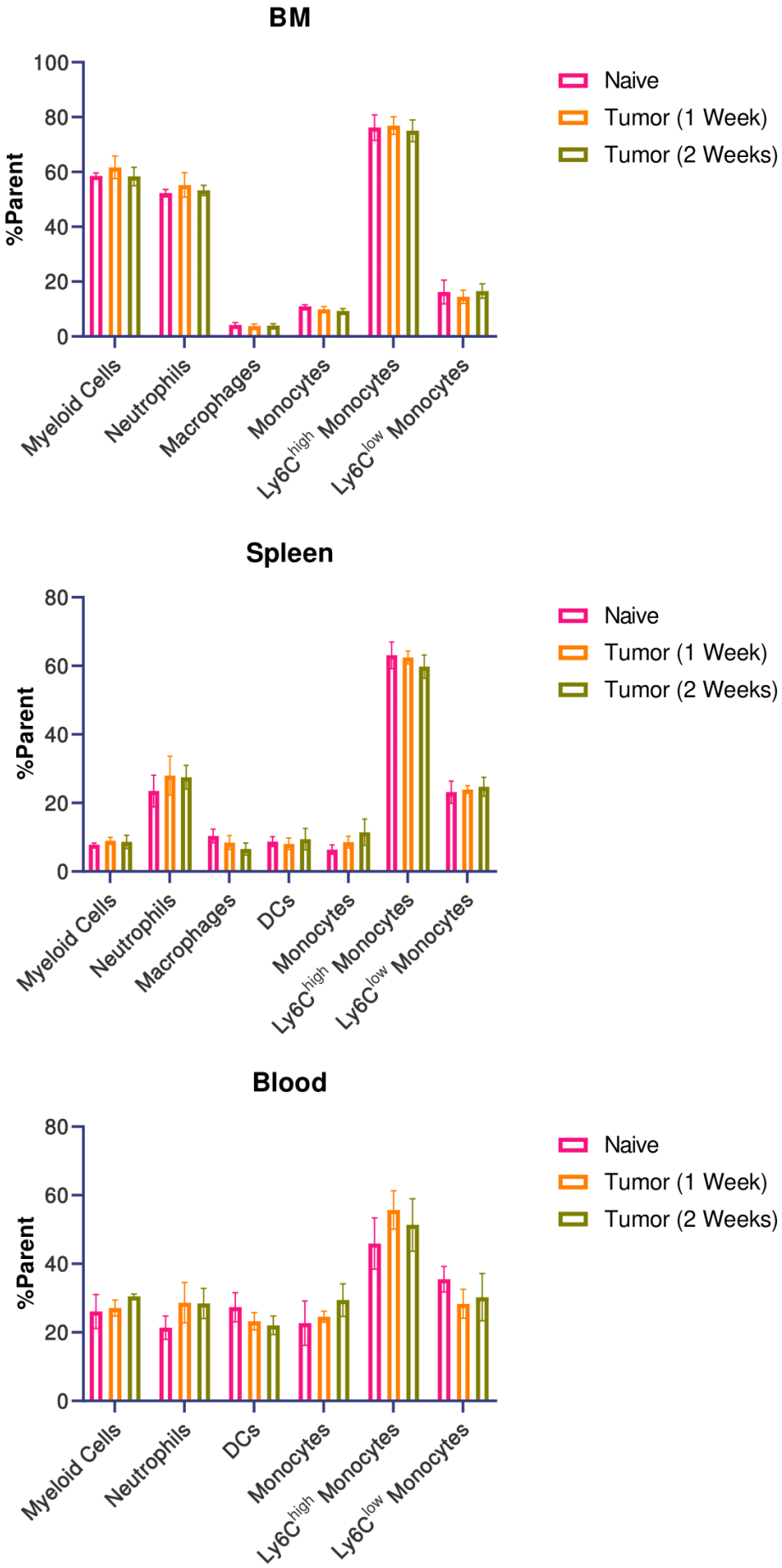
BM
%Parent
100
80
60
40
20
0
Myeloid Cells
Neutrophils
Macrophages
Monocytes
Ly6C^high Monocytes
Ly6C^low Monocytes
Naive
Tumor (1 Week)
Tumor (2 Weeks)
Spleen
%Parent
80
60
40
20
0
Myeloid Cells
Neutrophils
Macrophages
DCs
Monocytes
Ly6C^high Monocytes
Ly6C^low Monocytes
Naive
Tumor (1 Week)
Tumor (2 Weeks)
Blood
%Parent
80
60
40
20
0
Myeloid Cells
Neutrophils
DCs
Monocytes
Ly6C^high Monocytes
Ly6C^low Monocytes
Naive
Tumor (1 Week)
Tumor (2 Weeks)

**Figure 4.15. Myeloid cells (%Parent) for bone marrow (BM), splenocytes and blood cells.** Data are shown as means ± standard errors of the means. p values < 0.05 were considered significant, with levels of significance as follows: *p < 0.05; **p < 0.01; ***p < 0.001; ****p < 0.0001; ns, not significant.

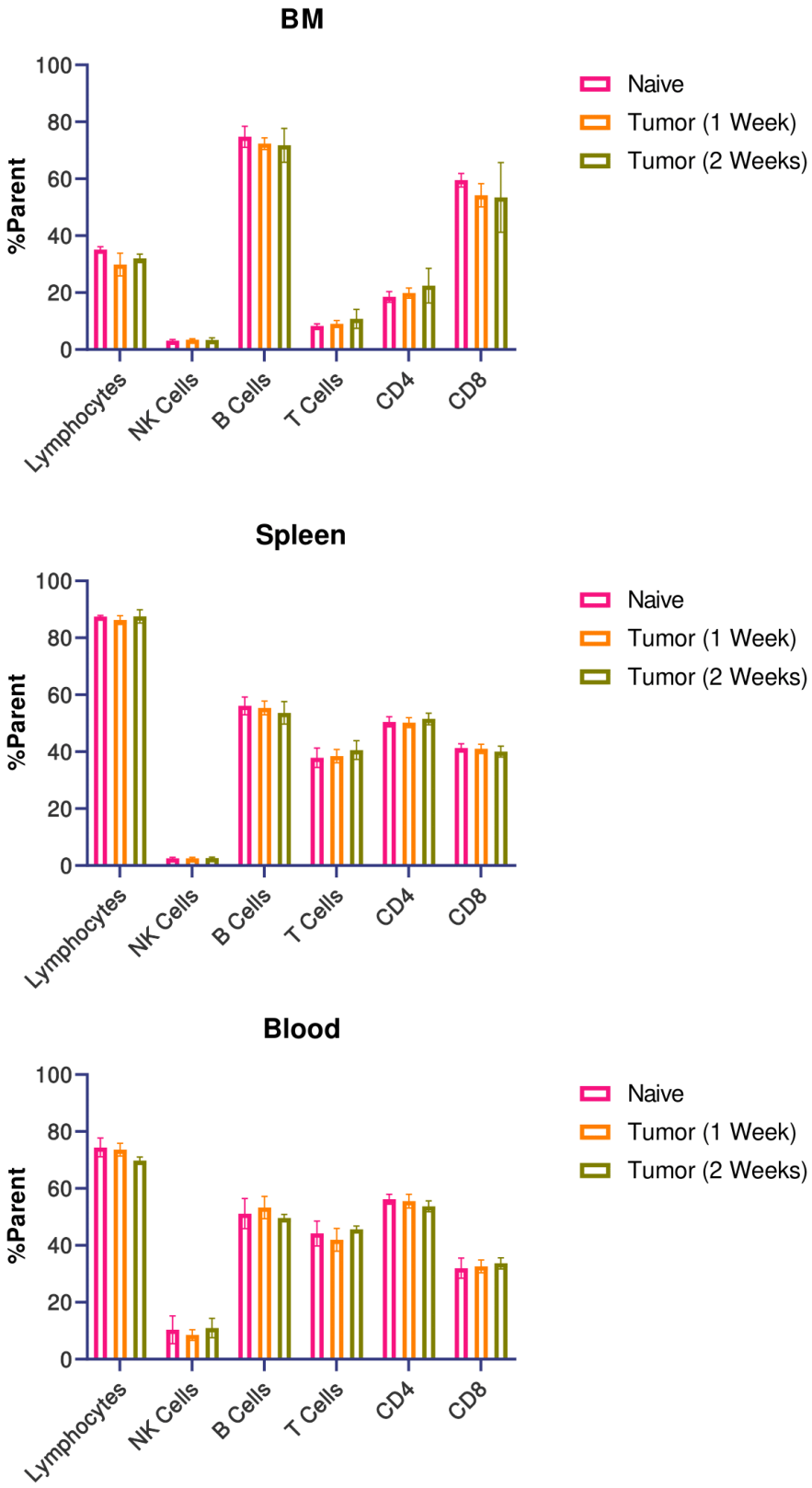

**Figure 4.16. Lymphoid cells (%Parent) for BM, splenocytes, and blood cells. (c)-** Progenitor cells (%Parent) for BM cells. Data are shown as means ± standard errors of the means. p values < 0.05 were considered significant, with levels of significance as follows: *p < 0.05; **p < 0.01; ***p < 0.001; ****p < 0.0001; ns, not significant. CD4, T helper cells; CD8, Cytotoxic T cells.

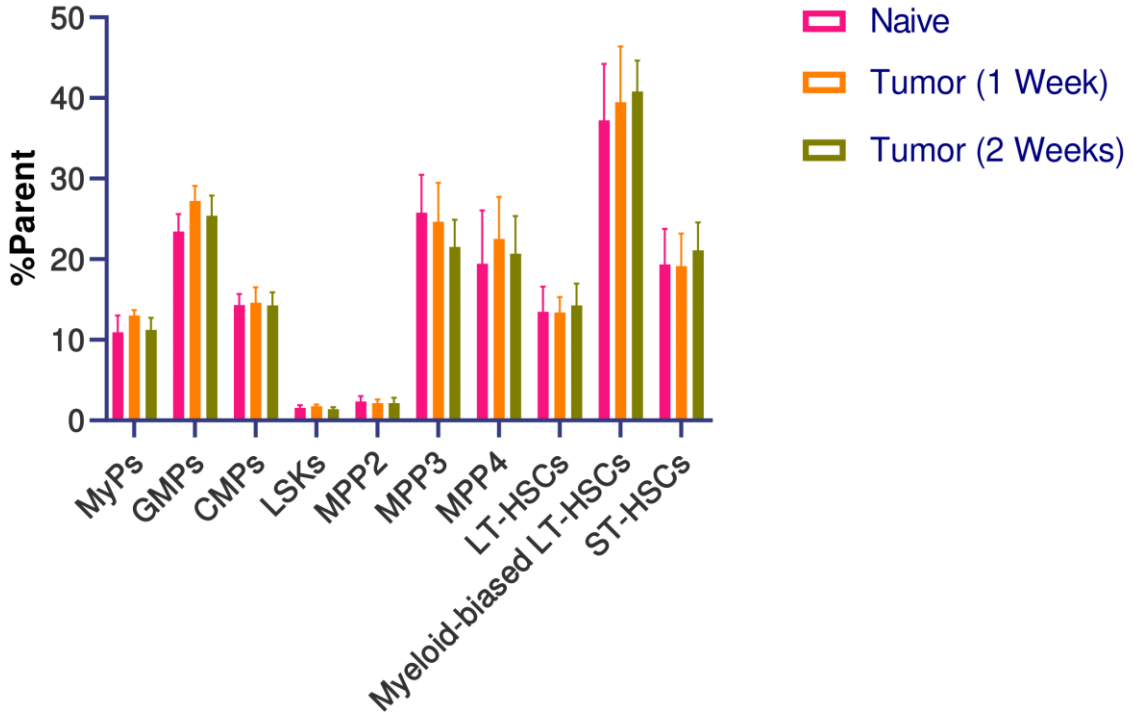


**Figure 4.17. Progenitor cells (%Parent) for BM cells**. Data are shown as means ± standard errors of the means. p values < 0.05 were considered significant, with levels of significance as follows: *p < 0.05; **p < 0.01; ***p < 0.001; ****p < 0.0001; ns, not significant. MyPs, Myeloid progenitors, GMPs, Granulocyte-macrophage progenitors; CMPs, Common myeloid progenitors; LSKs, Hematopoietic stem cells; MPP, Multipotent progenitor; MPP2, megakaryocyte/erythroid-biased MPPs; MPP3, Myeloid lineage-biased MPPs; MPP4, lymphoid lineage-biased MPPs; LT-HSCs, Long-term hematopoietic stem cells; ST-HSCs, Short-term hematopoietic stem cells.

After the establishment of the effect of tumor inoculation in immune cells and progenitors, we accessed the training state of BMDMs and splenocytes from the different groups. Thus, we determined inflammatory cytokine production following *in vitro* LPS restimulation (**Fig. 4.18 and 4.19**). The production of IL-6 and TNF was evaluated by ELISA.

It was observed that tumor inoculation affects the training state of both splenocytes and BMDMs, however in different, almost opposed ways.

Splenocytes from tumor-bearing mice show, after LPS stimulation, much higher production of IL-6 when compared to naive mice, but on the other side, the production of TNF is diminished in these cells.

In contrast, BMDMs from tumor-inoculated mice present higher TNF concentrations after LPS stimulation than IL-6 concentrations.

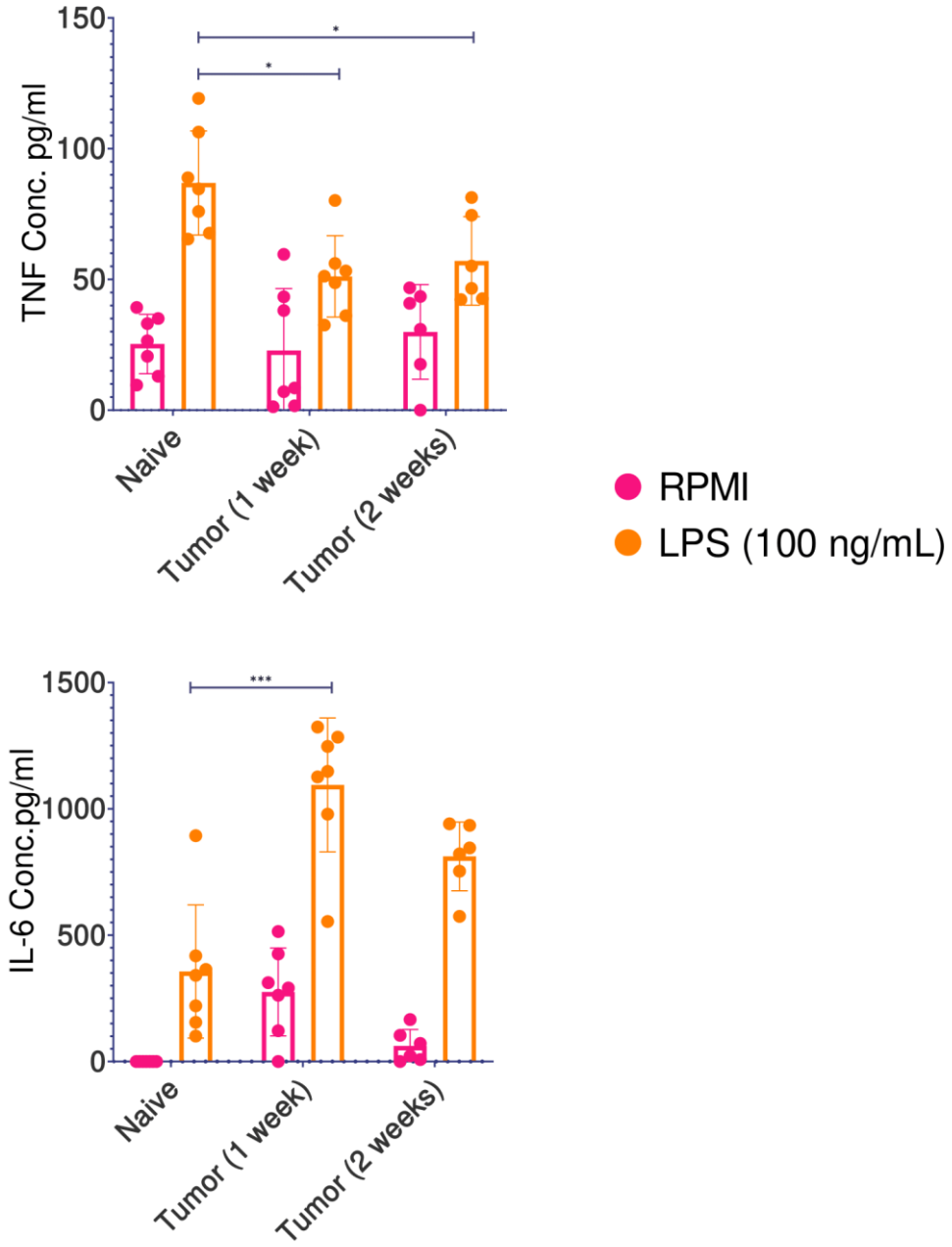


**Figure 4.18. Splenocytes production of TNF and IL-6 after LPS restimulation.** RPMI-stimulated cells were used as a negative control. Data are shown as means ± standard errors of the means. p values < 0.05 were considered significant, with levels of significance as follows: *p < 0.05; **p < 0.01; ***p < 0.001; ****p < 0.0001; ns, not significant. P values were derived from a Kruskal-Wallis analysis of variance (ANOVA) with a multiple-comparison test.

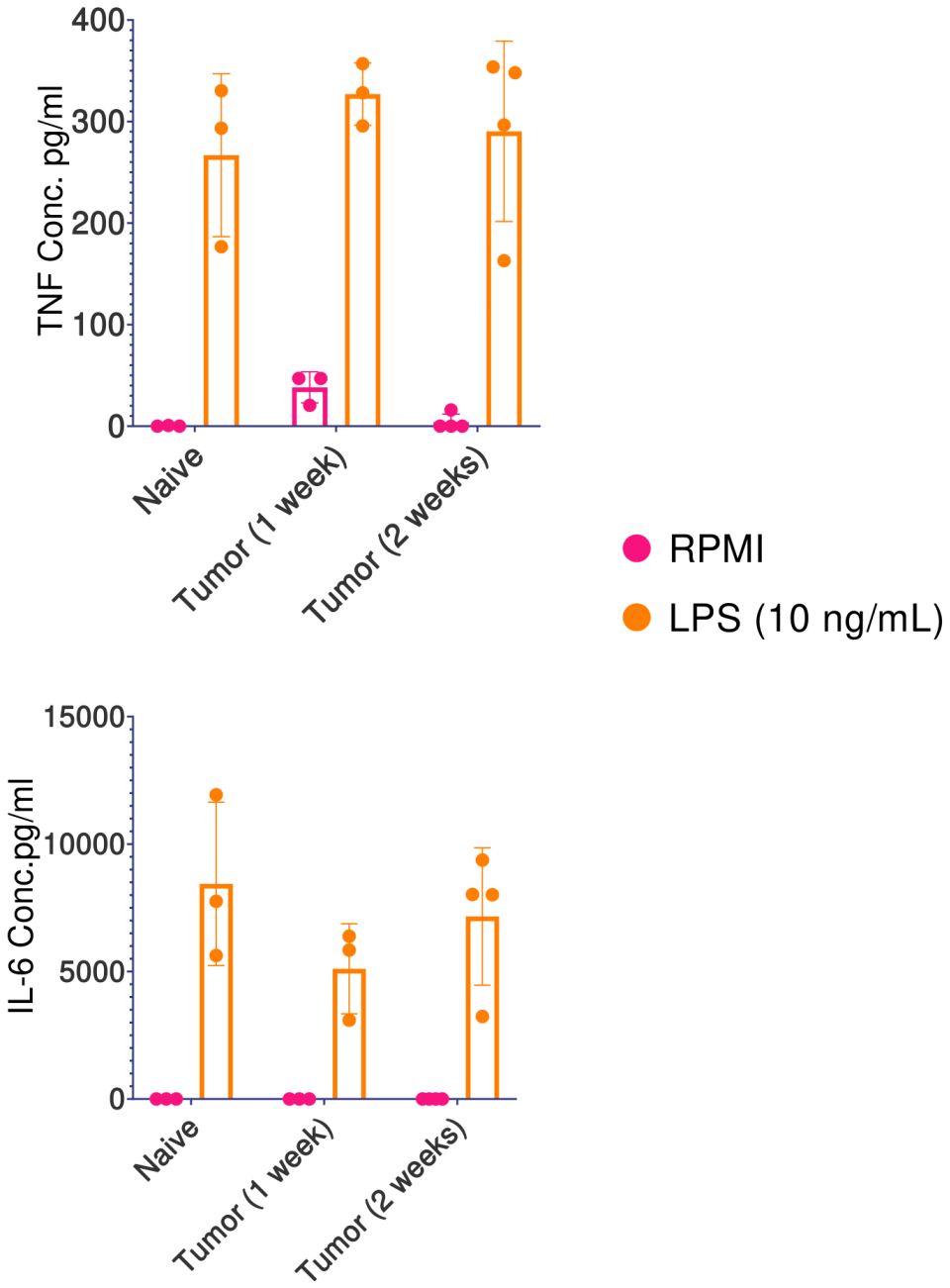


**Figure 4.19. BMDMs production of TNF and IL-6 after LPS stimulation.** RPMI-stimulated cells were used as a negative control. Data are shown as means ± standard errors of the means. p values < 0.05 were considered significant, with levels of significance as follows: *p < 0.05; **p < 0.01; ***p < 0.001; ****p < 0.0001; ns, not significant. P values were derived from a Kruskal-Wallis analysis of variance (ANOVA) with a multiple-comparison test.

Together these results suggest that although the effect of the tumor on the immune system is not seen in the number and percentages of immune cells and progenitors, it is clear that the tumor affects the immune state of innate immune cells.

# CHAPTER 5

# Discussion

In this study, we show how to optimally induce trained immunity in murine-derived BMDMs and how these cells respond in a tumoral environment. Besides, also established the effects of a tumor on the innate immune cells and their progenitors.

Despite all the increasing knowledge and research in the field of oncology, a lot of cancers still don't have an effective therapy established. One example of this is Anaplastic thyroid cancer, which doesn't have a reliable treatment nowadays.[26,32,67,68]

Immunotherapy has revolutionized cancer treatment, but the existing approaches are limited in their effectiveness. One of the most commonly used immunotherapies, known as checkpoint blockade therapy[45], only benefits a small percentage of patients and is often accompanied by severe side effects. These therapies primarily target the adaptive immune system, while neglecting the activation of the innate immune system.

In recent years, the activation of this side of the immune system has earned significant attention due to the discovery of trained immunity.[37–40] Trained immunity describes a phenomenon where innate immune cells, like monocytes and macrophages, undergo long-lasting functional changes upon encountering specific triggers. This empowers innate immune cells to mount a heightened response upon subsequent encounters with various pathogens and non-infectious stimuli.

Increasing evidence highlights the substantial role of the innate immune system in the context of cancer.[55,62] Although current understanding predominantly focuses on the infiltration of innate immune cells within the tumor, it is crucial to acknowledge that tumors can exert systemic effects through diverse mechanisms. Tumor-derived factors possess the capacity to impact innate immune cells circulating in the bloodstream, as well as their precursor cells located in the bone marrow.

Having this in mind, it is crucial to investigate new therapy approaches to anaplastic thyroid cancer, and trained immunity can be an excellent target for it.

Our approach aims to describe the optimal conditions for the induction of trained immunity in BMDMs, study their reaction in a tumor microenvironment, and understand in what way a tumor modulates the innate immune system.

In the first part of the project, we described the optimal conditions for the induction of trained immunity in an *in vitro* model in murine-derived BMDMs. Prior use of this model has explored

various aspects, however, the precise conditions required to effectively induce trained immunity have not yet been established.

In this model, microbial or endogenous stimuli, such as β-glucan, MDP, HK Candida, and BCG were added to BMDMs for 24 hours (training period), after which the cells were washed and allowed to rest in culture medium, followed by restimulation with unrelated antigens (LPS and Pam-3-cys).

This study provides several new insights into this basic model of trained immunity that will aid with the design of the next steps of the project. First, we found that the magnitude of the induction of trained immunity is highly correlated with the time that trained cells are left to rest and with the concentration used, most notably for BCG-trained cells. After a 2-day-rest period, trained BMDMs had a much higher response to the second trigger, but only when trained with a high concentration of BCG. The importance of resting time for the establishment of trained immunity has also been demonstrated in various studies [63] which is correlated with our findings. Besides this fact, BCG-trained cells were also the ones that showed the best response towards a trained phenotype, after LPS restimulation. This effect is dependent on NOD2 signaling, autophagy, and epigenetic changes.

Another observation of this study is that trained immunity does not only translate into an increased proinflammatory response of BMDMs. It involves a general increase in the responsiveness of the cells, as witnessed by the amplification of NO production after LPS restimulation. This NO production is correlated with metabolic activation and can regulate the production of inflammatory molecules. Besides, the high activation of the cells and the trained immunity phenotype did not affect their viability.

Heat-killed *Candida albicans* and Pam-3-cys were also tested as means to induce trained immunity on the murine-derived BMDMs. Pam-3-cys showed an induction of a high inflammatory response on BMDMs, not being able to induce trained immunity in these cells. Our concern was that P3C was affecting their viability, however, the DNA concentration of cells restimulated with 1 µg/mL was unaltered. When tested higher concentrations of this stimulus in trained cells, they showed a decrease in proinflammatory cytokine production. Pam-3-cys shown in previous studies to be an excellent stimulus for the induction of trained immunity in human monocytes[63], however in murine-derived BMDMs it didn't show to be the optimal choice.

This optimization of training assays to murine-derived BMDMs led us to use BCG at 45 µg/mL with a restimulation of LPS after 4 days as the optimal conditions to trained immunity induction.

Studies developed in human BMDMs trained with β-glucan showed that these cells elicit a trained response upon stimulation with tumor-derived factors.[61] This suggests that the activation of trained immune responses may play a role in the immunosurveillance mechanisms that hinder the progression of tumors.

To access this hypothesis in murine-derived BMDMs, we restimulated BCG-trained BMDMs with melanoma tumor culture medium in different concentrations. Our results are in line with the expectations, since BCG-trained macrophages, responded to the tumor-derived factor with an increase in proinflammatory cytokine production. In addition, LPS stimulation had a synergetic effect with the tumor factors which indicates that the induction of a trained response can occur in a tumor environment and that different stimuli can augment that response.

In parallel, MRI imaging was tested as a means to, in further steps of the project, access tumor growth. Using a wild-type C57BL/6J mouse, MRI allowed us to identify the subhyoid and tracheal regions of the mouse, including the thyroid lobes.

In order to proceed with the project, a scaled-down experiment had to be developed in BMDMs culture and differentiation. This kind of model improves the process of the experiment, reduces costs, increases speed, and helps with the overall feasibility of experiments. The aim was to analyze 21 different samples of BMDMs in the next step of the project. For this, bone-marrow cells were cultured in different-sized dishes and allowed to differentiate into BMDMs. Their training state and phenotype were analyzed.

The macrophage phenotype was analyzed by flow cytometry. The expression of the following markers was accessed Ly6C, CD68, F4/80, CD206, CD115, and CD11b. These markers were chosen based on the typical macrophage (M1) phenotype.

Macrophages are usually gated as CD45+ CD11b+ F4/80+ cells, so the expression of CD11b and F4/80 were assessed. As was expected the CD11b and F4/80 had the highest expression on these cells.

CD68 and CD206 are M2-like macrophage markers, so their expression was evaluated on these BMDMs to ensure the right phenotype. Their expression was observed to be very low on these BMDMs, which is in line with an M1-phenotype, showing that the size of the dish does not alter the phenotype of the macrophages.

On the other side, also Ly6C was analyzed since it is a monocyte marker. Once again, this marker was less expressed on these BMDMs, which confirms the full differentiation to macrophages.

As mentioned before, tumors can have systemic effects which can affect innate immune cells in circulation or even in the bone marrow. These changes could limit the response of BMDMs to training and for that reason, we analyzed to what extent circulating and progenitor cells may already be affected by the presence of a tumor *in situ*.

Alterations like this have been established for TC patients in previous studies [58], however, fewer studies have been developed in mouse models. To assess this issue, we analyzed tumor-bearing-mice, 1 or 2 weeks after tumor inoculation. Myeloid and lymphoid cells from the spleen, blood, and bone marrow were analyzed by flow cytometry together with bone marrow progenitors. The training state of splenocytes and BMDMs was analyzed after LPS stimulation and proinflammatory cytokine production was analyzed.

Although no relevant differences were observed in the flow cytometry results, through stimulation of splenocytes and BMDMs with LPS it was possible to observe that the tumor influences the innate immune system. The cells from tumor-bearing mice, after LPS stimulation, showed a variation in TNF and IL-6 production. However, this variation was inversed in splenocytes and BMDMs.

In conclusion, with these findings, we propose optimal conditions to induce a trained immunity phenotype in murine-derived BMDMs and show that these trained macrophages elicit a trained response after stimulation with tumor-derived factors resulting in anti-tumor immunity. Besides, we showed that tumor inoculation has an effect at a systemic level, indicating that rewiring of these cells through therapy might be a strategy to enable active tumor killing by immune cells. Our study paves the way to explore trained immunity induction as a therapy for anaplastic thyroid cancer.

## 5.1- Limitations and future directions

Like every research project, this study presents limitations. It is important to take them into account to prevent incorrect assumptions taken from the results. In this section, we explain the principal limitations and future directions of the study.

1) Due to the time limitations of the project, we were unable to establish an ATC mouse model. For that reason, all tumor-involved experiments were developed using an

already-established melanoma mouse model. Clinically, melanoma is, in general, an immunogenic tumor. We can extrapolate the results in this model to ATC, however, further analyses on systemic effect and training state of innate immune cells must be developed using an adequate ATC mouse model.

2) Another limitation is the sample size for the assessment of the training state of bone marrow cells and BMDMs. From 7 mice per group, only 3 per group were analyzed for proinflammatory cytokine production after LPS stimulation, which contributes to less robustness of our results. For bone marrow cells, we were unable to analyze the training state due to contaminations in the culture. Further analysis using an ATC mouse model, can give us a better understanding of the training effect of this kind of cancer in the innate immune system and how influences innate immune cells and their progenitors.

# CHAPTER 6

# Conclusion

The innate immune system was thought of as being rudimentary and just the first line of attack against pathogens. However, in the last decade, it was discovered that it can recall a past encounter. Through epigenetic modifications and rewiring of metabolic pathways caused by a first encounter, immune cells can induce a stronger innate immune response after a secondary stimulation.

To this innate immune memory, it was called trained immunity which has started to be investigated as an excellent therapeutic target.

In this research trained immunity was targeted as a therapy for anaplastic thyroid cancer. ATC is one of the most aggressive thyroid cancers, with almost no viable therapies nowadays. Since ATC is highly infiltrated by TAMs, we hypothesized that inducing trained immunity on macrophages derived from the bone marrow would help with overcoming the tolerance from the tumor microenvironment.

By using murine-derived BMDMs, we established an optimal way of inducing trained immunity in these healthy cells *in vitro*. This first achievement of the project enabled us to develop new *in vitro* training assays and evaluate the training state of BMDMs in different environments, including their reaction to tumor factors and when harvested from tumor-bearing mice.

Moreover, although an ATC mouse model was not available, it was possible to analyze the viability of using MRI as a mean to identify and possibly measure the thyroid- and tumors- of mice.

In conclusion, this study sheds light on the potential of trained immunity as a promising therapeutic approach for anaplastic thyroid cancer, a highly aggressive malignancy with limited treatment options.

The immunosuppressive nature of ATC represents a significant challenge, but the findings suggest that targeting the innate immune memory could overcome this obstacle and offer a novel avenue for treatment.

This research shows that murine-derived BMDMs can be induced to exhibit trained immunity optimally through stimuli such as the BCG vaccine and factors released by tumor cells, comparable to bacterial stimuli. Moreover, the study examines the impact of tumors *in situ* on the immune system, investigating training state by cytokine production and immune cell populations in tumor-bearing mice.

By providing a deeper understanding of how to target the bone marrow and induce trained immunity, this research opens new possibilities for developing effective therapies against ATC. Further exploration and clinical trials are warranted to validate the potential of trained immunity as a treatment paradigm in this aggressive form of thyroid cancer.

# CHAPTER 7

# References

1. WHO. Ghe-Leading-Causes-of-Death @ Www.Who.Int. Published online 2019.

2. Sung H, Ferlay J, Siegel RL, et al. Global Cancer Statistics 2020: GLOBOCAN Estimates of Incidence and Mortality Worldwide for 36 Cancers in 185 Countries. *CA Cancer J Clin*. 2021;71(3):209-249. doi:10.3322/caac.21660

3. Bray F, Ferlay J, Soerjomataram I, Siegel RL, Torre LA, Jemal A. Global cancer statistics 2018: GLOBOCAN estimates of incidence and mortality worldwide for 36 cancers in 185 countries. *CA Cancer J Clin*. 2018;68(6):394-424. doi:10.3322/caac.21492

4. Chu JJ, Mehrzad R. The biology of cancer. In: *The Link Between Obesity and Cancer*. ; 2022. doi:10.1016/B978-0-323-90965-5.00012-X

5. Nesta A V., Tafur D, Beck CR. Hotspots of Human Mutation. *Trends in Genetics*. 2021;37(8). doi:10.1016/j.tig.2020.10.003

6. Nenclares P, Harrington KJ. The biology of cancer. *Medicine (United Kingdom)*. 2020;48(2). doi:10.1016/j.mpmed.2019.11.001

7. Wang M, Zhao J, Zhang L, et al. Role of tumor microenvironment in tumorigenesis. *J Cancer*. 2017;8(5). doi:10.7150/jca.17648

8. Hanahan D, Weinberg RA. The Hallmarks of Cancer. *Cell*. 2000;100:57-70. doi:10.1107/S2059798322003928

9. Lazebnik Y. What are the hallmarks of cancer? *Nat Rev Cancer*. 2010;10(4):232-233. doi:10.1038/nrc2827

10. Hanahan D, Weinberg RA. Hallmarks of cancer: The next generation. *Cell*. 2011;144(5):646-674. doi:10.1016/j.cell.2011.02.013

11. Fouad YA, Aanei C. Revisiting the hallmarks of cancer. *Cancer Res*. Published online 2017.

12. Howell M, Shepherd M. The immune system. *Anaesthesia and Intensive Care Medicine*. 2021;22(8). doi:10.1016/j.mpaic.2021.06.006

13. Bonilla FA, Oettgen HC. Adaptive immunity. *Journal of Allergy and Clinical Immunology*. 2010;125(2 SUPPL. 2). doi:10.1016/j.jaci.2009.09.017

14. Sznarkowska A, Mikac S, Pilch M. MHC class I regulation: The origin perspective. *Cancers (Basel)*. 2020;12(5). doi:10.3390/cancers12051155

15. Boehm T, Swann JB. Origin and evolution of adaptive immunity. *Annu Rev Anim Biosci*. 2014;2. doi:10.1146/annurev-animal-022513-114201

16. Gulluoglu S. Cancer immunity. In: *Autoimmunity and Cancer*. ; 2022. doi:10.1007/978-3-030-75699-4_10

17. Ferrari SM, Fallahi P, Galdiero MR, et al. Immune and inflammatory cells in thyroid cancer microenvironment. *Int J Mol Sci*. 2019;20(18). doi:10.3390/ijms20184413

18. Li N, Wang Y, Xu H, Wang H, Gao Y, Zhang Y. Exosomes Derived from RM-1 Cells Promote the Recruitment of MDSCs into Tumor Microenvironment by Upregulating CXCR4 via TLR2/NF- B Pathway. *J Oncol*. 2021;2021. doi:10.1155/2021/5584406

19. Mantovani A, Marchesi F, Malesci A, Laghi L, Allavena P. Tumour-associated macrophages as treatment targets in oncology. *Nat Rev Clin Oncol*. 2017;14(7). doi:10.1038/nrclinonc.2016.217

20. Segura-Villalobos D, Ramírez-Moreno IG, Martínez-Aguilar M, et al. Mast Cell–Tumor Interactions: Molecular Mechanisms of Recruitment, Intratumoral Communication and Potential Therapeutic Targets for Tumor Growth. *Cells*. 2022;11(3). doi:10.3390/cells11030349

21. Sipos JA, Mazzaferri EL. Thyroid cancer epidemiology and prognostic variables. *Clin Oncol*. 2010;22(6):395-404. doi:10.1016/j.clon.2010.05.004

22. Cabanillas ME, McFadden DG, Durante C. Thyroid cancer. *The Lancet*. 2016;388(10061):2783-2795. doi:10.1016/S0140-6736(16)30172-6

23. Landa I, Ibrahimpasic T, Boucai L, et al. Genomic and transcriptomic hallmarks of poorly differentiated and anaplastic thyroid cancers. *Journal of Clinical Investigation*. 2016;126(3):1052-1066. doi:10.1172/JCI85271

24. Lowe NM, Loughran S, Slevin NJ, Yap BK. Anaplastic thyroid cancer: The addition of systemic chemotherapy to radiotherapy led to an observed improvement in survival - A single centre experience and the review of the literature. *The Scientific World Journal*. 2014;2014. doi:10.1155/2014/674583

25. Pellegriti G, Frasca F, Regalbuto C, Squatrito S, Vigneri R. Worldwide increasing incidence of thyroid cancer: Update on epidemiology and risk factors. *J Cancer Epidemiol*. 2013;2013. doi:10.1155/2013/965212

26. Smallridge RC, Marlow LA, Copland JA. Anaplastic thyroid cancer: Molecular pathogenesis and emerging therapies. *Endocr Relat Cancer*. 2009;16(1):17-44. doi:10.1677/ERC-08-0154

27. Nagarajah J, Le M, Knauf JA, et al. Sustained ERK inhibition maximizes responses of BrafV600E thyroid cancers to radioiodine. *Journal of Clinical Investigation*. 2016;126(11):4119-4124. doi:10.1172/JCI89067

28. Netea-Maier RT, Smit JWA, Netea MG. Metabolic changes in tumor cells and tumor-associated macrophages: A mutual relationship. *Cancer Lett*. 2018;413:102-109. doi:10.1016/j.canlet.2017.10.037

29. Rabold K, Netea MG, Adema GJ, Netea-Maier RT. Cellular metabolism of tumor-associated macrophages – functional impact and consequences. *FEBS Lett*. 2017;591(19):3022-3041. doi:10.1002/1873-3468.12771

30. Zubair K, You C, Kwon G, Kang K. Two faces of macrophages: Training and tolerance. *Biomedicines*. 2021;9(11). doi:10.3390/biomedicines9111596

31. Lv J, Liu C, Chen FK, et al. M2like tumour-associated macrophage secreted IGF promotes thyroid cancer stemness and metastasis by activating the PI3K/AKT/mTOR pathway. *Mol Med Rep*. 2021;24(2). doi:10.3892/mmr.2021.12249

32. Kreissl MC, Janssen MJR, Nagarajah J. Current treatment strategies in metastasized differentiated thyroid cancer. *Journal of Nuclear Medicine*. 2019;60(1):9-15. doi:10.2967/jnumed.117.190819

33. Aashiq M, Silverman DA, Na'ara S, Takahashi H, Amit M. Radioiodine-refractory thyroid cancer: Molecular basis of redifferentiation therapies, management, and novel therapies. *Cancers (Basel)*. 2019;11(9). doi:10.3390/cancers11091382

34. Vanden Borre P, Mcfadden DG, Gunda V, et al. The next generation of orthotopic thyroid cancer models: Immunocompetent orthotopic mouse models of BRAFV600E-positive papillary and anaplastic thyroid carcinoma. *Thyroid*. 2014;24(4). doi:10.1089/thy.2013.0483

35. Kirschner LS, Qamri Z, Kari S, Ashtekar A. Mouse models of thyroid cancer: A 2015 update. *Mol Cell Endocrinol*. 2016;421. doi:10.1016/j.mce.2015.06.029

36. Van Der Heijden CDCC, Noz MP, Joosten LAB, Netea MG, Riksen NP, Keating ST. Epigenetics and Trained Immunity. *Antioxid Redox Signal*. 2018;29(11):1023-1040. doi:10.1089/ars.2017.7310

37. Mulder WJM, Ochando J, Joosten LAB, Fayad ZA, Netea MG. Therapeutic targeting of trained immunity. *Nat Rev Drug Discov*. 2019;18(7):553-566. doi:10.1038/s41573-019-0025-4

38. Domínguez-Andrées J, Dos Santos JC, Bekkering S, et al. TRAINED IMMUNITY: ADAPTATION WITHIN INNATE IMMUNE MECHANISMS. *Physiol Rev*. 2023;103(1):313-346. doi:10.1152/physrev.00031.2021

39. Netea MG, Domínguez-Andrés J, Barreiro LB, et al. Defining trained immunity and its role in health and disease. *Nat Rev Immunol*. 2020;20(6):375-388. doi:10.1038/s41577-020-0285-6

40. Divangahi M, Aaby P, Khader SA, et al. Trained immunity, tolerance, priming and differentiation: distinct immunological processes. *Nat Immunol*. 2021;22(1):2-6. doi:10.1038/s41590-020-00845-6

41. Schrijver DP, Röring RJ, Deckers J, et al. Resolving sepsis-induced immunoparalysis via trained immunity by targeting interleukin-4 to myeloid cells. *Nat Biomed Eng*. Published online 2023. doi:10.1038/s41551-023-01050-0

42. Stienstra R, Netea-Maier RT, Riksen NP, Joosten LAB, Netea MG. Specific and Complex Reprogramming of Cellular Metabolism in Myeloid Cells during Innate Immune Responses. *Cell Metab*. 2017;26(1):142-156. doi:10.1016/j.cmet.2017.06.001

43. Esfahani K, Roudaia L, Buhlaiga N, Del Rincon S V., Papneja N, Miller WH. A review of cancer immunotherapy: From the past, to the present, to the future. *Current Oncology*. 2020;27(S2):87-97. doi:10.3747/co.27.5223

44. Chan ASH, Kangas TO, Qiu X, et al. Imprime PGG Enhances Anti-Tumor Effects of Tumor-Targeting, Anti-Angiogenic, and Immune Checkpoint Inhibitor Antibodies. *Front Oncol*. 2022;12. doi:10.3389/fonc.2022.869078

45. Havel JJ, Chowell D, Chan TA. The evolving landscape of biomarkers for checkpoint inhibitor immunotherapy. *Nat Rev Cancer*. 2019;19(3). doi:10.1038/s41568-019-0116-x

46. Marofi F, Motavalli R, Safonov VA, et al. CAR T cells in solid tumors: challenges and opportunities. *Stem Cell Res Ther*. 2021;12(1). doi:10.1186/s13287-020-02128-1

47. Geisel J, Kahl F, Müller M, et al. IL-6 and Maturation Govern TLR2 and TLR4 Induced TLR Agonist Tolerance and Cross-Tolerance in Dendritic Cells. *The Journal of Immunology*. 2007;179(9):5811-5818. doi:10.4049/jimmunol.179.9.5811

48. Kucerova P, Cervinkova M. Spontaneous regression of tumour and the role of microbial infection - possibilities for cancer treatment. *Anticancer Drugs*. 2016;27(4). doi:10.1097/CAD.0000000000000337

49. Clemente-Casares X, Santamaria P. Nanomedicine in autoimmunity. *Immunol Lett*. 2014;158(1-2). doi:10.1016/j.imlet.2013.12.018

50. Shi Y, van der Meel R, Chen X, Lammers T. The EPR effect and beyond: Strategies to improve tumor targeting and cancer nanomedicine treatment efficacy. *Theranostics*. 2020;10(17). doi:10.7150/thno.49577

51. Anselmo AC, Mitragotri S. Nanoparticles in the clinic. *Bioeng Transl Med*. 2016;1(1):10-29. doi:10.1002/btm2.10003

52. Yao CG, Martins PN. Nanotechnology Applications in Transplantation Medicine. *Transplantation*. 2020;104(4):682-693. doi:10.1097/TP.0000000000003032

53. Wu J. The enhanced permeability and retention (Epr) effect: The significance of the concept and methods to enhance its application. *J Pers Med*. 2021;11(8). doi:10.3390/jpm11080771

54. Schrijver DP, de Dreu A, Hofstraat SRJ, et al. Nanoengineering Apolipoprotein A1-Based Immunotherapeutics. *Adv Ther (Weinh)*. 2021;4(8). doi:10.1002/adtp.202100083

55. Priem B, van Leent MMT, Teunissen AJP, et al. Trained Immunity-Promoting Nanobiologic Therapy Suppresses Tumor Growth and Potentiates Checkpoint Inhibition. *Cell*. 2020;183(3):786-801.e19. doi:10.1016/j.cell.2020.09.059

56. van Leent MMT, Priem B, Schrijver DP, et al. Regulating trained immunity with nanomedicine. *Nat Rev Mater*. 2022;7(6):465-481. doi:10.1038/s41578-021-00413-w

57. Magadán S, Mikelez-Alonso I, Borrego F, González-Fernández Á. Nanoparticles and trained immunity: Glimpse into the future. *Adv Drug Deliv Rev*. 2021;175. doi:10.1016/j.addr.2021.05.031

58. Rabold K, Zoodsma M, Grondman I, et al. Reprogramming of myeloid cells and their progenitors in patients with non-medullary thyroid carcinoma. *Nat Commun*. 2022;13(1). doi:10.1038/s41467-022-33907-4

59. Mantovani A, Allavena P, Marchesi F, Garlanda C. Macrophages as tools and targets in cancer therapy. *Nat Rev Drug Discov*. 2022;0123456789. doi:10.1038/s41573-022-00520-5

60. de Ridder M, van Dijkum EN, Engelsman A, Kapiteijn E, Klümpen HJ, Rasch CRN. Anaplastic thyroid carcinoma: a nationwide cohort study on incidence, treatment and survival in the Netherlands over 3 decades. *Eur J Endocrinol*. 2020;183(2):203-209. doi:10.1530/EJE-20-0080

61. Li M, He L, Zhu J, Zhang P, Liang S. Targeting tumor-associated macrophages for cancer treatment. *Cell Biosci*. 2022;12(1). doi:10.1186/s13578-022-00823-5

62. Ding C, Shrestha R, Zhu X, et al. Inducing trained immunity in pro-metastatic macrophages to control tumor metastasis. *Nat Immunol*. Published online 2023. doi:10.1038/s41590-022-01388-8

63. Bekkering S, Blok BA, Joosten LAB, Riksen NP, Van Crevel R, Netea MG. In Vitro experimental model of trained innate immunity in human primary monocytes. *Clinical and Vaccine Immunology*. 2016;23(12). doi:10.1128/CVI.00349-16

64. Smith SG, Kleinnijenhuis J, Netea MG, Dockrell HM. Whole Blood Profiling of Bacillus Calmette–Guérin-Induced Trained Innate Immunity in Infants Identifies Epidermal Growth Factor, IL-6, Platelet-Derived Growth Factor-AB/BB, and Natural Killer Cell Activation. *Front Immunol*. 2017;8. doi:10.3389/fimmu.2017.00644

65. Quintin J, Saeed S, Martens JHA, et al. Candida albicans infection affords protection against reinfection via functional reprogramming of monocytes. *Cell Host Microbe*. 2012;12(2). doi:10.1016/j.chom.2012.06.006

66. Pathology of tumours in laboratory animals. Volume II--tumours of the mouse. *IARC Sci Publ*. 1979;23.

67. Cabanillas ME, McFadden DG, Durante C. Thyroid cancer. *The Lancet*. 2016;388(10061):2783-2795. doi:10.1016/S0140-6736(16)30172-6

68. Sipos JA, Mazzaferri EL. Thyroid cancer epidemiology and prognostic variables. *Clin Oncol*. 2010;22(6):395-404. doi:10.1016/j.clon.2010.05.004

# ANNEXES

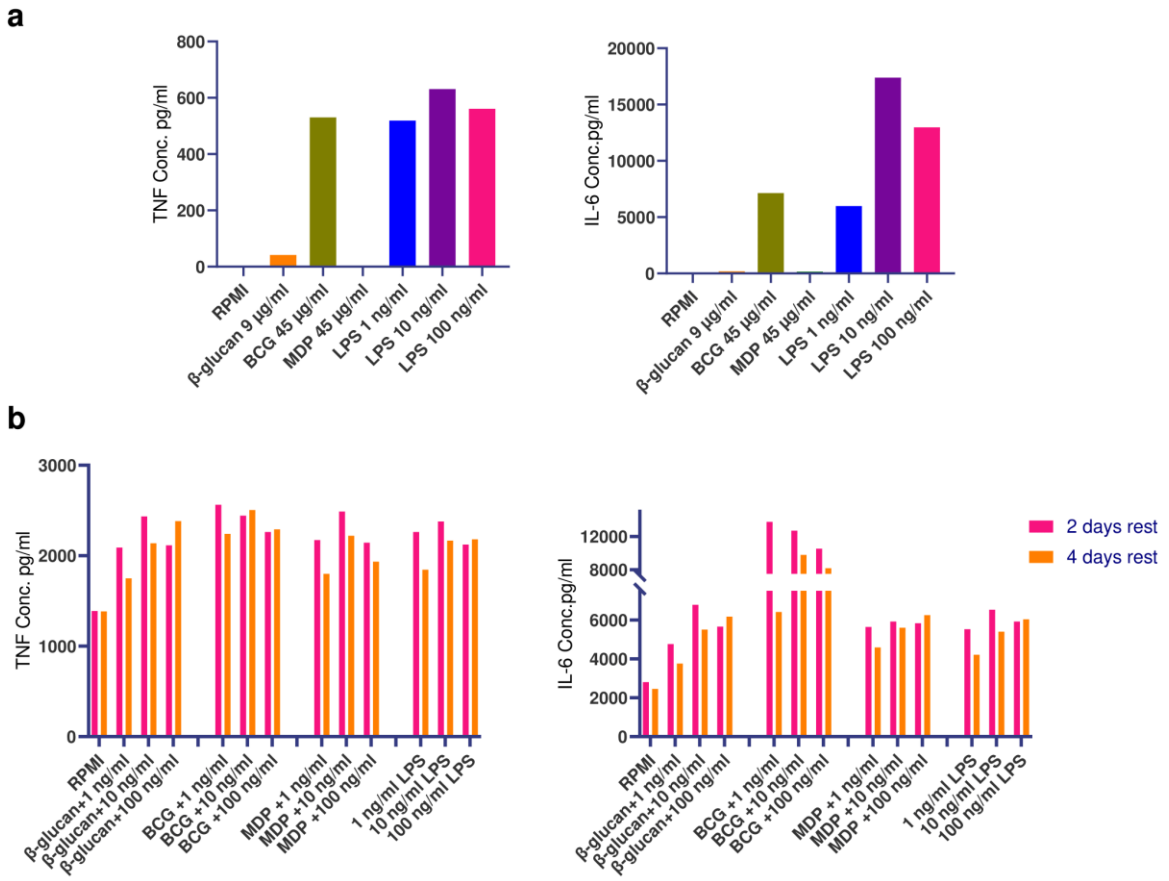


**Annex 1- Proinflammatory cytokine production with different LPS concentrations. (a)-** TNF and IL-6 production after the first stimulus. Cells were stimulated for 24 hours with β-glucan, BCG, MDP**,** or LPS. RPMI-stimulated cells were used as a control. **(b)-** TNF and IL-6 production after LPS restimulation (24h). After training the cells rested for 2 or 4 days. RPMI-stimulated cells were used as a negative control and LPS stimulated as a positive control. Data are shown as means ± standard errors of the means. p values < 0.05 were considered significant, with levels of significance as follows: *p < 0.05; **p < 0.01; ***p < 0.001; ****p < 0.0001; ns, not significant. P values were derived from a two-way analysis of variance (ANOVA) with a multiple-comparison test.

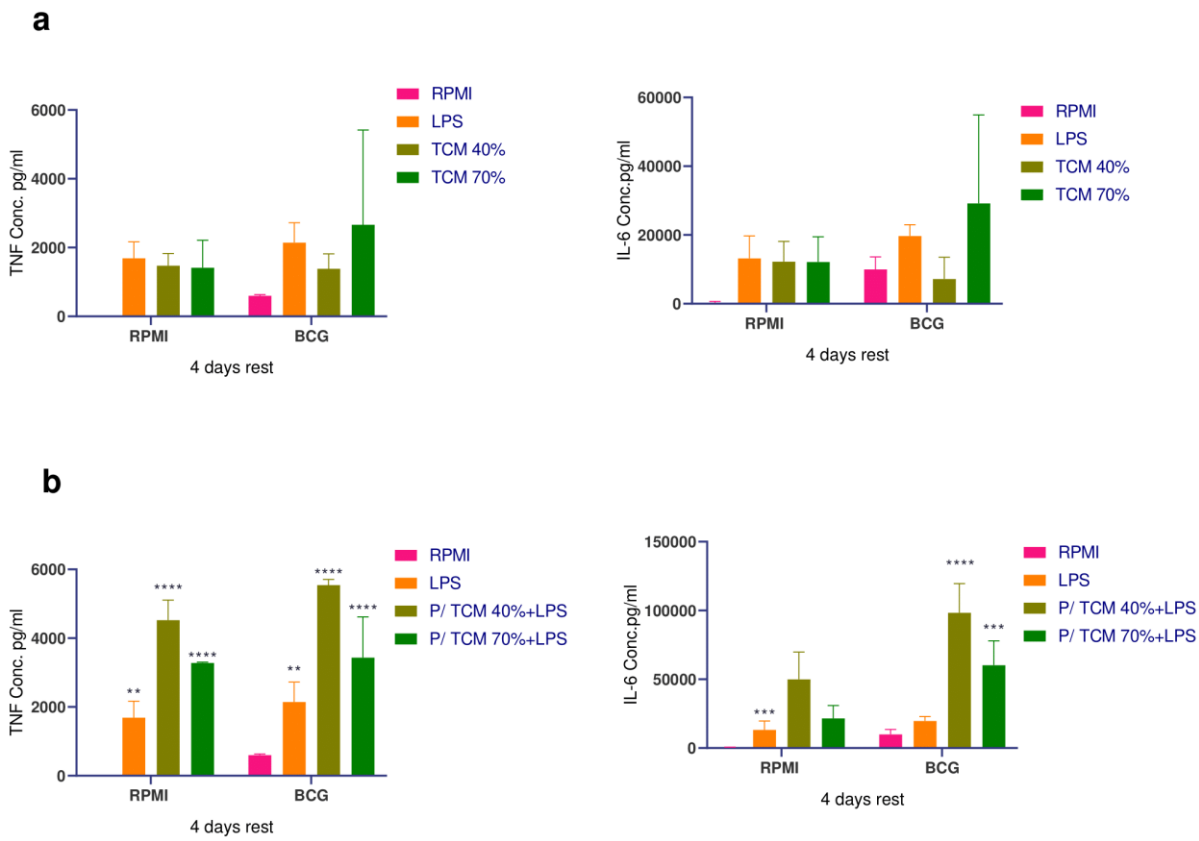


**Annex 2- TCM and LPS induce trained immunity phenotype. (a)-** TNF and IL-6 production after TCM restimulation. Cells were stimulated for 24 hours with BCG. After training cells rested for 4 days. BMDMs were restimulated with TCM. RPMI-stimulated cells were used as a control. **(b)-** TNF and IL-6 production after TCM and LPS restimulation. Cells were stimulated for 24 hours with BCG. After training cells rested for 4 days. BMDMs were restimulated with TCM and LPS. RPMI-stimulated cells were used as a control. Data are shown as means ± standard errors of the means. p values < 0.05 were considered significant, with levels of significance as follows: *p < 0.05; **p < 0.01; ***p < 0.001; ****p < 0.0001; ns, not significant. P values were derived from a two-way analysis of variance (ANOVA) with a multiple-comparison test.